# Modeling Moving Polarized Groups of Animals and Cells

Dissertation
der Mathematischen Fakultät
der Eberhard-Karls-Universität Tübingen
zur Erlangung des Grades eines

Doktors der Naturwissenschaften

vorgelegt von
Frithjof Lutscher
aus Göppingen

2000

| | |
|---|---|
| Tag der mündlichen Prüfung: | 20. Dezember 2000 |
| Dekan: | Prof. Dr. Ch. Lubich |
| Erster Berichterstatter: | Prof. Dr. K.P. Hadeler |
| Zweiter Berichterstatter: | Prof. Dr. W. Alt |

# Zusammenfassung in deutscher Sprache

Inhalt dieser Arbeit ist die Herleitung und Untersuchung eines mathematischen Modells für die Bildung von Fischschwärmen. Diese Schwärme zeichnen sich dadurch aus, daß alle Individuen in einem Schwarm annähernd dieselbe Bewegungsrichtung und Geschwindigkeit haben. Die Ränder eines Schwarms sind scharf, die Dichte innerhalb eines Schwarms ist nahezu gleichmäßig.

Wenn alle Individuen in einer Gruppe dieselbe Ausrichtung haben, spricht man von paralleler Orientierung oder *Polarisierung.* Im Gegensatz zu Schwärmen von Fischen oder Vögeln sind Mückenschwärme i.a. nicht polarisiert. In der englischen Sprache unterscheidet man polarisierte Gruppen (schools of fish, flocks of birds) von nicht polarisierten (shoal of fish, swarm of mosquitoes). Im folgenden bezeichnet "Schwarm" stets eine sich bewegende polarisierte Gruppe.

In einem Schwarm gibt es in der Regel keinen Anführer, der die Richtung vorgibt. Die Polarisierung wird erreicht, indem sich jedes Individuum parallel zu seinen Nachbarn orientiert. Dieser Ausrichtungsvorgang wird im Englischen mit *alignment* bezeichnet, und diese Bezeichnung wird hier übernommen. Außerdem paßt sich ein Individuum an die Geschwindigkeit seiner Nachbarn an. Fische, die hinter einen Schwarm zurückfallen, beschleunigen um aufzuholen, und ebenso verlangsamen Fische vor einem Schwarm ihre Geschwindigkeit.

Ausrichtungsprozesse lassen sich auch auf zellulärer Ebene finden. Aktin-Filamente beispielsweise sind längliche Polymere, die, wenn sie sich berühren, interagieren und aneinander ausrichten.

Man nimmt an, daß die Bildung von Fischschwärmen vor allem dem Schutz vor Freßfeinden dient. Eine große Gruppe erkennt einen Angreifer früher. Ein großer Schwarm schreckt Angreifer ab, weil er wie ein großes Individuum wirkt. Im Falle eines Angriffs verwirrt die Vielzahl gleich aussehender Individuen den Angreifer. Ein zweiter wichtiger Vorteil eines großen Schwarms scheint eine größere Effizienz bei der Suche nach Ressourcen zu sein. Außerdem lassen sich in einem Schwarm hydrodynamische Effekte zur einfacheren Fortbewegung ausnutzen.

In der Literatur finden sich vor allem zwei Zugänge zur Modellierung von Alignment mit Hilfe von partiellen Integro-Differentialgleichungen. In beiden Ansätzen geht es nur um die Ausrichtung und nicht um die räumliche Bewegung.

In einer Folge von Artikeln entwickeln und untersuchen Edelstein-Keshet, Ermentrout und Mogilner (1990, 1995, 1996) mehrere Modelle für Interaktion und Ausrichtung von Fibroblasten. Dabei wird angenommen, daß eine Partikel sich zum einen zufällig immer wieder neu ausrichtet, zum andern nach Interaktion mit einer anderen Partikel mit einer gewissen Wahrscheinlichkeit deren Ausrichtung annimmt. Ist die Rate der zufälligen Ausrichtungsänderung klein genug, so entsteht parallele Orientierung vieler Partikel.

In einem anderen Modell von Geigant et al. (1997) wird angenommen, daß je zwei Aktin-Filamente mit einer gewissen Rate interagieren und sich aufgrund dieser Interaktion neu ausrichten. Sowohl die Interaktionsrate als auch die Wahrscheinlichkeitsverteilung der neuen Orientierung hängen vom Winkel zwischen den beiden interagierenden Filamenten ab. Ist die Winkeldifferenz je zweier Filamente nach einer Interaktion geringer als vorher und ist ferner die Varianz der Wahrscheinlichkeitsverteilung klein, so entsteht auch in diesem Modell parallele

Orientierung vieler Filamente.

In der vorliegenden Arbeit wird die Bewegung der Individuen im Raum von Anfang an explizit in die Modellierung einbezogen. Die Gesamtdichte aller Individuen ist strukturiert nach Ort und Geschwindigkeit (Richtung und Betrag). Der Bewegungsprozeß im Raum wird durch die lineare Boltzmanngleichung beschrieben. Die Interaktion wird zunächst unabhängig vom Raumpunkt mit Hilfe einer Differentialgleichung modelliert. Dann nimmt man an, daß die Interaktion an jedem Raumpunkt nach denselben Regeln abläuft und verbindet die Differentialgleichung additiv mit der Boltzmanngleichung. Dieses Vorgehen ist ähnlich dem bei der Herleitung von Reaktions-Diffusionsgleichungen. Reaktions-Transportgleichungen sind allerdings besser geeignet, Interaktionen zu modellieren, die von der Bewegungsrichtung der interagierenden Teilchen abhängen. Auch vermeiden Reaktions-Transportgleichungen das unrealistische Phänomen unendlicher Ausbreitungsgeschwindigkeit, das für Reaktions-Diffusionsgleichungen bekannt ist.

Im ersten Kapitel wird angenommen, daß sich Individuen mit konstantem Betrag der Geschwindigkeit $\gamma_*$ im eindimensionalen Raum bewegen und ihre Richtung zufällig mit der Rate $\mu_*$ ändern. Die Gesamtdichte $u$ wird in die der nach rechts und links laufenden Individuen aufgeteilt: $u = u^+ + u^-$. Bei der Modellierung des Alignmentprozesses wird angenommen, daß Individuen ihre Richtung nach der Richtung der Mehrheit wählen. Das führt zu einer weiteren, diesmal dichteabhängigen Rate $a(u)u^+u^-$. Die Funktion $a$ hängt von der Gesamtdichte ab und ist positiv. Das resultierende Modell ist ein Modell für korrelierte Zufallsbewegung, in dem statt der konstanten Umkehrrate die dichteabhängige Umkehrrate

$$\mu(u^+, u^-) = a(u)u^+u^- - \frac{\mu_*}{2}$$

steht, die positive und negative Werte annimmt. An dieser Umkehrrate läßt sich ablesen, daß Alignment und zufällige Umkehr einander entgegenwirken. Schwärme bilden sich, wenn der polarisierende Effekt des Alignments stärker ist als die ausgleichende Wirkung der zufälligen Bewegung. Die Modellgleichungen sind:

$$\begin{aligned} u_t^+ + \gamma u_x^+ &= \mu(u^+, u^-)(u^+ - u^-), \\ u_t^- - \gamma u_x^- &= \mu(u^+, u^-)(u^- - u^+). \end{aligned}$$

Das hergeleitete Modell wird analytisch und numerisch untersucht. Lösungen zu nichtnegativen Anfangswerten bleiben nichtnegativ und die Gesamtmasse aller Individuen bleibt konstant. Die stationäre Lösung $u^+ = u^- = \text{const.}$ beschreibt die Situation, daß beide Richtungen gleich stark vertreten und konstant im Raum sind. Ist die Umkehrrate größer als die "Alignmentrate" $a(u)u^+u^-$, so ist $\mu$ negativ und die stationäre Lösung ist linear stabil. Ist $\mu$ positiv, so ist sie instabil. Diese Instabilität ist das Charakteristikum von Alignment.

Mittels der Charakteristikenmethode zeigt man Existenz von Lösungen auf der ganzen reellen Achse. Aufgrund von Fortsetzungs- und Symmetrieargumenten erhält man daraus Lösungen auf beschränkten Intervallen mit geeigneten Randbedingungen. Es wird untersucht, unter welchen Bedingungen an die Umkehrrate diese Lösungen global in der Zeit existieren. Unter der Annahme, daß bei sehr hohen Dichten die Tendenz zur gemeinsamen Ausrichtung schwächer ist, wird

die Existenz eines invarianten Gebiets gezeigt. Zusammen mit einer a priori Abschätzung für das Maximum der Lösung und ihrer Ableitung ergibt sich daraus ein Beweis für globale Existenz.

Das qualitative Verhalten des Modells wird im Falle periodischer Randbedingungen genauer untersucht. Der Zustand, daß beide Dichten $u^{\pm}$ räumlich konstant und gleich groß sind, ist stationär. Für große Werte von $\mu_*$ ist dieser Zustand stabil, für kleine Werte dagegen instabil. Die Bifurkation ist keine Standardbifurkation. Alle Eigenwerte überqueren gleichzeitig die imaginäre Achse. Durch die Einführung eines viskosen Terms kann aus dieser Bifurkation eine Reihe von Hopf-Bifurkationen gemacht werden. Im Fall $\mu_* = 0$ lassen sich $\omega$-Limesmengen mit Hilfe einer Lyapunov Funktion beschreiben.

Schließlich wird das Modell zur Schwarmbildung mit einem einfachen Populationsmodell gekoppelt, das beschreibt, wie eine zu kleine Population ausstirbt, eine hinreichend große Population jedoch bis zu einer gewissen Kapazität wächst. Es kann kann analytisch und numerisch gezeigt werden, daß eine Population, die ohne Alignment aussterben würde, sich mit Alignment erholen kann.

Im nächsten Kapitel wird das eindimensionale Modell auf zwei Raumdimensionen erweitert. Dabei wird immer noch angenommen, daß der Betrag der Geschwindigkeit $\gamma_*$, mit der sich Individuen bewegen, konstant bleibt. Die Dichte $u(t, x, s)$ hängt ab von Ort $x \in \mathbb{R}^2$ und Geschwindigkeit $s \in V = \gamma_* S^1$. Die Gesamtdichte an einem Ort ist $\bar{u}(t, x) = \int_V u(t, x, s) ds$. Individuen richten ihre Geschwindigkeit an der mittleren Geschwindigkeit $\bar{s}(t, x) = \int_V \sigma u(t, x, \sigma) d\sigma / \bar{u}$ aus. Die ortsunabhängige Reaktionsgleichung lautet:

$$u_t = a(\bar{u})[s\bar{s} - |\bar{s}|^2]u.$$

Die Funktion $a$ ist positiv und entspricht der Funktion $a$ im eindimensionalen Modell. Diese Gleichung wird mit den Modellen von Edelstein-Keshet et al. (1995) und Geigant et al. (1997) verglichen. Dazu wird eine allgemeine Gleichung für Gewinn-Verlust-Prozesse hergeleitet, die alle drei Modelle als Spezialfälle enthält.

Das Alignmentmodell mit räumlicher Bewegung lautet

$$u_t + s \cdot \nabla_x u = -\mu_*(u - \frac{\bar{u}}{|V|}) + a(\bar{u})[s\bar{s} - |\bar{s}|^2]u,$$

wobei der erste Term auf der rechten Seite zufällige Neuausrichtung modelliert. Dieses Modell erhält die Gesamtmasse und Positivität. Ist $\mu_*$ klein genug, so ist die konstante stationäre Lösung instabil wie schon im eindimensionalen Fall. Existenz von Lösungen auf ganz $\mathbb{R}^2$ wird mittels des Charakteristikenansatzes gezeigt. Numerische Simulationen runden das Kapitel ab.

Im letzten Kapitel wird ein Modell hergeleitet und untersucht, in dem Individuen ihre Geschwindigkeit an die lokale Situation anpassen. Zur Vereinfachung wird zunächst angenommen, daß sich alle Individuen in dieselbe Richtung bewegen. Die Dichte der Individuen wird mit $u$, ihre Geschwindigkeit mit $\gamma$ bezeichnet. Es wird eine optimale Dichte $u_*$ angenommen, die Individuen zu erreichen suchen, und eine optimale Geschwindigkeit $\gamma_*$, mit der sie sich bewegen wollen. Ist die Dichte an einer Stelle geringer als die optimale Dichte und gleichzeitig der Gradient der Dichte positiv, dann beschleunigt ein Individuum an dieser Stelle, um zu

Stellen größerer Dichte zu kommen. Analoge Überlegungen für die drei anderen möglichen Fälle führen zu einer "erwarteten Geschwindigkeit" $E(u, u_x)$. Setzt man nun $E = \gamma$, so ergibt sich eine Diffusionsgleichung, in der der dichteabhängige Diffusionskoeffizient das Vorzeichen wechselt. Das Problem ist also nicht wohlgestellt. Daher nimmt man an, daß Individuen ihre Geschwindigkeit mit einer gewissen Verzögerung und einem Fehler an die erwartete Geschwindigkeit anpassen. Man erhält eine Differentialgleichung für die Geschwindigkeit. Insgesamt hat man also ein System von zwei Gleichungen

$$\begin{aligned} u_t + (\gamma u)_x &= 0, \\ \tau \gamma_t &= \beta \gamma_{xx} + E(u, u_x) - \gamma. \end{aligned}$$

Die Verzögerung wird durch $\tau$ gemessen, die "Varianz" des Fehlers wird durch $\beta$ bestimmt.

Um dieses System zu untersuchen, regularisiert man es zunächst, indem man in der ersten Zeile den Term $\varepsilon u_{xx}$ auf der rechten Seite hinzufügt. Dann entsteht ein parabolisches System, falls $\tau > 0$, und ein parabolisch/elliptisches System, falls $\tau = 0$. Wählt man für die Dichte eine konstante Funktion $\bar{u}$ und für die Geschwindigkeit $\gamma_*$, so ist $(\bar{u}, \gamma_*)$ eine stationäre Lösung des Systems. Sie ist linear stabil, falls $\bar{u} > u_*$. Gilt hingegen $\bar{u} < u_*$ und ist $\varepsilon$ klein genug, so ist die konstante Lösung instabil.

Zuerst wird gezeigt, daß für $\tau > 0$ und auch für $\tau = 0$ glatte Lösungen global existieren. Im Fall $\tau = 0$ kann man mit Hilfe der Viskositätsmethode die Existenz von Lösungen für $\varepsilon = 0$ zeigen. Man findet, daß die Lösungen für beliebig lange Zeiten stetig bleiben, wenn nur die Anfangsdaten glatt sind. Dies ist bei Erhaltungsgleichungen im allgemeinen nicht so.

Zuletzt wird der Prozeß der Geschwindigkeitsanpassung mit dem Umkehrprozeß des Alignment verbunden. Dabei wird angenommen, daß Individuen ihre Geschwindigkeit nur an Nachbarn ausrichten, die sich in dieselbe Richtung bewegen wie sie selbst. Es ergibt sich ein Modell von vier Gleichungen, zwei für die Dichten $u^{\pm}$ und zwei für die entsprechenden Geschwindigkeiten $\gamma^{\pm}$. Der Umkehrprozeß wird durch die Umkehrfunktion $\mu$ vom Anfang beschrieben, die Geschwindigkeitsanpassung durch die parabolische (oder elliptische) Gleichung oben. Es wird gezeigt, daß im Fall $\tau = 0$ die Existenzresultate von oben auf das System mit zwei Richtungen übertragen werden können. Insbesondere existieren auch hier Lösungen, die für beliebig lange Zeiten stetig bleiben, wenn die Anfangswerte glatt sind.

Zum ersten Mal werden in dieser Arbeit die Anpassungsprozesse in Orientierung und Geschwindigkeit innerhalb eines Schwarms in einem einzigen Modell beschrieben. Analytische Resultate und numerische Simulationen zeigen, daß das Modell qualitativ richtige Lösungen besitzt. Es wäre nun wünschenswert, die Anpassung der Geschwindigkeit auch in zwei Raumdimensionen zu modellieren und das Verhalten des Modells mit biologischen Experimenten zu vergleichen.

# Contents

# Chapter 1

# Introduction

## 1.1 Biological Background

Most animal species form groups at some stage during their life cycle. The structure of the group depends on and reflects the functional importance of grouping in a certain phase and environment. Depending on the species and the shape such groups are called packs, herds, schools, flocks, swarms etc. In this work we derive and study a model for *moving polarized groups* such as schools of fish or flocks of birds.

By *movement* we always denote a change of the spatial location of an individual. The mere change of the orientation is called *turning*. The process by which an individual turns to adapt its orientation to that of its neighbors is called *alignment*. A group is *polarized* if all members have about the same orientation in space. Keeping a common orientation, individuals can travel large distances together. On the contrary, there are groups in which all individuals move but the group as a whole remains stationary or drifts only slowly. Individuals in such groups are not polarized, e.g. mosquitos. Somewhat in between is the behavior of sparrows for example, which form moving polarized groups but the direction of group movement changes frequently such that the group as a whole does not travel far. These frequent changes of the group direction shall not be addressed here. The amount of biological literature about moving polarized groups and fish schools in particular is so large that we can list only some important features and give a few references at the end.

If the overall number of individuals in a certain area is very small then no schools form. If a school forms then its size can vary from less than ten to more than a thousand individuals. The edges of such a group are relatively sharp and the density within a group is nearly uniform. The distance between two neighboring fish is approximately twice the width of the zone in which swimming movement creates vortices in the water. Individuals tend to disperse in order to avoid overcrowding. Individuals can move faster in a group than alone, but usually there are no collisions even though the group as a whole may turn and swirl frequently.

In small moving polarized groups there sometimes seems to be a leader which directs the movement of the others, e.g. in V-shaped constellations of about a dozen birds. In larger groups however there is no apparent leader, in fact the leading position (relative to the direction of movement) changes continuously.

Sometimes external cues may explain observed polarization, but frequently there is no detectable external cue. The question then is how and why these groups are formed and maintained.

Alignment can also be observed on the cellular and subcellular level. We name a few examples. Actin filaments are rod-like polymers which are the main building part of the cyto-skeleton. They appear as disordered loose meshwork as well as in highly polarized arrays or in bundles with two mutually orthogonal axes of orientation. Filaments in loose meshwork can reorient themselves due to interaction with others in order to form large arrays in parallel orientation. Fibroblasts are part of the connective tissue and play a role in wound healing. They move, come into contact with others, align with them and adhere which leads to clusters in parallel orientation. Alignment also occurs in purely chemical systems. In liquid crystals, for example, areas of unordered and of parallel oriented particles can be found as well as the transition between them.

In all these examples on the microscopic level, direct contact between particles is essential for polarized patterns to evolve. Particles touch one another and interact. They change their direction, adhere, move. On the macroscopic level visual perception is essential for the formation of moving polarized groups. For fish the lateral line is the most important organ for orientation: they are still able to join a school even if they wear temporal blinders.

For some time researchers could not explain the observed behavior without assuming a group leader or some external influence which determines the common direction. Some authors even postulated a "group mind" and the emergence of a "superindividual". This situation changed in the late 1980's when concepts from dynamical systems theory were applied to describe individual behavior. Group structure was understood as emerging from rules for individuals. A relatively recent approach is the so called JLS-approach, according to which every individual makes decisions whether to join a group, stay in it or leave it (JLS-decisions). The behavior of the group is determined by the net effect of the individual JLS-decisions.

It is now commonly agreed upon that the striking patterns which can be found in moving polarized groups result from a twofold adaptation process: Individuals adapt their *orientation of movement* to that of their neighbors, i.e. they *align* with them. Within a moving group individuals also adapt their *speed* to that of the others. For example, a fish lagging behind increases the number and amplitude of tail movements. Even if there are only two fish, these two tend to swim parallel to each other and equalize their velocities.

With this new understanding of *how* groups form the focus of the question *why* they form shifted from the group level to the individual level. On this level, due to evolutionary selection pressure, individuals adjust their behavior as to maximize their evolutionary fitness. The most widely accepted explanation for the formation of fish schools is that individuals try to avoid predation. In a larger group there is an antipredator advantage of vigilance, i.e. an approaching predator is detected earlier because more fish are attentive. The risk of being detected does not increase in a large group. Hence, an individual reduces its risk of predation by joining a group because the probability of an individual in a group to be caught decreases as the group size increases. This effect is called the "abatement effect". Predators hesitate to attack large schools since the school as a whole acts as

a single individual which is much larger than the predator. Even if a predator attacks a school, its focus from one single prey is easily distracted and the attack may fail. Other factors for schooling are resource exploitation (search for food), mating or energy saving through hydrodynamic effects.

An early but very detailed treatment of fish schools is the monograph by Radakov [55] which contains experiments, data, theories and even consequences for industrial fishing. The most up to date and comprehensive overview of animal grouping is the book edited by Parrish and Hamner [49] which addresses all questions from data collection and analysis to behavioral ecology and modeling and offers an excellent bibliography. A description of the JLS-approach together with a discussion of the advantages of schooling against predation is given by Pitcher [52]. Okubo was one of the first who used dynamical systems to describe animal aggregation in general and fish schooling in particular [45]. References for the behavior of filaments and fibroblasts can be found in the work by Geigant [13] and Edelstein-Keshet and Ermentrout [10].

## 1.2 Mathematical Models for Alignment

During the last years orientation processes of animals and cells have received much attention in mathematical modeling [4, 48]. There are two general frameworks to approach the problem: the Lagrangian and the Eulerian [18]. In the Lagrangian framework the state of every single individual is given by a set of characteristic factors (location, age,...) and the evolution of each factor in time is described by (ordinary or stochastic) differential equations [44] or by a set of local rules in cellular automata [9, 10, 61]. These models can take into account many details of interaction. Numerical simulations of these models show a behavior similar to the behavior observed in nature or experiments [58, 63]. On the other hand it is often hard, if not impossible, to treat such models analytically.

In Eulerian models the density of individuals is structured by a set of variables and the evolution of the density is described by partial (integro-) differential equations. These models pose some challenging mathematical problems but they cannot account for all biologically relevant details. They are only applicable for a sufficiently large number of individuals. They are often used to find a smallest set of rules or dependencies which describes the observed behavior. In the present work we focus on the Eulerian approach only. The transition from Lagrangian to Eulerian models is a delicate one [12] and shall not be addressed here.

In the existing literature, there are mainly two different approaches to model alignment processes within the Eulerian framework. One is developed by Edelstein-Keshet et al. [10, 41, 42] and describes the orientation and binding behavior of fibroblasts. The other is by Geigant et al. [13, 14] to model interaction and orientation of actin filaments. Both assume a spatially homogeneous distribution of particles and neglect movement in space (for an exception see [40]). This simplification is justified if movement happens on a much slower time scale than turning. We describe both approaches here and compare them to the model developed later in Chapter 3.

Three models for fibroblast behavior are presented and investigated by Edelstein-Keshet, Ermentrout and Mogilner [10, 41, 42], henceforth abbreviated by Edelstein-

Keshet et al. For Model I two classes of cells are considered: free cells and bound cells. Their densities depend on the orientation angle $\theta \in [-\pi, \pi]$ and are denoted by $C(\theta, t)$ for the free cells and $P(\theta, t)$ for the bound cells. Free cells turn at random and interact with other free or bound cells. When a free cell in direction $\theta$ interacts with any other cell in direction $\theta'$, it can either keep its direction or switch to $\theta'$. If it aligns with its interaction partner at $\theta'$ then it adheres to it and becomes a bound cell. The probability of alignment may depend on the angular difference $\theta - \theta'$ and also on whether the interaction partner is a free or a bound cell. Bound cells break loose from aligned clusters with a rate $\gamma$. Hence, the model equations are gain and loss equations for the two classes of particles with parameters $\varepsilon, \gamma, \beta_{1,2} > 0$ :

$$\begin{aligned} P_t &= \beta_1 CK * C + \beta_2 PK * C - \gamma P, \\ C_t &= \varepsilon \Delta_\theta C - \beta_1 CK * C - \beta_2 CK * P + \gamma P. \end{aligned}$$

The one dimensional Laplacian describes random turning of free cells. Interaction is modeled by the convolution terms, where

$$(CK * C)(\theta) = C(\theta) \int_{-\pi}^{\pi} K(\theta - \theta') C(\theta') d\theta'$$

for instance gives the total number of free cells which turn into direction $\theta$ upon interaction with free cells in direction $\theta$. The exact shape of the kernel is less important than its symmetries. Three different shapes of $K$ are considered. The kernel can have a single hump around $\theta = 0$ which describes parallel orientation of cells head-to-head only. Double hump kernels can describe head-to-head as well as head-to-tail parallel orientation with the humps at $\theta = 0, \pm\pi$. Finally, if kernels have humps at $\theta = \pm\pi/2$ they describe bundles in which particles are parallel to either of two mutually orthogonal lines.

Model II describes gradual rotation rather than instantaneous alignment. There is no binding mechanism for aligned cells, only one density $C(\theta, t)$ is considered. This density of cells induces a potential $W * C$ and particles undergo an angular drift according to the corresponding potential field. The model equation in this case is

$$C_t = \varepsilon \Delta_\theta C - \nabla_\theta \cdot (C \nabla (W * C)).$$

The kernel $W$ has a shape as the kernel $K$ above.

In Model III, finally, turning is again instantaneous to one of the directions of the two interaction partners. There is no binding of aligned cells and the equation for the density $C(\theta, t)$ reads

$$C_t = \varepsilon \Delta_\theta C - C(Q(C) * C),$$

where the convolution term is

$$(Q(C) * C)(\theta) = \int_{-\pi}^{\pi} Q_1(C(\theta) - C(\theta')) Q_2(\theta - \theta') C(\theta') d\theta'.$$

The kernel $Q_2$ has the same meaning and shape as $K$ in Model I. The function $Q_1$ reflects the observation that bigger clusters grow at the expense of smaller ones when they interact. It is assumed to be monotone increasing, bounded and odd.

The behavior of all models is similar: The total cell density is constant and there is a homogeneous, i.e. $\theta$-independent steady state solution. A linear stability analysis shows that this state is stable for large random turning parameter $\varepsilon$ and becomes unstable as $\varepsilon$ decreases. Which of the modes grows fastest depends on the chosen kernel. This instability is the characteristic feature of alignment and hence alignment behavior results from a competition between random turning and interaction-controlled directed turning.

The situation that all cells are completely aligned is described by a $\delta$-distribution with respect to the angular variable $\theta$. In the limiting case, $\varepsilon = 0$, when there is no random turning, such a state of complete alignment is a (generalized) solution and this solution is linearly stable. The situation of two $\delta$-peaks is unstable. For weak but nonzero angular diffusion the peaks are smoothed out. An approximate formula for the shape of a smoothed peak is given. Also, the 3D case is investigated by the same means. Orientation is then determined by a vector in $S^2 \subset \mathbb{R}^3$.

An extension of these models to include spatial dependence was considered in [40]. All densities now depend on time $t \in \mathbb{R}^+$, orientation $\theta \in S^{n-1} \subset \mathbb{R}^n$ and space $x \in \mathbb{R}^n$ for $n = 2, 3$. Particles are assumed to move randomly in space, which is modeled by the Laplacian with respect to $x$. The orientation of a particle does not influence its movement. The derivation of the interaction terms is similar to the non-spatial case above. The convolution kernels depend on the spatial as well as on the orientational variables. Integration takes place over $S^{n-1} \times \mathbb{R}^n$. Hence the equations are non-local in space. Equations for Model I read:

$$\begin{aligned} P_t &= \beta_1 CK * C + \beta_2 PK * C - \gamma P, \\ C_t &= \varepsilon_1 \Delta_x C + \varepsilon_2 \Delta_\theta C - \beta_1 CK * C - \beta_2 CK * P + \gamma P. \end{aligned}$$

A bifurcation analysis at the homogeneous stationary state, i.e. at functions constant on $S^{n-1} \times \mathbb{R}^n$, yields three different behaviors: If the spatial diffusion is large and the orientational diffusion is small then particles remain evenly distributed in space but become polarized. If the spatial diffusion is small and the orientational diffusion is large then centers of aggregation of non-aligned particles form. If both diffusion rates are small then aligned spatially separated clusters form. The space dependent version of Models II and III show a similar linearization behavior.

Geigant et al. [14] present a planar model for alignment of filaments due to actin-actin interaction. It is a special case of a model for pattern formation on $S^1$ by Geigant [13] and describes how actin filaments form large arrays in which all filaments are oriented in one single or two mutually orthogonal directions. Filaments are characterized by their orientation angle $\theta \in [-\pi, \pi]$. When a filament with orientation $\theta'$ meets another with orientation $\theta''$, then the two interact with a certain rate $\zeta = \zeta(\theta' - \theta'')$. Upon interaction the filament with orientation $\theta'$ turns into a new direction $\theta$ with some probability $\omega = \omega(\theta' - \theta, \theta' - \theta'')$, which depends on the angular difference of the interaction partners *and* to the new direction. The density of filaments at time $t$ in direction $\theta$ is denoted by $f(t, \theta)$ and the model equation is a gain and loss equation for the different directions:

$$\begin{aligned} f_t(t,\theta) &= -f(t,\theta) \int_{-\pi}^{\pi} \zeta(\theta - \theta') f(t,\theta') d\theta' \\ &+ \int_{-\pi}^{\pi} \int_{-\pi}^{\pi} \zeta(\theta' - \theta'') \omega(\theta' - \theta, \theta' - \theta'') f(t,\theta') f(t,\theta'') d\theta' d\theta''. \end{aligned}$$

A similar equation was derived in the context of dominance in social populations by Jäger and Segel [30]. Individuals are characterized by a value of dominance in $[0, 1]$ rather than by an orientation angle. Every encounter between two individuals results in a winner and a looser and an individual's value of dominance increases or decreases accordingly.

The total mass of filaments is constant and the equation is rotationally invariant. The homogeneous state, where $f$ is a constant, is stationary. As above, we speak of alignment if this situation is unstable. The stability behavior depends on some qualitative properties of the parameter functions $\zeta$ and $\omega$. The authors consider several cases, we only mention a few here.

Suppose filaments at all angles interact equally, then $\zeta$ is a constant. If also the turning is independent of the interaction angles, then $\omega = \text{const.}$ and the homogeneous state is stable. If the turning depends on the angular differences then $\omega$ is called *attractive* if the angular difference between two filaments decreases after interaction. It is called *attractive/repulsive* if the difference decreases at acute angles and increases at obtuse angles. The turning probability $\omega$ is a peak around the new direction $\theta$ and turning is more precise if the peak is narrower and sharp. If $\omega$ is attractive and turning is precise enough, then the homogeneous state is unstable and filaments start to align in one single direction. If $\omega$ is attractive/repulsive then head-to-head as well as head-to-tail parallel orientation emerges.

In the limiting case where all filaments are oriented in the same direction the density $f$ becomes a $\delta$-distribution with respect to the orientation angle $\theta$. If the turning is exact, i.e. $\omega$ is a peak in the new direction $\theta$ then such a $\delta$-distribution is indeed a solution to the equation. It is linearly stable. For small imprecision of turning a narrow peak solution is expected.

Among other complex phenomena of swarm formation and aggregation, gliding myxobacteria show behavior of alignment and movement. They form so-called "streets" in which the rod-like bacteria have the same orientation in space and glide either past each other or parallel to each other. They reverse their direction of movement depending on the surrounding density of other bacteria. This behavior was modeled by Pfistner [50]. The problem is essentially one-dimensional. Bacteria move on the line either to the right or to the left with average speed $\gamma_*$. The density $u$ is split accordingly into the right and left moving fraction $u^{\pm}$. Bacteria are assumed to perceive the densities in a neighborhood of length $2R$ of their position. They change direction with some rate $\mu^{\pm}$ which depends on the densities in the perception interval. The resulting model is the following system of hyperbolic equations.

$$\begin{aligned} u_t^+(t,x) + \gamma_* u_x^+(t,x) &= -\mu^+ u^+(t,x) + \mu^- u^-(t,x), \\ u_t^-(t,x) - \gamma_* u_x^-(t,x) &= \mu^+ u^+(t,x) - \mu^- u^-(t,x), \end{aligned}$$

where the turning frequencies are defined with some function $\Lambda$ and weight functions $\alpha, \beta$ as

$$\mu^{\pm} = \Lambda\left(\int_{-R}^{R} \alpha(r) u^{\pm}(t, x \pm r) + \beta(r) u^{\mp}(t, x \pm r) dr\right).$$

The function $\Lambda$ is assumed monotone increasing and positive. If a bacterium moves to the right and perceives many others going to the right then its tendency to reverse its direction is small. On the other hand, if many others move left, then its tendency to turn increases. If both directions are equally present, bacteria usually do not turn. This behavior is captured in the following assumptions on the weight functions:

$$\alpha < 0, \qquad \beta > 0, \qquad |\alpha| > \beta.$$

The model is non-local in space. To obtain a local model, the integrals in the definition of $\Lambda$ are approximated by local Taylor series. Then the turning rates depend on the densities $u^{\pm}$ and on the gradients $u_x^{\pm}$.

Stationary swarms are investigated in the spatially local model. They are defined by the condition that the density $u = u^+ + u^-$ is unchanged in time and the flux $u^+ - u^-$ vanishes identically. Then obviously $u^+(t,x) = u^-(t,x) = u(t,x)/2$. The system now reduces to a single implicit ordinary differential equation. Conditions for the existence of stationary swarms are given and their shape is computed. A three dimensional generalization of the model in the form of a Boltzmann-like equation is given by Pfistner and Alt but not investigated more closely [51].

Although these myxobacteria clearly show alignment behavior by the formation of streets and by the density dependent change of their direction of movement, the observed stationary swarms contain bacteria moving in both directions equally. The swarm is not polarized. It retains its shape since individuals turn as they reach the boundary of the swarm and move back into the swarm. This is not the behavior of schools to be modeled in the present work. But the two models by Pfistner and Alt are special cases of so called reaction transport equations. This type of equations shall also be the basis of the present work. We briefly recall some important facts about them.

## 1.3 Review of Reaction Transport Equations

Movement in space and interaction with the environment are two fundamental features of living organisms. Reaction transport equations are a natural approach to describe movement and interaction processes in particular if the interaction depends on the direction of movement [21]. At the same time reaction transport equations avoid unwanted effects such as infinite propagation speed which occurs in reaction diffusion equations.

Spreading in space is modeled by the linear Boltzmann equation. Particles are characterized by their position in space $x \in \Omega \subset \mathbb{R}^n$ and their velocity $s \in V \subset \mathbb{R}^n$. In the simplest case $V$ is a sphere or a ball of some radius $\gamma_*$. Particles move in straight lines with their respective velocity, stop according to a Poisson process with parameter $\mu_*$ and choose a new direction $s'$ according to a kernel $K(s,s')$. The density $u(t,x,s)$ satisfies the *transport equation*

$$u_t(t,x,s) + s \cdot \nabla_x u(t,x,s) = -\mu_* u(t,x,s) + \mu_* \int_V K(s,s') u(t,x,s') ds' \tag{1.1}$$

on $\mathbb{R}_+ \times \Omega \times V$. Integrating over all velocities we get the total density at one point $x \in \Omega$ as $\bar{u}(t,x) = \int_V u(t,x,\sigma) d\sigma$. Interaction processes are modeled independently

of the spatial variable. If the interaction depends only on the total density then it is described by an ordinary differential equation

$$\frac{d}{dt}\bar{u}(t) = f(\bar{u}(t)) \tag{1.2}$$

for some suitable function $f$. Similarly to the modeling approach with reaction diffusion equations, simultaneous spread and interaction is given by the *reaction transport equation*

$$u_t + s \cdot \nabla_x u = -\mu_* u + \mu_* \int_V K(s, s')u(s')ds' + f(\bar{u}). \tag{1.3}$$

However, equation (1.3) does not preserve positivity of $u$ in general. Particles can only be deleted from the velocity class in which they are. Modeling the reaction term as in (1.2) does not account for this fact since it does not keep track of the velocity classes. Schwetlick [59] studied reaction equations of the form

$$\frac{\partial}{\partial t}u(t, s) = f(u, \bar{u})(t, s). \tag{1.4}$$

In particular, for a birth-death process with density dependent mortality $g$ and fertility $m$, Hadeler [19] proposes the function

$$f(u, \bar{u}) = \frac{1}{|V|}m(\bar{u})\bar{u} - g(\bar{u})u.$$

If we reduce equation (1.1) to the simplest case where particles move on the line with constant speed, i.e. $n = 1$ and $V = \{\pm\gamma_*\}$, we obtain the following system of two equations

$$\begin{aligned} u_t^+ + \gamma_* u_x^+ &= -\frac{\mu_*}{2}(u^+ - u^-), \\ u_t^- - \gamma_* u_x^- &= -\frac{\mu_*}{2}(u^- - u^+), \end{aligned} \tag{1.5}$$

where $u^\pm(t, x) = u(t, x, \pm\gamma_*)$ denotes the density of right and left moving particles. This is the Goldstein-Kac model for the correlated random walk [31]. It preserves positivity for $u^\pm$ jointly. Introducing the total density $u(t, x) = u^+(t, x) + u^-(t, x)$ and $v(t, x) = u^+(t, x) - u^-(t, x)$ this system can be written as

$$\begin{aligned} u_t + \gamma_* v_x &= 0, \\ v_t + \gamma_* u_x &= -\mu_* v. \end{aligned} \tag{1.6}$$

Differentiating and substituting one can derive the following telegrapher's equation for the density $u$ alone:

$$u_{tt} + \mu_* u_t = \gamma_*^2 u_{xx}.$$

Dividing this equation by $\mu_*$ and letting $\mu_*, \gamma_* \to \infty$ with $\gamma_*^2/\mu_* = D = \text{const.}$ we formally get the diffusion equation

$$u_t = Du_{xx}. \tag{1.7}$$

This *parabolic limit* can also be obtained from (1.6) if we write $\tilde{v} = \gamma_* v$ for the flux and make the same limiting process in the second equation. Then

$$\begin{aligned} u_t + \tilde{v}_x &= 0, \\ D u_x &= -\tilde{v}. \end{aligned} \tag{1.8}$$

Holmes was the first to introduce reactions to (1.5) and realize that one can still derive a telegrapher's equation if the reaction depends only on the total density [29]. The system reads

$$\begin{aligned} u_t^+ + \gamma_* u_x^+ &= -\frac{\mu_*}{2}(u^+ - u^-) + \frac{1}{2} f(u), \\ u_t^- - \gamma_* u_x^- &= -\frac{\mu_*}{2}(u^- - u^+) + \frac{1}{2} f(u), \end{aligned} \tag{1.9}$$

and leads to the telegrapher's equation

$$u_{tt} + (\mu_* - f'(u)) u_t = \gamma_*^2 u_{xx} + \mu_* f(u).$$

Taking the same limit as above, i.e. $\mu_*, \gamma_* \to \infty$ with $\gamma_*^2/\mu_* = D = \text{const.}$, we formally get the reaction diffusion equation

$$u_t = D u_{xx} + f(u).$$

These limiting processes were made analytically precise and approximation theorems were derived by Hillen and Müller [26].

Equation (1.9) and several generalizations have been widely studied and used to model biological phenomena, including birth-death, activator-inhibitor, epidemic spread etc. Hadeler investigated existence and speed of traveling fronts [19], the application to disease models [20] and models for several species [21]. Hillen [22, 23, 24] introduced boundary conditions, proved existence results for mild and classical solutions and derived an invariance principle. He used energy methods and Lyapunov functionals. He also showed the existence of Turing patterns in a system of two species. In order to model movement depending on some external signal, the velocity $\gamma_*$ and the turning rate $\mu_*$ can be chosen to depend on this signal [27, 28]. A one dimensional free boundary value problem for (1.9) was studied by Kuttler [35].

In several space dimensions, equation (1.1) was applied to cell movement by Othmer et al. [46]. According to the underlying discrete stochastic model it was called a *velocity jump process*. Hadeler gave a detailed account of the relevance and applications of reaction transport equations in biological modeling [21]. He discussed in particular the connections between the diffusion equation, the transport equation and the Cattaneo system. Hillen and Othmer considered (1.1) with an additional external signal to study chemotaxis in $n$ dimensions and derived the classical parabolic chemotaxis equations as the parabolic limit [25]. A detailed mathematical analysis of (1.3) was done by Schwetlick [59, 60]. He generalized the approximation results about parabolic limits to higher dimensions and studied existence and minimal speeds for traveling fronts. Boundary conditions in higher dimensional domains were introduced and existence of mild solutions was shown. Regularity of stationary solutions was studied and also convergence to stationary solutions was shown under some assumptions on $f$.

## 1.4 Overview of the Results

The main goal of this work is to develop and investigate a mathematical model for moving polarized groups on the basis of reaction transport equations.

In Chapter 2 this is done in one space dimension assuming constant speed. Formally, the model equations look similar to (1.5) but the constant turning rate $\mu_*$ is replaced by a density dependent turning function $\mu = \mu(u^+, u^-)$. Interaction is purely local, i.e. the turning function depends pointwise on $u^{\pm}$.

The most important feature of the turning function is that it changes sign. The dispersion relation shows that the sign change of $\mu$ corresponds to a change in the stability behavior of the homogeneous equilibrium solution. Hence the sign change reflects the transition from dispersal to alignment and shows that random turning and alignment are two competing mechanisms.

Using the methods of characteristics, local existence of mild and classical solutions is shows and conditions for global existence are discussed. An invariance result is used to show that solutions exist globally and are bounded for the reasonable assumption that dispersal is stronger than alignment at high densities. Then, on a bounded interval with periodic boundary conditions, the bifurcation from the stationary state for increasing strength of alignment is investigated. This bifurcation is not a standard bifurcation since all eigenvalues cross the imaginary axis at the same parameter value. By introducing a viscosity term, this transition is split into a series of Hopf bifurcations.

Finally a predator-prey system is superimposed on the model equation. Analytically and by simulations it is shown that an aligning prey may survive where a non aligning prey would go extinct.

Then, in Chapter 3 the model is generalized to two space dimensions still assuming constant speed. It is investigated for a discrete set of velocities and some simulations are shown. Again, by using the method of characteristics, existence and uniqueness of solutions is shown. The model is compared to the alignment models cited and explained above. A general equation is presented which comprises all these models as special cases. From this equation one obtains an interpretation of individual behavior in the 2D model equation. The general equation also yields an interesting observation in the 1D case.

In the last chapter speed adaptation is included into the one-dimensional model. It is assumed that there is a *preferred density* and that individuals speed up or slow down in order to be in areas of preferred density. The resulting model consists of altogether four equations: a conservation law with source term for each of the densities and a parabolic or elliptic equation for the adaptation process of their respective speeds. The coupling between the equations is highly nonlinear.

For simplicity, the speed adaptation process is first studied in one direction only. There is one equation for the density and one for the speed. Linearization shows that the uniform density distribution is unstable as long as the density is below the preferred density. The model is regularized by introducing a viscosity term in the equation for the density. For the resulting parabolic or parabolic/elliptic system global existence of smooth solutions is shown. In the next step estimates for weak solutions are shown to hold independent of the viscosity parameter. Then,

by a compact imbedding theorem, one gets solutions for vanishing viscosity.

Finally it is shown that the vanishing viscosity method can be extended to the system of four equations for two directions and two speeds.

*It is my pleasure to acknowledge the support I got from so many people during the last three years. Even though I cannot mention all of them here, I them to know that I am very thankful for all the help and encouragement I received.*

*I am especially grateful to Prof. Dr. K.P. Hadeler. As my supervisor he chose the topic of this work and through his guidance and criticism helped me get along. I am thankful to all the members of the biomathematics group in Tübingen for valuable discussions and indispensable technical support. In particular I want to express my thanks to Thomas Hillen for patient explanations and encouragement.*

*I am grateful to all the participants and the staff at the IMA (Institute of Mathematics and its Applications) special program "Mathematics in Biology". In particular I want to thank Leah Edelstein-Keshet, Mark Lewis and Hans Weinberger for many fruitful discussions and their encouragement. The stay at the IMA in Minneapolis was supported by the DAAD (German Academic Exchange Service).*

*The work in Tübingen was supported by a position within the special program DANSE (Dynamics, Analysis, efficient Simulation and Ergodic Theory) from the DFG (German Research Council).*

# Chapter 2

# Alignment in 1 Dimension

We derive and analyze a model equation for alignment in one space dimension based on the random walk system (1.5) for constant particle speed. We get a system of equations similar to (1.5) but with non-linear density dependent turning function $\mu$ instead of the turning rate $\mu_*$. Having investigated some basic properties of the model we show existence of solutions, regularity and positivity. We discuss the question of global (in time) solutions.

The case of periodic boundary conditions on a bounded interval is given detailed attention. It is closely related to no flux boundary conditions and describes continued interaction between particle patches. A detailed linear analysis is performed and $\omega$-limit sets are characterized.

To discuss the benefit of alignment for survival of a population we superimpose a simple predator–prey model and show analytically and numerically that alignment can lead to survival of a population which would go extinct otherwise.

Since the particle speed is assumed constant throughout this chapter we simplify notation and write $\gamma = \gamma_*$.

## 2.1 A Simple Model in 1D

We derive the reaction term modeling alignment in one spatial dimension with two velocities $s \in \{\pm\gamma\}$ and denote the corresponding densities by $u^\pm$. We first discuss the desired features of an alignment system in the absence of motion. The general form of the reaction term is $\dot{u}^\pm = f^\pm(u^+, u^-)$. The alignment process is symmetric with respect to left and right and preserves total mass. Hence the system can be written in the following form

$$\begin{aligned} \dot{u}^+ &= f(u^+, u^-), \\ \dot{u}^- &= -f(u^+, u^-). \end{aligned} \tag{2.1}$$

The symmetry condition $f(u^+, u^-) = -f(u^-, u^+)$ has to be satisfied. In particular,

$$f(u/2, u/2) = 0 \quad \text{for} \quad u = u^+ + u^- \geq 0,$$

hence the state where both directions are equally distributed is stationary, no direction has an advantage over the other. The states $(u^+, 0)$ and $(0, u^-)$ represent

complete alignment, all particles have the same direction. These states should be stationary and hence we need

$$f(0,u^-) = f(u^+,0) = 0 \quad \text{for} \quad u^\pm \geq 0.$$

This condition also implies preservation of positivity. Furthermore we require that these two stationary states are stable. Of course we cannot achieve stability against a change in total number of particles. We can only require stability against changes in the relative size of the two groups. This stability is expressed as

$$D_1 f(u^+,0) < D_2 f(u^+,0), \quad D_1 f(0,u^-) < D_2 f(0,u^-) \quad \text{for} \quad u^\pm \geq 0$$

where $D_j$ denotes the partial derivative with respect to the $j$-th variable. We write $f$ in the form

$$f(u^+,u^-) = f_1(u) f_2(p), \quad p = u^+/u, \quad u = u^+ + u^-.$$

Then $f_2$, which depends on the relative density of right moving particles, models the qualitative behavior and $f_1$ is a positive function which depends only on the total density. The assumptions about stationary states translate into

$$f_2(0) = f_2(1) = 0, \quad f_2(1/2) = 0,$$

and the stability conditions give

$$f_2'(0) < 0, \quad f_2'(1/2) > 0, \quad f_2'(1) < 0.$$

Given that there are no other stationary states we find

$$f_2(p) < 0 \quad \text{for} \quad 0 < p < 1/2; \quad f_2(p) > 0 \quad \text{for} \quad 1/2 < p < 1.$$

An obvious candidate is

$$f_2(p) = p(1-p)(p-1/2).$$

With this choice (2.1) becomes

$$\begin{aligned} \dot{u}^+ &= \frac{f_1(u)}{u^3} u^+ u^- (u^+ - u^-), \\ \dot{u}^- &= \frac{f_1(u)}{u^3} u^+ u^- (u^- - u^+). \end{aligned} \tag{2.2}$$

We call $a(u) = f_1(u)/u^3$ and discuss possible choices of $a$ and hence of $f_1$ later. We introduce the space variable and insert the reaction term (2.2) into the correlated random walk model to the to arrive at

$$\begin{aligned} u_t^+ + \gamma u_x^+ &= \frac{\mu_*}{2}(u^- - u^+) + a(u) u^+ u^- (u^+ - u^-), \\ u_t^- - \gamma u_x^- &= \frac{\mu_*}{2}(u^+ - u^-) + a(u) u^+ u^- (u^- - u^+), \end{aligned} \tag{2.3}$$

where $a > 0$. To get a proper Cauchy problem we have to specify initial conditions

$$u^\pm(0,x) = u_0^\pm(x), \qquad x \in \Omega \subset \mathbb{R}, \tag{2.4}$$

and boundary conditions, which will be done below 2.1.2. The system can be written in the equivalent form

$$\begin{aligned} u_t + \gamma v_x &= 0, \\ v_t + \gamma u_x &= -\mu_* v + \frac{a(u)}{2}(u^2 - v^2)v, \end{aligned} \tag{2.5}$$

with total mass $u = u^+ + u^-$ as above and $v = (u^+ - u^-)$.

One cannot get a proper diffusion limit from system (2.5) as it was possible from system (1.6). Nonetheless it is interesting to consider formally the limit process $\gamma, \mu_* \to \infty$. The second equation of (2.5) written in terms of the flux $\tilde{v} = \gamma v$ reads

$$\tilde{v}_t + \gamma^2 u_x = -\mu_* \tilde{v} + \frac{a(u)}{2}(u^2 - \frac{\tilde{v}^2}{\gamma^2})\tilde{v}.$$

If we assume that the alignment process scales with $\mu_*$, i.e. $a(u) = \mu_* \bar{a}(u)$, then for $\gamma, \mu_* \to \infty$ with $\gamma^2/\mu_* = D$ we get

$$D u_x = \left( \frac{\bar{a}(u)}{2} u^2 - 1 \right) \tilde{v}, \tag{2.6}$$

which for $a = 0$ is (1.8). The expression in brackets changes sign in general. But the minus sign on the right hand side of (1.8) is essential to get the diffusion equation instead of backward diffusion. Formally, backward diffusion can produce aggregation and hence we expect pattern formation in the hyperbolic model, too.

Looking at the literature about aggregation phenomena one finds many approaches which lead to ill-posed problems and are then regularized by different techniques. For example, a thorough discussion of model derivation which leads to ill-posed problems is given in [5, 38]. Possible regularization techniques are discretization [38, 47], inclusion of higher order terms as in the Cahn-Hilliard equations [7] or integral formulations [2], to name but a few.

According to the sign change in (2.6) we say that the model (2.3) or (2.5) has a "diffusive character" if the sign of the factor

$$-\mu_* + \frac{a(u)}{2}(u^2 - v^2) \tag{2.7}$$

in front of $v$ in (2.5) is negative. The following generalization of (2.3) gives better insight into the process.

All terms on the right hand side of (2.3) contain the factor $(u^+ - u^-)$. We introduce a density dependent turning function $\mu(u^+, u^-)$ and write

$$\begin{aligned} u_t^+ + \gamma u_x^+ &= \mu(u^+, u^-)(u^+ - u^-), \\ u_t^- - \gamma u_x^- &= \mu(u^+, u^-)(u^- - u^+), \end{aligned} \tag{2.8}$$

which becomes (2.3) for $\mu(u^+, u^-) = a(u)u^+u^- - \mu_*/2$. Now it is clear what happens. Particles turn randomly according to the turning rate $\mu_*$. The alignment process enters the equations with opposite sign ($a > 0$). We call $a(u)u^+u^-$ the *alignment rate*. If it is small compared to $\mu_*$, then particles turn from the direction of higher density to the direction of lower density. But if the aligning forces are strong enough, then particles turn into the direction which already carries more particles. What we observe is the competition of two processes. A diffusive character is given if random turning is stronger than alignment, i.e. $\mu(u^+, u^-) < 0$.

### 2.1.1 Basic Properties of the model

Before we show existence of solutions to (2.8) we look at some properties of (2.3) which indicate that it is a reasonable model for alignment.

We give a heuristic argument why (2.3) should preserve positivity. Suppose that smooth solutions are positive until $t_0$ and at $(t_0, x_0)$ the density $u^+$ has a minimum with $u^+(t_0, x_0) = 0$. Then at $(t_0, x_0)$ we find

$$u_t^+ = \frac{\mu_*}{2} u^- > 0$$

and hence $u^+$ increases. This idea will be made mathematically precise and generalized to (2.8) in Lemma 2.2.3.

From the first equation of (2.5) it is obvious that the total mass $\int u = \int u^+ + u^-$ is conserved. This makes sense biologically.

#### Dispersion Relation

The homogeneous state where both directions are equally distributed is described by $u^+ = u^- = \text{const}$. It corresponds to constant solutions $\bar{u} > 0$, $\bar{v} = 0$ of system (2.5). Looking at the dispersion relation of the corresponding linear system we see that there are unstable modes provided that the random turning rate is small. The linearization of (2.5) is

$$\begin{aligned} u_t + \gamma v_x &= 0, \\ v_t + \gamma u_x &= [(a/2)\bar{u}^2 - \mu_*]v. \end{aligned}$$

The ansatz $u(t,x) = e^{\lambda t}U(x), v(t,x) = e^{\lambda t}V(x)$ gives

$$\begin{aligned} \lambda U + \gamma V_x &= 0, \\ \lambda V + \gamma U_x &= [(a/2)\bar{u}^2 - \mu_*]V, \end{aligned}$$

which can be reduced to the single equation

$$-\gamma^2 U_{xx} = ((a/2)\bar{u}^2 - \mu_* - \lambda)\lambda U.$$

Assuming that $U$ is a linear combination of exponentials $e^{ikx}$ for different $k$ we get the dispersion relation from the quadratic equation for $\lambda$ :

$$\lambda((a/2)\bar{u}^2 - \mu_* - \lambda) = \gamma^2 k^2.$$

The solutions are

$$\lambda_{1,2} = \left(\frac{a}{4}\bar{u}^2 - \frac{\mu_*}{2}\right) \pm \frac{1}{2}\sqrt{((a/2)\bar{u}^2 - \mu_*)^2 - 4\gamma^2 k^2}.$$

For small modes $k$, the discriminant is positive, for large $k$ it is negative. In both cases the sign of the real part $\Re\lambda$ is determined by the sign of the first term $a\bar{u}^2/4 - \mu_*/2$.

For large $\mu_*$ all modes are stable, and they become unstable all at the same value $\mu_* = a\bar{u}^2/2$. For smaller values of $\mu_*$ all modes are unstable. This transition is certainly *not* a standard bifurcation. It will appear again later where we investigate it more closely by adding a viscosity term (see 2.3.3). It can also be observed in

the telegrapher's equation when the damping term changes sign and becomes a forcing term [22]. There are other mathematical models in biology which have an infinite range of unstable wave numbers, e.g. mechanical models for mesenchymal morphogenesis [43]. The parameter $\mu_*$ is a measure of randomness in turning in the model. If it is small enough then the homogeneous situation is unstable. A similar behavior is found in the models by Geigant et al. [14] and by Edelstein-Keshet et al. [10, 40], although there only finitely many modes become unstable.

**Perfect Schools**

The case of complete alignment would appear as a solution where all individuals move in the same direction. The density in the other direction is zero. Evidently such a solution can exist only if $\mu_* = 0$. In that case initial data $u_0^+(x)$ together with $u_0^-(x) = 0$ lead to unidirectional schools in form of a simple wave

$$u^+(t,x) = u_0(x - \gamma t), \qquad u^-(t,x) = 0. \tag{2.9}$$

If $u_0^+$ is not smooth then we can interpret (2.9) as a weak solution (in the sense of conservation laws). The particular case where $u_0^+$ is the characteristic function of some interval is called a *perfect school* since the density within the school is uniform and the edges are sharp.

Somewhat more interesting is the case that two perfect schools of the same height move in opposite directions. Then even when the two schools meet neither direction has an advantage over the other and the net effect of interaction should be zero. The schools should move on unchanged. Consider the equations on the real line and denote by $u^\pm(t,x) = u_0^\pm(x \mp \gamma t)$ two perfect schools with $u_0^\pm = \chi_{I^\pm}$ for intervals $I^\pm$. We have to show that

$$\int_0^\infty \int_{-\infty}^\infty u^\pm \phi_t \pm \gamma u^\pm \phi_x = \int_0^\infty \int_{-\infty}^\infty \mp a(u) u^+ u^- (u^+ - u^-)\phi - \int_{-\infty}^\infty u_0^\pm \phi$$

for all test functions $\phi \in \mathcal{C}^1(\mathbb{R}^2)$ with compact support in $[0,\infty) \times \mathbb{R}$. If $u^+$ or $u^-$ vanishes, then the product $u^+u^-$ vanishes. But wherever both densities are nonzero they are the same and hence the difference $u^+ - u^-$ vanishes. Hence the first term on the right hand side is zero. The remaining equations for $u^\pm$ decouple and are just the weak formulation for left and right moving waves. They are obviously satisfied.

### 2.1.2 Boundary Conditions

We introduce boundary conditions and investigate their influence on the behavior of solutions. Of course the 1D problem is a model problem for the more realistic 2D or even 3D case. However, the 1D boundary conditions may appear somewhat artificial. Dirichlet boundary conditions say that particles are absorbed at the boundary (homogeneous) or released at the boundary, always directed inward with respect to the domain (inhomogeneous). Homogeneous Neumann boundary conditions describe the situation where individuals turn around at the boundary. If we identify the two endpoints of the interval we get a circle and speak of periodic boundary conditions.

For inhomogeneous Dirichlet boundary conditions stationary solutions can be calculated explicitly. Solutions in the case of homogeneous Neumann boundary

conditions are a subset of solutions of the case of periodic boundary conditions, defined by a certain symmetry condition.

Boundary conditions for reaction random walk systems on the interval $[0, l]$ have been discussed by Hillen [22]. They are as follows.

- $u^+(t,0) = 0$, $u^-(t,l) = 0$ in the homogeneous Dirichlet case,
- $u^+(t,x) = u^-(t,x)$ for $x \in \{0,l\}$ in the homogeneous Neumann case,
- $u^\pm(t,0) = u^\pm(t,l)$ in the periodic case.

In the $u,v$-notation this can be expressed as

- $u(t,0) = -v(t,0)$, $u(t,l) = v(t,l)$ in the homogeneous Dirichlet case,
- $v(t,x) = 0$ for $x \in \{0,l\}$ in the homogeneous Neumann case,
- $u(t,0) = u(t,l)$, $v(t,0) = v(t,l)$ in the periodic case.

The system has the general form

$$\begin{aligned} u_t + \gamma v_x &= 0, \\ v_t + \gamma u_x &= g(u,v), \end{aligned} \tag{2.10}$$

with some function $g$. Regardless of the boundary conditions we can make the following observation about stationary solutions.

LEMMA 2.1.1
*Stationary solutions of (2.10) are constant in $v$ and monotone in $u$.*

PROOF.
The first equation gives $v_x = 0$, i.e. $v$ is a constant at a stationary solution. Then the second equation becomes a one dimensional ordinary differential equation $u_x = f_v(u)$ with parameter $v$. ∎

### The Dirichlet Problem

We consider stationary solutions of the inhomogeneous Dirichlet problem without random turning, i.e. system (2.10) with the reaction term from (2.5):

$$g(u,v) = a/2(u^2 - v^2)v \tag{2.11}$$

for $a = \text{const.}$, and the following conditions on the left and right boundary of the interval $[0,l]$,

$$u^+(0) = u_l^+, \quad u^-(l) = u_r^-.$$

At a stationary solution, $v$ is a constant by Lemma 2.1.1 and the boundary condition for $u = u^+ + u^-$ assumes the form

$$u(0) = 2u_l^+ - v, \quad u(l) = 2u_r^- + v.$$

The second equation of (2.10) yields a Riccati equation for $u$,

$$u_x = \frac{av}{\gamma}(u^2 - v^2),$$

and thus by integration we get

$$\frac{u-v}{u+v} = \frac{u(0)-v}{u(0)+v} e^{(2av^2/\gamma)x} = \frac{u_l^+ - v}{u_l^+} e^{(2av^2/\gamma)x}.$$

Using the boundary conditions, we find a transcendental equation for $v$:

$$\frac{(u_l^+ - v)(u_r^- + v)}{u_l^+ u_r^-} = e^{-(2av^2/\gamma)l}.$$

The left hand side of this equation describes a parabola which passes through the point $(0,1)$. The bell shaped curve on the right has its maximum at $(0,1)$. Hence we always have the trivial solution $v = 0$, $u^+ = u^- = \text{const}$. We discuss the case $u_l^+ > u_r^-$, the other case is obtained by symmetry. There is always a nontrivial positive solution for $v$. If the curvature of the bell shaped curve at $(0,1)$ is large enough, then there are also two negative solutions for $v$ (compare the two plots below).

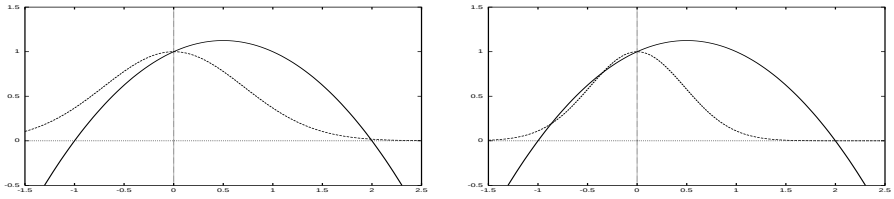

The solution corresponding to a given $v$ can be represented as

$$u^+(x) = \frac{v u_l^+}{u_l^+ - (u_l^+ - v)e^{(2av^2/\gamma)x}}, \qquad u^-(x) = u^+(x) - v.$$

This solution is monotonically increasing if $v > 0$ and monotonically decreasing if $v < 0$. The situation in case $v > 0$ is clear: There are more $u^+$-particles coming in at the left boundary than $u^-$-particles at the right boundary. On their way through the interval the predominance of $u^+$ makes $u^-$-particles turn around and align. Increasing the length of the interval leads to increasing $v$ which in turn leads to decreasing the number of $u^-$-particles that arrive at the left boundary.

For sufficiently large intervals the curvature of the bell shaped curve at 0 is large enough such that there appear negative solutions for $v$. Hence we have $u^- > u^+$ throughout the interval even though the supply of $u^-$-particles at the right boundary is less than the supply of $u^+$-particles at the left boundary. It is hard to imagine that such a solution can bifurcate from a homogeneous equilibrium. But assume that initially particles come in only on the right, i.e. $u_r^- > 0, u_l^+ = 0$. Now particles start to move in from the left. They will be turned and aligned by the dominance of the left moving direction. Once this dominance has been established, it is not broken if the influx of $u^+$-particles at the left boundary is increased continuously.

We conjecture that the stationary solution with $v > 0$ is stable and the one with $v = 0$ is unstable. From the two solutions with negative $v$ one should be unstable and the other should be stable.

### Homogeneous Neumann Boundary Conditions

Because of the reflection at the boundary, homogeneous Neumann boundary conditions play a similar role as the $\mu_*$-term: they act against complete alignment. Near the boundary there will always be particles in opposite directions which are then again subject to alignment. Thus we have the case that the two stationary solutions $(u^+, 0)$ and $(0, u^-)$ of the reaction differential equation are not compatible with the boundary condition. As a consequence of Lemma 2.1.1 we note the following.

COROLLARY 2.1.2
*The stationary states of (2.8) with homogeneous Neumann boundary conditions necessarily satisfy $v = 0$ and hence are of the form $u^+ = u^- = \text{const}$.*

These stationary solutions are unstable for small $\mu_*$. We expect oscillating behavior. Computer simulations show the following: One starts with $u^+ \equiv u^- \equiv 1$ and adds a small perturbation on $u^+$, for example a narrow pulse. Then this pulse travels to the right gaining in height constantly but the width of course remains unchanged. At the boundary the pulse turns and continues to gain height while the density of the other direction decreases.

Solutions for homogeneous Neumann boundary conditions are not studied explicitly because they are a subset of solutions for periodic boundary conditions.

### Periodic Boundary Conditions

The case of periodic boundary conditions may be thought of as particles moving on a circle. A detailed qualitative study of this case is done in Section 2.3. Here we only show the connection between homogeneous Neumann and periodic boundary conditions.

We say that two functions $u^+, u^-$ on $\Omega = [0, l]$ satisfy the *mirror symmetry condition* on $\Omega$ if

$$u^+(x) = u^-(l - x) \quad \text{for} \quad x \in \Omega. \tag{2.12}$$

LEMMA 2.1.3
*Suppose the initial data $u_0^\pm$ on $\Omega$ satisfy the mirror symmetry condition (2.12). Then this symmetry is preserved under the flow generated by (2.3) with periodic boundary conditions.*

PROOF.
Let $u_0^+$ be given and set $u_0^-(x) = u_0^+(l - x)$ according to (2.12). Then in particular $u_0^+(l/2) = u_0^-(l/2)$ and we can solve the Neumann problem on $[0, l/2]$. Let $w^\pm$ denote the solutions to the homogeneous Neumann problem. We now set

$$u^\pm(t, x) = \begin{cases} w^\pm(t, x) & \text{for} \quad x \in [0, l/2] \\ w^\mp(t, l - x) & \text{for} \quad x \in [l/2, l]. \end{cases}$$

Then straightforward computations show that $u^\pm$ satisfies the differential equations on $\Omega$ as well as the periodic boundary conditions. Uniqueness of solutions (which will be shown along with existence in Section 2.2) now gives the desired result. ∎

COROLLARY 2.1.4
*Solutions to the homogeneous Neumann problem on* $[0, l/2]$ *are in 1 to 1 correspondence with solutions on* $[0, l]$ *with periodic boundary conditions which are symmetric in the sense of (2.12).*

PROOF.
Suppose initial conditions $w_0^{\pm}$ are given on $[0, l/2]$ which satisfy the homogeneous Neumann boundary condition $w_0^{\pm}(x) = w_0^{\mp}(x)$ for $x \in \{0, l/2\}$. Set

$$u_0^{\pm}(x) = \begin{cases} w_0^{\pm}(x) & \text{for} \quad x \in [0, l/2] \\ w_0^{\mp}(l-x) & \text{for} \quad x \in [l/2, l]. \end{cases} \tag{2.13}$$

Then $u_0^{\pm}$ define initial conditions to a periodic boundary problem and satisfy (2.12). Since this symmetry is conserved by the theorem we simply restrict the solutions $u^{\pm}$ to $[0, l/2]$ to get a solution to the homogeneous Neumann problem. Uniqueness of solutions is shown in the next section. ■

## 2.2 Existence of Solutions

We show existence and uniqueness of solutions for the general system (2.8) under mild conditions for the turning function $\mu(u^+, u^-)$. We then discuss positivity and regularity of solutions. We suggest several different alignment rates which are biologically meaningful and ensure global existence of solutions.
First we consider the case $\Omega = \mathbb{R}$. System (2.8) has the characteristic equations

$$\dot{t} = 1, \quad \dot{x} = \pm\gamma \quad \text{and} \quad \dot{u}^{\pm} = \pm\mu(u^+, u^-)(u^+ - u^-).$$

We can integrate the last equations along the characteristics $x \pm \gamma t = \text{const.}$ and obtain

$$u^{\pm}(z) = u_0^{\pm} \pm \int_{z_0}^{z} \mu(u^+, u^-)(u^+ - u^-)(y)dy. \tag{2.14}$$

A pair of functions $(u^+, u^-) \in L^{\infty}([0, T) \times \mathbb{R})^2$ is called a *mild solution* if (2.14) is satisfied.

THEOREM 2.2.1
*Suppose* $\mu : \mathbb{R}^2 \to \mathbb{R}$ *is locally Lipschitz continuous. Then for all initial data* $(u_0^+, u_0^-) \in (L^{\infty} \cap L^1)(\mathbb{R})^2$ *there exists a unique mild solution*

$$(u^+, u^-) \in L^{\infty}\left([0, T), (L^{\infty} \cap L^1)(\mathbb{R})^2\right)$$

*of (2.8) for some* $T > 0$ *which satisfy the initial conditions* $u^{\pm}(0) = u_0^{\pm}$.

PROOF.
We introduce the following notations

$$\begin{array}{lll} \tilde{Y} := (L^{\infty} \cap L^1)(\mathbb{R}) & \text{with norm} & \|u\|_{\tilde{Y}} = \|u\|_{L^{\infty}} + \|u\|_{L^1} \\ Y := L^{\infty}([0, t_0), \tilde{Y}) & \text{with norm} & \|u\|_Y = \sup_{0 \le t < t_0} \|u(t, \cdot)\|_{\tilde{Y}} \\ \\ X := Y \times Y & \text{with norm} & \|(u^+, u^-)\|_X = \max(\|u^+\|_Y, \|u^-\|_Y). \end{array}$$

Choose initial data $u_0^{\pm} \in \tilde{Y}$. For all $w^{\pm} \in Y$ with $w^{\pm}(0,\cdot) = u_0^{\pm}$ the initial value problem

$$\begin{aligned} u_t^+ + \gamma u_x^+ &= \mu(w^+, w^-)(w^+ - w^-), \\ u_t^- - \gamma u_x^- &= \mu(w^+, w^-)(w^- - w^+), \\ u^{\pm}(0,\cdot) &= u_0^{\pm}, \end{aligned}$$

can be solved along the characteristics $x \pm \gamma t = \text{const.}$ with the new variable $z = z_0 \pm \gamma t$.
We define the operator $\mathcal{G} \colon = (\mathcal{G}_1, \mathcal{G}_2) \colon X \to X$ by (2.14):

$$\mathcal{G}_1(w^+, w^-)(z) \colon = u^+(z) = u_0^+(z_0) + \frac{1}{\gamma} \int_{z_0}^{z} \mu(w^+, w^-)(w^+ - w^-)(y)dy$$

and $\mathcal{G}_2(w^+, w^-) \colon = u^-$ analogously.
We estimate the norm of $\mathcal{G}$ for small times $t_0$. Choose $k_0$ such that $\|u_0^{\pm}\|_{\tilde{Y}} \leq k_0$, and $N > k_0 + \varepsilon$ for some $\varepsilon > 0$. Then for $(w^+, w^-) \in B(N, X)$ we find

$$\|\mathcal{G}_1(w^+, w^-)\|_Y \leq k_0 + \frac{1}{\gamma} \sup_{B(N,\mathbb{R}^2)} (\mu)|z - z_0| \left(\|w^+\|_Y + \|w^-\|_Y\right).$$

We get the estimate

$$\|\mathcal{G}(w^+, w^-)\|_X \leq k_0 + 2t_0 N \sup_{B(N,\mathbb{R}^2)} (\mu).$$

Choosing $t_0$ small enough, i.e.

$$t_0 < \frac{\varepsilon}{2N \sup_{B(N,\mathbb{R}^2)}(\mu)},$$

gives

$$k_0 + 2t_0 N \sup_{B(N,\mathbb{R}^2)} (\mu) \ < \ -\varepsilon + N + 2t_0 N \sup_{B(N,\mathbb{R}^2)} (\mu) \ < \ N$$

and hence $\mathcal{G}$ maps $B(N, X)$ into itself. Finally we show the contraction property. Choose $(w^+, w^-), (\tilde{w}^+, \tilde{w}^-) \in B(N, X)$. Then

$$\begin{aligned} & \|\mathcal{G}(w^+, w^-) - \mathcal{G}(\tilde{w}^+, \tilde{w}^-)\|_X \\ = \ & \left\| \frac{1}{\gamma} \int_{z_0}^{z} \left[\mu(w^+, w^-)(w^+ - w^-) - \mu(\tilde{w}^+, \tilde{w}^-)(\tilde{w}^+ - \tilde{w}^-)\right](y)dy \right\|_Y \\ = \ & \left\| \frac{1}{2\gamma} \int_{z_0}^{z} (\mu(w^+, w^-) + \mu(\tilde{w}^+, \tilde{w}^-))(w^+ - \tilde{w}^+ + \tilde{w}^- - w^-)(y)dy \right\|_Y \\ & + \left\| \frac{1}{2\gamma} \int_{z_0}^{z} (\mu(w^+, w^-) - \mu(\tilde{w}^+, \tilde{w}^-))(w^+ + \tilde{w}^+ - w^- - \tilde{w}^-)(y)dy \right\|_Y \\ \leq \ & t_0 \left[ \sup_{B(N,\mathbb{R}^2)} (\mu) + NLip(\mu, N) \right] \|w^{\pm} - \tilde{w}^{\pm}\|_X, \end{aligned}$$

where $Lip(\mu, N)$ is the Lipschitz constant of $\mu$ on $B(N, \mathbb{R}^2)$. Hence we get a contraction for

$$t_0 < \frac{1}{\sup_{B(N,\mathbb{R}^2)}(\mu) + NLip(\mu, N)}.$$

If we choose $T$ such that it satisfies both the conditions for $t_0$ above, then the operator $\mathcal{G}$ has a unique fixed point which by construction is the solution to the system of equations. ∎

Remark

1. For a nonnegative solution $(u^+, u^-)$ the integral $\int u^+ + u^- dx$ is the total mass of particles. From the first equation of (2.5) it follows that the total mass is conserved as long as $u^+ - u^- = v \to 0$ for $|x| \to \infty$. If the initial data have compact support, then this condition is certainly satisfied. In the proof above we showed that if the initial data are merely integrable then solutions are also integrable and hence the total mass is conserved also in this case.

2. An explicit representation of solutions to (1.5) in terms of Bessel functions is given by Hadeler [21]. Discontinuities of the initial data are transported only along characteristics (compare also Reed [56]) and solutions are as smooth as the initial data. The proof of Theorem 2.2.1 can be modified to show that if the initial data are in $\mathcal{C}_b^k(\mathbb{R})$ and if $\mu$ has Lipschitz continuous derivatives up to order $k$ then solutions of (2.8) exist locally and are $n$ times continuously differentiable.

Now we use Theorem 2.2.1 in order to prove existence of solutions for $\Omega = [0, l]$ with either periodic or homogeneous Neumann boundary conditions. A mild solution is defined by (2.14) via restriction and has to satisfy the respective boundary conditions.

Theorem 2.2.2
*Let $\Omega$ as above and $\mu\colon \mathbb{R}^2 \to \mathbb{R}$ be locally Lipschitz continuous. Then for all initial data $u_0^\pm \in L^\infty(\Omega)$ there exists a unique mild solution*

$$(u^+, u^-) \in L^\infty\left([0, T) \times \Omega\right)^2$$

*of (2.8) for some $T > 0$.*

Proof.
By Corollary 2.1.4 it suffices to prove the claim for periodic boundary conditions. Let $\hat{u}_0^\pm(x) = u_0^\pm(x \bmod l), x \in \mathbb{R}$ be the periodic continuation of the initial data to $\mathbb{R}$. The proof of Theorem 2.2.1 with $\tilde{Y} = L^\infty(\mathbb{R})$ instead of $\tilde{Y} = (L^\infty \cap L^1)(\mathbb{R})$ gives a unique solution $(u^+, u^-) \in L^\infty([0, T) \times \mathbb{R})$ for some time $T > 0$. We claim that this solution is periodic with period $l$. Hence it can be restricted to $\Omega$ with periodic boundary conditions. Uniqueness of solutions on $\mathbb{R}$ implies uniqueness of solutions on $\Omega$ by continuation. In order to see that solutions on $\mathbb{R}$ remain periodic, set $w^\pm(t, x) = \hat{u}^\pm(t, x + l)$. Then

$$\begin{aligned}(w_t^+ + \gamma w_x^+)_{|(t,x)} &= (\hat{u}_t^+ + \gamma \hat{u}_x^+)_{|(t,x+l)} = \mu(\hat{u}^+, \hat{u}^-)(\hat{u}^+ - \hat{u}^-)_{|(t,x+l)} \\ &= \mu(w^+, w^-)(w^+ - w^-)_{|(t,x)}\end{aligned}$$

and similarly for $w^-$. Hence, the functions $w^\pm$ satisfy (2.8) with initial data $w^\pm(0, x) = \hat{u}^\pm(0, x + l) = \hat{u}_0^\pm(x)$. By uniqueness then $w^\pm = \hat{u}^\pm$. ∎

If the initial data $u_0^\pm$ are in $\mathcal{C}^k(\Omega)$ and satisfy the following compatibility conditions at the boundary

$$\frac{\partial^j}{\partial x^j} u_0^\pm(0) = \frac{\partial^j}{\partial x^j} u_0^\pm(l), \qquad 1 \le j \le k,$$

then the periodic continuation of $u_0^\pm$ gives functions $\hat{u}_0^\pm \in \mathcal{C}_b^k(\mathbb{R})$. By the remark above, we then get solutions of (2.8) which are $k$-times continuously differentiable and can be restricted to $\Omega$ with periodic boundary conditions. For homogeneous Neumann boundary conditions the compatibility conditions for derivatives are

$$\frac{\partial^j}{\partial x^j} u_0^+(0) = (-1)^j \frac{\partial^j}{\partial x^j} u_0^-(0), \quad \frac{\partial^j}{\partial x^j} u_0^+(l) = (-1)^j \frac{\partial^j}{\partial x^j} u_0^-(l), \quad 1 \le j \le k.$$

LEMMA 2.2.3
*Suppose the turning function $\mu \in \mathcal{C}^{1,1}$ satisfies*

$$\mu(u^+, 0) \le 0, \qquad \mu(0, u^-) \le 0. \tag{2.15}$$

*Then for nonnegative initial data $u_0^\pm \in \mathcal{C}_b^1(\mathbb{R})$ solutions stay nonnegative as long as they exist in $\mathcal{C}^1$. If nonnegative initial data on a bounded interval with periodic or homogeneous Neumann boundary conditions are continuously differentiable and satisfy the boundary conditions together with their derivatives, then solutions stay nonnegative as long as they exist in $\mathcal{C}^1$. Condition (2.15) is in particular satisfied for $\mu(u^+, u^-) = a(u)u^+u^- - \mu_*/2$.*

PROOF.
It suffices to prove the first claim. By assumption, solutions are continuously differentiable for some positive time. Then along the characteristics, they satisfy the characteristic equations

$$\dot{u}^\pm = \pm\mu(u^+, u^-)(u^+ - u^-).$$

The right hand side is locally Lipschitz continuous. If $u^+ = 0$ then $\dot{u}^+ \ge 0$ by (2.15) and hence $u^+$ cannot become negative along characteristics. A similar argument applies to $u^-$. ∎

### 2.2.1 Global Existence

We now examine under which conditions solutions exist globally in time. First we show some numerical evidence that finite time blow-up may occur depending on the alignment rate. Then we reconsider the reaction differential equation (2.1) and discuss conditions on the function $a$ in (2.3) which are biologically meaningful and ensure global existence of solutions.

Reflection of particles at a boundary with Neumann conditions interferes with the alignment process. We exploit this fact to numerically produce arbitrarily fast growing solutions. Using Corollary 2.1.4, we impose periodic boundary conditions on $\Omega = [0, 1]$ and choose initial data $u_0^\pm(x) = \pm 1/2 \sin(2\pi x) + 1/2$ which satisfy the mirror symmetry condition (2.12). The parameters are $a = 1, \gamma = 1$ and $\mu_* = 0$. Since the symmetry between $u^+$ and $u^-$ is preserved, we only show the profile of $u^+$. We plot the density every time a rotation is completed.

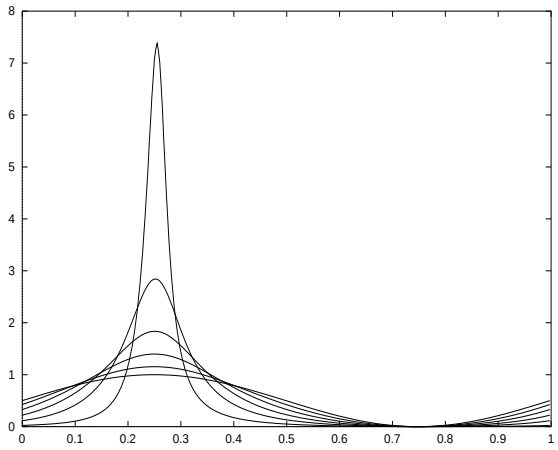


We observe the following: The initial function is the one with the lowest maximum. Each time the two peaks for $u^+$ and $u^-$ interact they become higher and narrower. After 5 rotations the gradients become so steep that the numerical scheme produces negative values. Simulations on finer grids show the same behavior.

Going back to the biological interpretation, we see that for $a = \text{const.}$ the alignment rate grows with the density. It is clear that this may lead to arbitrarily high densities. Biological observations show that in reality the tendency to align decreases at high densities. Individuals even try to move away from others when the density becomes too high. We consider a few different cases.

**Homogeneous Reaction Term**

Still assuming $\mu_* = 0$ and going back to the derivation of the model (2.2), we recall that the function $a(u)$ contains a factor $1/u^3$. If we set $a(u) = 1/u^3$ then the right hand side of (2.8) is homogeneous of degree 0 but non-constant and hence cannot be continuous at $(0, 0)$. Therefore we set

$$a(u) = \frac{a_*}{1 + u^3}, \qquad a_* > 0, \tag{2.16}$$

and thereby preserve the important feature that $a \to 0$ as $u \to \infty$. For small $u^\pm$ (2.16) is close to the constant $a_*$ and for large $u^\pm$ it is close to the homogeneous case.

Lemma 2.2.4
*Suppose the turning function $\mu$ is locally Lipschitz and chosen such that the right hand side of system (2.8) is bounded. Then for initial data $u_0^\pm \in L^\infty(\mathbb{R})$ the solution exists globally in time. This argument applies in particular to the choice of $\mu$ as in (2.16).*

Proof.
By assumption we have $|\mu(u^+, u^-)(u^+ - u^-)| \le M$ for some $M > 0$ and all $u^\pm$. Then along the characteristics we have

$$\begin{aligned} |u^\pm(t,x)| &\le |u_0^\pm(x - \gamma t)| + \int_0^t |\mu(u^+, u^-)(u^+ - u^-)(\tau, x \mp \gamma\tau)| d\tau \\ &\le |u_0^\pm(x - \gamma t)| + Mt. \end{aligned}$$

Hence the norm of solutions grows at most linearly with $t$. According to Theorem 2.2.1 we can continue the solution for all times. ∎

**Homogeneous Alignment Rate**

Next we consider an alignment rate which is homogeneous of degree zero. We choose

$$a(u) = a_*/u^2, \quad a_* > 0. \tag{2.17}$$

With this choice the function $\mu$ is bounded on $\mathbb{R}^2\backslash\{0\}$ and the right hand side of system (2.8) is locally Lipschitz.

COROLLARY 2.2.5
*Suppose the turning function $\mu$ is bounded and the right hand side of (2.8) is locally Lipschitz continuous. Then the $L^\infty$-norm of solutions grows at most exponentially in time and hence solutions exist globally. This argument applies in particular to the choice of $\mu$ as in (2.17).*

PROOF.
By assumption we have $|\mu(u^+, u^-)| \leq M$ for some $M > 0$ and all $u^\pm$. Then

$$\begin{aligned} |u^\pm(t,x)| &\leq |u_0^\pm(x-\gamma t)| + \int_0^t |\mu(u^+,u^-)(u^+-u^-)(\tau, x \mp \gamma(t-\tau))| d\tau \\ &\leq |u_0^\pm(x-\gamma t)| + M\int_0^t (|u^+|+|u^-|)(\tau, x-\gamma(t-\tau)) d\tau. \end{aligned}$$

Adding the two equations for $u^+$ and $u^-$ we get the estimate

$$\|u^+(t)\| + \|u^-(t)\| \leq \|u_0^+\| + \|u_0^-\| + 2M\int_0^t (\|u^+(\tau)\| + \|u^-(\tau)\|) d\tau.$$

Hence again with Gronwall's Lemma we see

$$\|u^+(t)\| + \|u^-(t)\| \leq (\|u_0^+\| + \|u_0^-\|) e^{2Mt},$$

which completes the proof. ∎

Numerical simulations show the contrast to the previous situation. The parameters are the same as above except that now $a(u) = 1/(1+u^3)$ for the left figure and $a(u) = 1/u^2$ for the right figure. The solution is plotted every time 5 rotations were completed. Note also the different scales on the vertical axis.

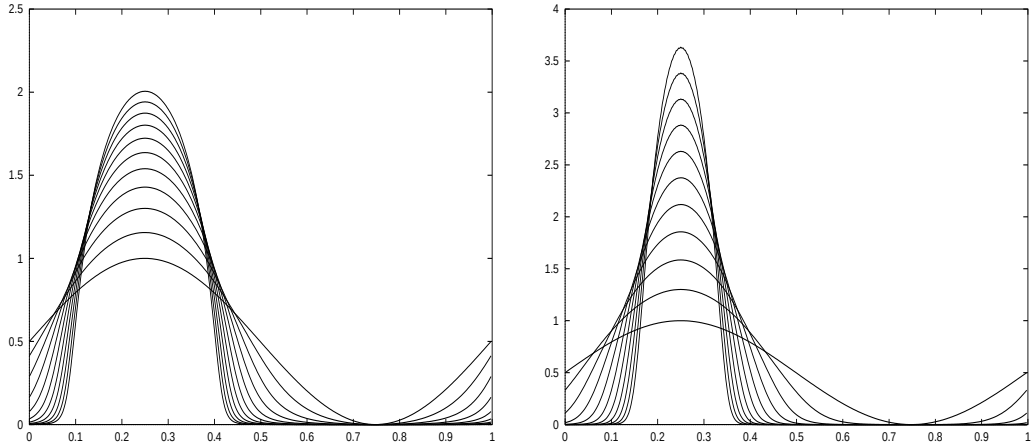


**Dispersal at high densities**

If the density of animals in a school or a flock becomes too high or the distance between individuals becomes too small they spread out again. This effect has been modeled e.g. by Grünbaum [17], who assumed a "target density". If the density is lower than the target density then individuals aggregate and align whereas if the density is higher than the target density then individuals spread out again. This spreading process is more or less random and parallel orientation is, at least momentarily, destroyed. Other models assume a "target distance" which has a similar effect (for references see [17]).

It has also been observed that no schools or flocks can form if the overall density of individuals is too low. Individuals then do not meet others sufficiently often to form a school.

However, there is some discussion whether such concepts as target density and target distance are biologically realistic. In particular it is not clear how to measure these quantities.

If we resume the idea of alignment and random turning as two competing factors for the formation of moving polarized groups then we can find both of the observed behaviors without assuming a target density (compare [10]). We take $a(u) = a_*/(1+u^3)$ and $\mu_* > 0$. The turning function

$$\mu(u^+, u^-) = \frac{a_* u^+ u^-}{1+u^3} - \frac{\mu_*}{2} \tag{2.18}$$

is smooth and bounded on $\mathbb{R}^2_+$. We choose $2a_* \sqrt[3]{4} > 3\mu_*$ such that $\sup \mu > 0$. We observe that $\mu < 0$ for $(u^+, u^-)$ close to $(0,0)$ as well as for large values of $u^\pm$.

LEMMA 2.2.6
*Choose $\mu$ as in (2.18). Then there exist thresholds $0 < \Sigma_1 < \Sigma_2 < \infty$ such that $[0, \Sigma_j]^2, j = 1, 2$ is invariant for the system of equations (2.8), i.e. if the initial data are continuously differentiable on $[0, l]$ and satisfy $0 \le u_0^\pm \le \Sigma_j$ then solutions satisfy $0 \le u^\pm(t) \le \Sigma_j$ as long as they exist in $\mathcal{C}^1(\Omega)$.*

PROOF.
Fix $u^- > 0$. Then $\mu(u^+, u^-)$ as a function of $u^+ \ge 0$ has exactly two zeros, denote

by $z = z(u^-)$ the larger one. Now set

$$\Sigma_2 = \sup_{u^->0} z(u^-) < \infty.$$

Then $\mu(\Sigma_2, u^-) \leq 0$ for all $u^- \in [0, \Sigma_2]$. By symmetry we also have $\mu(u^+, \Sigma_2) \leq 0$ for all $u^+ \in [0, \Sigma_2]$. To apply the invariance principle [24] we have to show that the vector field points inward at the boundaries of $[0, \Sigma_2]^2$. There are four parts of the boundary. The outer normal on $\{(u^+, 0) : 0 \leq u^+ \leq \Sigma_2\}$ is $(0, -1)$, and the condition that the vector field points inward at $(u^+, 0)$ translates into $\mu(u^+, 0) \leq 0$. If one of its arguments vanishes, then $\mu$ is negative and hence the condition is satisfied. By symmetry, the vectorfield also points inward on $\{(0, u^-) : 0 \leq u^- \leq \Sigma_2\}$. The outer normal on $\{(\Sigma_2, u^-) : 0 \leq u^- \leq \Sigma_2\}$ is $(1, 0)$. The condition

$$\mu(\Sigma_2, u^-)(\Sigma_2 - u^-) \leq 0$$

is satisfied by the definition of $\Sigma_2$ on $0 \leq u^- \leq \Sigma_2$. By symmetry, the condition is also satisfied on the last part of the boundary, $\{(u^+, \Sigma_2) : 0 \leq u^+ \leq \Sigma_2\}$. Hence the region $[0, \Sigma_2]^2$ is invariant for the system (2.3). The same arguments work for $\Sigma_1$, defined as the infimum over the smaller zero. ■

The two thresholds $\Sigma_{1,2}$ emerge from the competition between aligning forces and random turning. Densities below $\Sigma_1$ are too low for schools to form. Aligned groups are torn apart by random movement. Densities above $\Sigma_2$ are too high. As an aligned group reaches this critical density it disperses again.

The two effects can be seen in the following simulation. For the same initial values as above we choose parameters $\mu_* = 0.1$ and $a_* = 5$ such that $u_0^{\pm} < \Sigma_2$. Initially the peak grows, but then it becomes wider and forms a plateau as the maximal density is reached. Outside the peak a low but nonzero uniform density is established.

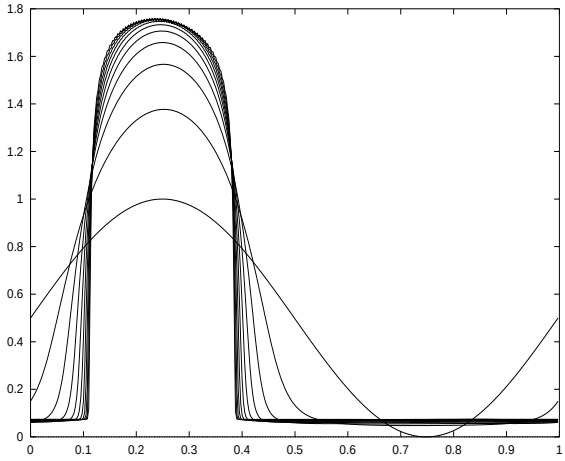


For parabolic equations local existence results together with existence of invariant domains are frequently used to show global existence of solutions. Since hyperbolic operators do not have similar regularization properties, this method does not carry over to system (2.3). Instead, we have to show a-priori bounds for the derivatives independently of the invariant domain.

We show global a-priori estimates for $u^{\pm}$ and $u_x^{\pm}$ on $\mathbb{R}$. If the initial data satisfy the compatibility conditions at the boundary then these estimates carry over to the case of periodic boundary conditions by continuation arguments.

THEOREM 2.2.7
*Choose $\mu$ as in (2.18). Suppose $u^{\pm}(t) \in \mathcal{C}^1(\mathbb{R})$ are solutions to system (2.3) for $t \in [0, t_0)$. Then the $\mathcal{C}^1$-norm of $u^{\pm}$ is bounded exponentially in time and hence solutions can be continued until infinity.*

PROOF.
We use the representation of solutions obtained by integration along characteristics, i.e.

$$u^{\pm}(t,x) = u_0^{\pm}(x - \gamma t) + \int_0^t \mu(u^+, u^-)(u^{\pm} - u^{\mp})(\tau, x \mp \gamma(t-\tau))d\tau. \tag{2.19}$$

The function $\mu$ is bounded and hence by Corollary 2.2.5 we get

$$\|u^+(t)\| + \|u^-(t)\| \leq (\|u_0^+\| + \|u_0^-\|)e^{2\|\mu\|t}.$$

Differentiating (2.19) with respect to $x$ gives

$$\begin{aligned} u_x^{\pm}(t,x) \quad = \quad & u_{0,x}^{\pm}(x - \gamma t) + \int_0^t \{D_1\mu(u^+, u^-)u_x^+(u^+ - u^-) \\ & + D_2\mu(u^+, u^-)u_x^-(u^+ - u^-) \\ & + \mu(u^+, u^-)(u_x^+ - u_x^-)\}(\tau, x - \gamma(t-\tau))d\tau, \end{aligned}$$

where $D_j$ denotes the derivative with respect to the $j$-th variable. From the choice of $\mu$ we see that $D_j\mu(u^+, u^-)u^{\pm}$ is bounded independently of $u^{\pm}$. The third term under the integral can be estimated as above. Altogether we find

$$\|u_x^+(t)\| + \|u_x^-(t)\| \leq \|u_{0,x}^+\| + \|u_{0,x}^-\| + 6\int_0^t \|\mu\|_{C^1}(\|u_x^+(\tau)\| + \|u_x^-(\tau)\|)d\tau.$$

Hence again with Gronwall's Lemma we see

$$\|u_x^+(t)\| + \|u_x^-(t)\| \leq (\|u_{0,x}^+\| + \|u_{0,x}^-\|)e^{6\|\mu\|_{C^1}t},$$

which completes the proof. ∎

## 2.3 Periodic Boundary Conditions

In the absence of random turning, i.e. $\mu_* = 0$, we describe the global dynamics of (2.3) and characterize $\omega$-limit sets. Then we examine bifurcations from the stationary states as $\mu_*$ decreases from large values to zero. Finally we introduce a viscosity term in order to investigate the bifurcation behavior where all eigenvalues cross the imaginary axis at once.

### 2.3.1 Global Dynamics for $\mu_* = 0$

In the following we always assume $a(u) > 0, \mu_* = 0$ and impose periodic boundary conditions on $\Omega = [0, l]$. From Lemma 2.1.1 we find the following characterization of stationary states.

COROLLARY 2.3.1
*At a stationary state $u^\pm$ are constant. Either $u^+$ and $u^-$ are equal or one of the two directions vanishes.*

The case $u^+ = u^-$ is unstable. The other stationary states are linearly stable as we see from the following more general consideration: If all particles are aligned in one direction, then $u^+ = 0$ or $u^- = 0$, which implies that the right hand side of the system (2.3) vanishes. The nonzero direction is then a simple wave on the circle with time period $l/\gamma$.

LEMMA 2.3.2
*A simple wave $u^+ > 0, u^- = 0$ ($u^- > 0, u^+ = 0$) is linearly stable with respect to the positive cone.*

PROOF.
Assume $u^- = 0$. We introduce small perturbations $w^\pm$ with $w^- \geq 0$ and linearize (2.3) around the simple wave $(u^+, 0)$. We obtain the system

$$\begin{aligned} w_t^+ + \gamma w_x^+ &= a(u)u^+(x)^2 w^-, \\ w_t^- - \gamma w_x^- &= -a(u)u^+(x)^2 w^-. \end{aligned}$$

The second equation is independent of the first and the system preserves positivity. The total mass of $w^-$ is a Lyapunov function:

$$\frac{d}{dt}\int_\Omega w^- dx = -\int_\Omega a(u)u^+(x)^2 w^-(x) dx \leq 0.$$

Hence the total mass of $w^-$ is decreasing along trajectories until the integral on the right hand side vanishes. This is only the case if $w^- = 0$ a.e. The convergence $w^- \to 0$ is also pointwise provided $u^+$ does not vanish at any point of $\Omega$. This can be seen by following the characteristic of $w^-$. ∎

It is clear that $u_0^+ > u_0^-$ does not imply $u^+(t) > u^-(t)$ for all $t > 0$. Using computer simulations one can even find initial values which satisfy $u_0^+(x) > u_0^-(x)$ for all $x \in \Omega$ and for which eventually $u^+$ vanishes and all individuals move to the left. If, however, in the beginning the minimal density in one direction is higher than the maximal density in the other, then it is true that the lower density will vanish eventually.

LEMMA 2.3.3
*Suppose* $\max u_0^- < \min u_0^+$. *Then* $u^- \to 0$ *as* $t \to \infty$.

SKETCH OF THE PROOF. Work along the characteristics and use the characteristic equations for $u^\pm$. We have $\dot{u}^+(0, x) > 0$ and $\dot{u}^-(0, x) < 0$ for all $x \in \mathbb{R}$. Then for small times $t > 0$ we find $\max u^-(t) < \max u_0^- < \min u_0^+ < \min u^+(t)$. Hence we

can iterate the argument. ■

The two sets $\{(u^+,0)\}$, $\{(0,u^-)\}$ describing complete alignment are local attractors but not all initial data lead to complete alignment. The respective basins of attraction are separated by a basin boundary. As a consequence of Lemma 2.1.3, a part of the basin boundary is characterized by the symmetry condition (2.12).

COROLLARY 2.3.4
*The set* $X_S = \{(u^+,u^-) \ : u^+(x) = u^-(l-x)\}$ *is invariant for the alignment system (2.3) and therefore part of the basin boundary.*

Another part of the basin boundary is given by perfect schools in opposite directions.

COROLLARY 2.3.5
*For all* $c \geq 0$ *the set* $X_c = \{(u^+,u^-) \ : u^+(x), u^-(x) \in \{0,c\}\}$ *is invariant for the alignment system (2.3) and therefore part of the basin boundary.*

Computer simulations suggest that solutions in $X_S$ which remain bounded have their limit set in some $X_c$. We construct a Lyapunov functional to show this analytically.

LEMMA 2.3.6
*The functional*

$$(u^+,u^-) \mapsto \int_0^l \ln((u^+ + 1)(u^- + 1))(t,x)dx$$

*is non-negative and decreasing along trajectories of the system (2.3).*

PROOF.
Solutions are non-negative and so $(u^+ + 1)(u^- + 1) \geq 1$. Then the integrand is non-negative. Differentiating with respect to $t$ gives

$$\begin{aligned}
& \frac{d}{dt}\int_0^l \ln((u^+ + 1)(u^- + 1))(t,x)dx \\
= & \int_0^l \frac{u_t^+(u^- + 1) + u_t^-(u^+ + 1)}{(u^+ + 1)(u^- + 1)}(t,x)dx \\
= & \int_0^l \frac{-\gamma u_x^+ + a u^- u^+(u^+ - u^-)}{u^+ + 1}(t,x)dx \\
& \quad + \int_0^l \frac{\gamma u_x^- - a u^- u^+(u^+ - u^-)}{u^- + 1}(t,x)dx \\
= & \int_0^l \gamma \frac{\partial}{\partial x}(\ln(u^- + 1) - \ln(u^+ + 1))(t,x)dx \\
& \quad + \int_0^l a(u) u^+ u^-(u^+ - u^-)\left(\frac{1}{u^+ + 1} - \frac{1}{u^- + 1}\right)(t,x)dx \\
= & -\int_0^l \frac{a(u) u^+ u^-(u^+ - u^-)^2}{(u^+ + 1)(u^- + 1)}(t,x)dx \quad \leq \quad 0
\end{aligned} \tag{2.20}$$

The last equality holds since the integral over the derivative vanishes due to the periodic boundary conditions. ∎

Suppose that for given initial data $(u_0^+, u_0^-) \in L^2(\Omega)^2$ the $\omega$-limit set $\omega((u^+, u^-))$ is nonempty. Then on the limit set the integral in (2.20) vanishes for all $t$. In particular, $u^+u^-(u^+ - u^-) = 0$ a.e. in $[t, t + l/\gamma] \times \Omega$. If for solutions $u^\pm$ we have $\Lambda'(t_0) = 0$ then on $[t_0, t_0 + l/\gamma]$ these solutions are traveling waves:

$$u^\pm(t_0 + \tau, x) = u^\pm(t_0, x \mp \gamma\tau) =: U_0^\pm(x \mp \gamma\tau).$$

Suppose there are sets $I^\pm$ of positive measure on which $U_0^\pm$ do not vanish. Then by following the characteristics we find some $\tau_0 \in [t_0, t_0 + l/\gamma]$ such that $U_0^\pm(x \mp \gamma\tau_0)$ do not vanish on some common set $I$ of positive measure. This then implies that $U^\pm$ agree on this set. Hence it follows that $U_0^\pm$ can assume only one nonzero value. We summarize these results in the following theorem.

THEOREM 2.3.7
*Consider the alignment system (2.3) with $\mu_* = 0$ and $a > 0$ on $\Omega = [0, l]$ with periodic or Neumann boundary conditions. Then the functional from Lemma 2.3.6 decreases along trajectories. If $(u^+, u^-) \in L^2(\Omega)^2$ is in some $\omega$-limit set then the right hand side of (2.3) vanishes a.e. Either one direction is zero or $u^\pm \in X_c$ for some $c > 0$.*

### 2.3.2 Bifurcation as $\mu_*$ decreases

Stationary solutions of (2.3) are spatially constant, and the values of $u^\pm$ at a stationary solution are given by the equilibrium points of

$$\dot{u}^\pm = \pm(a(u)u^+u^- - \frac{\mu_*}{2})(u^+ - u^-).$$

In $u, v$-coordinates, there always is the stationary point $\bar{u} > 0, \bar{v} = 0$. For large values of $\mu_*$ it is the only stationary point. As $\mu_*$ decreases below

$$\mu_b(\bar{u}) := a(\bar{u})\bar{u}^2/2. \tag{2.21}$$

we observe a pitchfork bifurcation and the additional equilibrium points are given by $\bar{u} > 0, \bar{v}^2 = \bar{u}^2 - \frac{2\mu_*}{a(\bar{u})}$. The linearization of system (2.5) around a solution $(\bar{u}, \bar{v})$

$$\begin{aligned} u_t + \gamma v_x &= 0, \\ v_t + \gamma u_x &= A(\bar{u}, \bar{v})u + B(\bar{u}, \bar{v})v, \end{aligned}$$

can be reduced to the following telegraph equation for $u$:

$$u_{tt} - Bu_t = \gamma^2 u_{xx} - \gamma A u_x,$$

where

$$A = \frac{a'(\bar{u})}{2}(\bar{u}^2 - \bar{v}^2)\bar{v} + a(\bar{u})\bar{u}\bar{v}, \quad B = \frac{a(\bar{u})}{2}(\bar{u}^2 - 3\bar{v}^2) - \mu_*. \tag{2.22}$$

The eigenvalue problem is

$$\gamma^2 u_{xx} - \gamma A u_x - \lambda(\lambda - B)u = 0, \tag{2.23}$$

with periodic boundary conditions $u(0) = u(l)$.

**Linear Analysis at $\bar{v} = 0$ i.e. $u^+ = u^-$**

We have $A = 0$ and $B = a(\bar{u})\bar{u}^2/2 - \mu_*$. Fourier transform of (2.23) yields the following formula for the eigenvalues $\lambda$ corresponding to the modes $k \in \mathbb{Z}$ :

$$\lambda_{1/2}(k) = \frac{B}{2} \pm \sqrt{\frac{B^2}{4} - \frac{k^2\pi^2\gamma^2}{l^2}}. \tag{2.24}$$

We consider only perturbations of zero mass, i.e. $k \neq 0$. The sign of the real part of $\lambda$ is determined by the sign of $B$. For $\mu_* > \mu_b(\bar{u})$ we have $B < 0$ and hence $\Re\lambda_{1/2}(k) < 0$ for all $k \in \mathbb{Z}$. For $\mu_* < \mu_b(\bar{u})$ the coefficient $B$ changes sign and eigenvalues of all wavenumbers become positive simultaneously.

**Global Behavior for Large $\mu_*$**

For large enough $\mu_*$ the homogeneous state $u^+ = u^- = \text{const.}$ is even globally stable.

LEMMA 2.3.8
*Suppose $a(u) = a_*/(1 + u^k)$ for $k = 2, 3$ and set $\bar{\mu}_b := \sup_{\bar{u}} \mu_b(\bar{u})$. Then for $\mu_* > \bar{\mu}_b$ every solution of (2.3) in $L^2(\Omega)^2$ converges to a homogeneous distribution $u^+ = u^- = \text{const}$.*

PROOF.
The $L^2$-norm is a Lyapunov function for the system:

$$\frac{d}{dt}\int_0^l u^2 + v^2 dx = \int_0^l \left(\frac{a(u)}{2}(u^2 - v^2) - \mu_*\right) v^2 dx \leq (\bar{\mu}_b - \mu_*)\int_0^l v^2 dx < 0.$$

Hence $\int u^2 + v^2 dx$ decreases until $\int v^2 dx = 0$. Integrating the functional above over one period in time we see that on limit sets we even have

$$\int_0^{l/\gamma}\int_0^l v^2(t + \tau, x) dx d\tau = 0,$$

which implies that $u^+ = u^- = \text{const}$. This constant, however, is determined by the total mass of the initial data and the length of the interval. Hence the $\omega$-limit set for each trajectory is exactly one point. ∎

**Linear Analysis at $\bar{v} \neq 0$**

For values $\mu_* < \mu_b$ the coefficient $A$ is real:

$$A = \left(\frac{a'(\bar{u})}{a(\bar{u})}\mu_* + a(\bar{u})\bar{u}\right)\sqrt{\bar{u}^2 - \frac{2\mu_*}{a(\bar{u})}}.$$

For the eigenvalue equation (2.23) with periodic boundary conditions we make the ansatz $v = e^{i\sigma x}$ with $\sigma \in \mathbb{R}$ and get

$$\sigma^2 + i\frac{A}{\gamma}\sigma = \frac{\lambda^2 - B\lambda}{\gamma^2}.$$

We set $\lambda = \alpha + i\beta$ and find equations for the real and imaginary part. Comparing the coefficients we get the following equations for $\alpha, \beta, \sigma$.

$$\sigma^2 = \frac{\alpha B - \alpha^2 + \beta^2}{\gamma^2}, \qquad \sigma = \frac{\beta B - 2\alpha\beta}{A\gamma} = \frac{2\pi k}{l}.$$

We eliminate $\beta$ from the equations and arrive at

$$\left(\frac{l}{2\pi k\gamma}\right)^2 = \frac{(B-2\alpha)^2 - A^2}{(B-2\alpha)^2(\alpha B - \alpha^2)}. \tag{2.25}$$

We are interested in the sign of $\alpha$. The right hand side as a function of $\alpha$ vanishes as $\alpha \to \infty$. It has poles at $\alpha = B, B/2, 0$ and zeros at $(B \pm A)/2$. If both of these zeros are negative then the right hand side of (2.25) is negative for $\alpha > 0$ and hence there are no intersections with horizontal lines of the value $l^2/(2\pi k\gamma)^2$ for $\alpha > 0$. The situation is stable. If, on the other hand, one of the zeros is positive then the graph of the right hand side of (2.25) intersects the lines for all $k > 0$ with positive $\alpha$. Hence the situation is unstable. Once again, all modes become unstable at the same time.

LEMMA 2.3.9
*For $\mu_* < \mu_b(\bar{u})$ the constant stationary solution $(\bar{u}, \bar{v})$ with $\bar{v} \neq 0$ is linearly stable if and only if $B^2 > A^2$.*

The expression $B^2 - A^2$ is a polynomial of degree 3 in $\mu_*$ which vanishes at zero. Depending on the derivative $a'(\bar{u})$ we consider several cases.

1. For $0 > a'(\bar{u}) > -a(\bar{u})/\bar{u}$ we have $B^2 < A^2$ for all $0 < \mu_* < \mu_b$.
2. For $a'(\bar{u}) < -a(\bar{u})/\bar{u}$ there is a value $\mu_1 < \mu_b$ such that $B^2 > A^2$ for $\mu_* < \mu_1$ and $B^2 < A^2$ for $\mu_* > \mu_1$.

As a special case, consider $a(u) = 1/(1+u^3)$. Then $a'(u) < 0$ and $a'(\bar{u})\bar{u} > -a(\bar{u})$ iff $2\bar{u}^3 < 1$. Hence if the total mass $\bar{u}$ is too low then the situation is unstable. If it is high enough then the situation is linearly stable if the difference of $u^+$ and $u^-$ is large enough (compared to $\mu_*$). In case $a(u) = 1/(1+u^2)$ the results are similar, the critical value of $\bar{u}$ being 1.

### 2.3.3 The System with Viscosity

We introduce a viscosity term into the equations. Looking at the homogeneous steady state, we find a series of Hopf bifurcations as $\mu_* \to 0$. Decreasing the viscosity for small fixed $\mu_* > 0$ also leads to Hopf bifurcations. Limit sets for the system with viscosity are compact. The system reads in $u, v$-notation (compare (2.10))

$$\begin{aligned} u_t + \gamma v_x &= \varepsilon u_{xx}, \\ v_t + \gamma u_x &= g(u,v) + \varepsilon v_{xx}, \end{aligned} \tag{2.26}$$

on $\Omega = [0, l]$ with periodic boundary conditions. Linearizing at $\bar{u} = \text{const.}, \bar{v} = 0$ gives

$$\begin{aligned} u_t + \gamma v_x &= \varepsilon u_{xx}, \\ v_t + \gamma u_x &= Bv + \varepsilon v_{xx}, \end{aligned} \tag{2.27}$$

with $B = a(\bar{u})\bar{u}^2/2 - \mu_*$ as in (2.22). Decreasing $\mu_* \to 0$ is equivalent to increasing $B$. The results below are formulated in terms of $B$. Fourier transform of (2.27) gives

$$\begin{aligned} \hat{u}_t + ik\gamma\hat{v} &= -k^2\varepsilon\hat{u}, \\ \hat{v}_t + ik\gamma\hat{u} &= B\hat{v} - k^2\varepsilon\hat{v} \end{aligned} \tag{2.28}$$

for $k \in \mathbb{Z}$. The eigenvalues of the system for $l = \pi$ are given by

$$\lambda_{1,2}(k) = \frac{1}{2}\left(B - 2k^2\varepsilon \pm \sqrt{B^2 - 4k^2\gamma^2}\right), \tag{2.29}$$

which is the analogue of (2.24). Again, we restrict ourselves to perturbations of zero mass, i.e. $k \neq 0$.

### Bifurcation for fixed viscosity

We fix $\varepsilon > 0$ such that $\varepsilon \ll 2\gamma$. For $B \leq 0$ all eigenvalues have negative real part. At $B = 2\varepsilon$ we have

$$\lambda_{1,2}(1) \in i\mathbb{R}\backslash\{0\}, \quad \Re\lambda_{1,2}(k) \neq 0 \text{ for } |k| > 1, \quad \frac{d(\Re\lambda_{1,2}(1))}{dB} = 1$$

and hence we observe a Hopf bifurcation. As we increase the value of $B$, the parabola on which the eigenvalues lie is shifted to the right but retains its shape. There is a series of Hopf bifurcations at $B = 2k^2\varepsilon$ for $k = \pm 2, \pm 3, ... \pm n$ until $B$ has reached its maximum. We plot the eigenvalues for $|k| < 8$ for the parameter values $\varepsilon = 0.01$ and $\gamma = 1$.

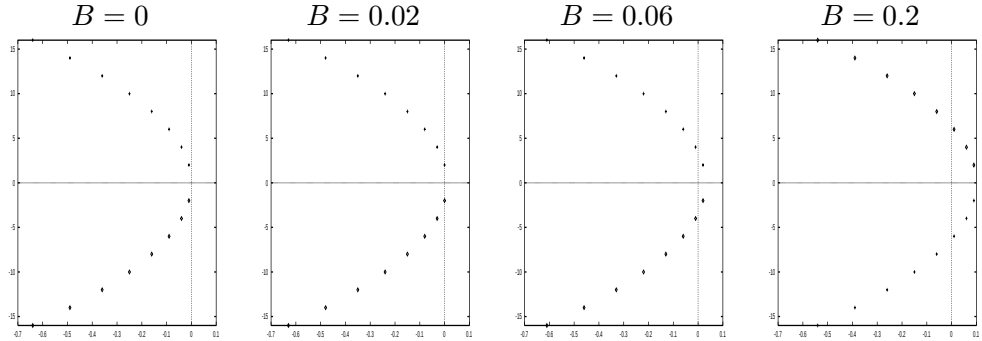


### Bifurcation for fixed turning rate

Now we fix $B > 0$. There is a number $k_1$ such that $\lambda_{1,2}(1), ...\lambda_{1,2}(k_1) \in \mathbb{R}$ and $\lambda_{1,2}(k_1 + j) \notin \mathbb{R}$ for $j > 0$. For large $\varepsilon$ the real parts of all eigenvalues are negative. At $\varepsilon = B/2$ the first mode becomes unstable as $\lambda_1(1)$ passes through zero. Starting with $\lambda_{1,2}(k_1 + 1)$ eigenvalues cross the imaginary axis and a Hopf bifurcation occurs. The parabola on which the non-real eigenvalues lie becomes more straight

as $\varepsilon \to 0$. We plot the first eigenvalues for the values $B = 1.5$ and $\gamma^2 = 0.1$.

$\varepsilon = 0.25$ $\varepsilon = 0.1$ $\varepsilon = 0.05$ $\varepsilon = 0.02$

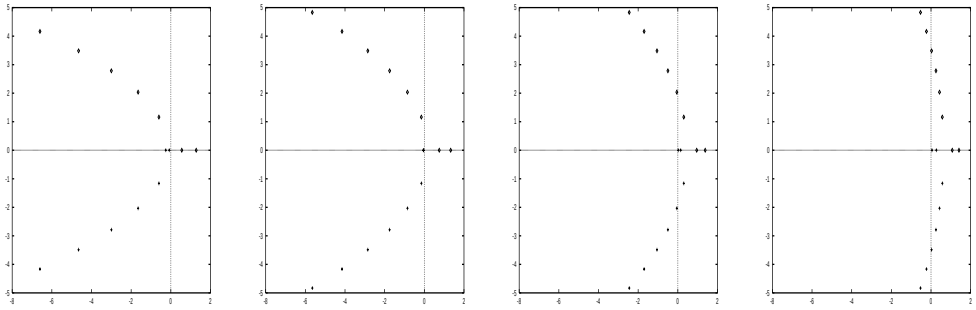

**Long Time Behavior**

Solutions of (2.26) are smooth even if the initial data are not, since the parabolic operator regularizes. To investigate limit sets of (2.26) we examine the energy functional

$$\frac{d}{dt}\int_0^l u_x^2 + v_x^2 dx = -\int g(u,v)_x v_x dx - 2\varepsilon \int u_{xx}^2 + v_{xx}^2 dx. \tag{2.30}$$

We assume that the partial derivatives $g_u$ and $g_v$ are bounded by some constant $C$. Then we get

$$\begin{aligned} |g(u,v)_x v_x| \leq \;& |g_u||u_x v_x| + |g_v| v_x^2 \leq \; \tfrac{1}{2}|g_u|(u_x^2 + v_x^2) + |g_v| v_x^2 \\ \leq \;& \tfrac{3}{2} C (u_x^2 + v_x^2). \end{aligned} \tag{2.31}$$

To estimate the second integral on the right hand side we integrate the equation

$$u_x(y) - u_x(x) = \int_x^y u_{xx}(s) ds$$

over $[0, l]$ and use the Cauchy-Schwarz inequality to get

$$|u_x(y)| l \leq \int_0^l \int_x^y |u_{xx}| ds dx \leq l \int_0^l |u_{xx}| dx \leq l\sqrt{l}\sqrt{\int u_{xx}^2}.$$

A similar estimate for $v$ leads to

$$u_x^2(x) + v_x^2(x) \leq l \int u_{xx}^2 + v_{xx}^2 dx.$$

Integrating again with respect to $x$ and multiplying by $-\varepsilon$ gives the inequality

$$-\varepsilon l^2 \int u_{xx}^2 + v_{xx}^2 dx \leq -\varepsilon \int u_x^2 + v_x^2 dx. \tag{2.32}$$

Inserting (2.31) and (2.32) into (2.30) we get

$$\frac{d}{dt}\int u_x^2 + v_x^2 dx \leq \left(\frac{3Cl}{2} - \frac{2\varepsilon}{l^2}\right) \int u_x^2 + v_x^2 dx. \tag{2.33}$$

LEMMA 2.3.10
*Suppose the derivatives $g_u$ and $g_v$ are globally bounded by some constant $C$. Then for $\varepsilon > 3Cl^3/4$ the energy integral is a Lyapunov functional. The limit sets of system (2.26) consist of constant functions. This argument applies in particular to the alignment system (2.3) with $a(u) = 1/(1+u^k)$ for $k = 2, 3$ and $\varepsilon > 3l^3/2$.*

PROOF.
We may assume $\mu_* = 0$. Then $g(u,v) = u^2 - v^2/(2(1+u^k))$ in the notation of (2.26). We show that we can choose $C = 2$. Note that we always have $0 \le |v| \le u$.

$$\begin{aligned}\frac{\partial}{\partial u}g(u,v) &= \frac{\partial}{\partial u}\frac{u^2-v^2}{2(1+u^3)}v = \frac{2uv(1+u^3)-3(u^2v-v^3)u^2}{2(1+u^3)^2}\\ &= \frac{-u^4v+3u^2v^3+2uv}{2(1+u^3)^2} \le \frac{4u^5+2u^2}{2(1+u^3)^2} \le 2,\\ \frac{\partial}{\partial v}g(u,v) &= \frac{u^2-3v^2}{2(1+u^3)} \le \frac{2u^2}{(1+u^3)} < 2.\end{aligned}$$

The case $a(u) = \frac{1}{1+u^2}$ is similar. ∎

We know from the bifurcation analysis that Lemma 2.3.10 cannot hold for arbitrarily small viscosity. But we can show that limit sets are compact for all $\varepsilon > 0$ if $g$ is bounded.

LEMMA 2.3.11
*Suppose $g$ is globally bounded. Then for all $\varepsilon > 0$ the limit set of any solution to the system (2.26) is compact in $L^2(\Omega)^2$ as well as in $\mathcal{C}(\Omega)^2$. This argument applies in particular to the alignment system with $a(u) = 1/(1+u^3)$.*

PROOF.
We assume $|g| \le M$. We integrate by parts the first integral on the right hand side of (2.30) and use the Cauchy-Schwarz and Young inequality to get

$$\int g(u,v)v_{xx}dx \le M\int |v_{xx}|dx \le M\sqrt{l}\sqrt{\int v_{xx}^2 dx} \le \frac{M^2 l}{4\varepsilon} + \varepsilon\int v_{xx}^2 dx.$$

Inserting this back into (2.30) we have

$$\frac{d}{dt}\int u_x^2 + v_x^2 dx \le \frac{M^2 l}{4\varepsilon} + \varepsilon\int v_{xx}^2 dx - 2\varepsilon\int u_{xx}^2 + v_{xx}^2 dx. \tag{2.34}$$

Finally we use (2.32) again and arrive at

$$\frac{d}{dt}\int u_x^2 + v_x^2 dx \le \frac{M^2 l}{4\varepsilon} - \frac{\varepsilon}{l^2}\int u_x^2 + v_x^2 dx. \tag{2.35}$$

This inequality is of the form

$$\dot\phi(t) \le \frac{M^2 l}{4\varepsilon} - \frac{\varepsilon}{l^2}\phi(t) =: F(\phi).$$

We know the solutions of $\dot\psi = F(\psi)$ and hence can estimate $\phi$ by

$$\phi(t) \le \phi(0)e^{-\frac{\varepsilon}{l^2}t} + \frac{M^2 l^3}{4\varepsilon^2}\left(1 - e^{-\frac{\varepsilon}{l^2}t}\right).$$

We get that $\phi$, and hence $\int u_x^2 + v_x^2$, is globally bounded. With the following standard estimate we also get global bounds for $u$ and $v$ :

$$|v(x)| \leq u(x) \leq \frac{\bar{u}}{l} + \sqrt{l}\sqrt{\int u_x^2 + v_x^2 dx}.$$

The imbeddings of $H^1(\Omega)^2$ into $L^2(\Omega)^2$ and $\mathcal{C}(\Omega)^2$ are compact so that trajectories are precompact in these spaces. Hence the limit sets are nonempty and compact. ■

## 2.4 Alignment in Predator-Prey Systems

The formation of fish schools is considered a strategy against predation. We show analytically and numerically that an aligning prey may survive where it would go extinct without the formation of schools.

Neglecting space for the moment, we denote by $\alpha(u)$ the reproduction rate of prey in the absence of predators. In order to keep the model simple we assume that the predator has abundant food sources besides the prey species in question and that its density $w_0$ can be assumed constant. Then

$$\dot{u} = \alpha(u)u - \beta(u)uw_0, \tag{2.36}$$

where $\beta(u)$ is the predation rate. We assume logistic growth for the prey in absence of predators and a saturation functional response $\beta$. We have $\dot{u} = 0$ at $u = 0$. For a suitable choice of parameters we observe an Allee effect, i.e. $\dot{u} < 0$ for very small and very large values of $u$, and $\dot{u} > 0$ for intermediate values of $u$. Therefore we simplify again and choose the population dynamics of the prey to be

$$\dot{u} = p(u) = p_* u(u - s_1)(s_2 - u), \tag{2.37}$$

where $0 < s_1 < s_2$ and $p_* > 0$. The value $s_1$ is the extinction threshold, the capacity is denoted by $s_2$. We insert (2.37) into (2.5) and get

$$\begin{aligned} u_t + \gamma v_x &= p_* u(u - s_1)(s_2 - u), \\ v_t + \gamma u_x &= \left(\frac{a(u)}{2}(u^2 - v^2) - \mu_*\right) v, \end{aligned} \tag{2.38}$$

where we always assume $a(u) = a_*/(1 + u^3)$ with $a_* > 0$.

### Linearization

Spatially constant stationary solutions of (2.38) are $(\bar{u}, \bar{v})$ with $\bar{u} \in \{0, s_1, s_2\}$ and $\bar{v} = 0$ or $\bar{v}^2 = \bar{u}^2 - 4\mu_*/a$. Linearization of (2.38) leads to a system of the form

$$\begin{aligned} u_t + \gamma v_x &= Cu, \\ v_t + \gamma u_x &= Au + Bv, \end{aligned} \tag{2.39}$$

where $A, B$ are as in (2.22) and $C = -3p_*\bar{u}^2 + 2p_*(s_1 + s_2)\bar{u} - p_* s_1 s_2$. Again, we look for eigenvalues $\lambda = \alpha + i\beta$ and similarly as above we find the equation

$$\left(\frac{l^2}{2\pi k\gamma}\right)^2 = \frac{(B + C - 2\alpha)^2 - A^2}{(B + C - 2\alpha)^2(C - \alpha)(\alpha - B)}, \tag{2.40}$$

where $k$ is the mode of the eigenfunction on the interval $[0, l]$ with periodic boundary conditions. We interpret the right hand side of (2.40) as a function $\Gamma(\alpha)$ and look for intersections with horizontal lines of the values on the left hand side for positive $\alpha$. The function $\Gamma$ has zeros for $\alpha = (B + C \pm A)/2$ and poles at $\alpha = B, C, (B + C)/2$. As $\alpha \to \infty$ it is negative and approaches zero. We discuss only the cases with $\bar{v} = 0$ here, which implies that $A = 0$.

1. $\bar{u} = \bar{v} = 0$
   We find $B, C < 0$. All zeros of $\Gamma$ are negative and hence $\Gamma(\alpha) < 0$ for $\alpha > 0$. The real part of all eigenvalues $\lambda$ is negative and the situation is stable.

2. $\bar{u} = s_1, \bar{v} = 0$
   Now $C > 0$ and hence one of the poles of $\Gamma$ occurs at a positive value. The value $\Gamma(0)$ is large if $a_*$ is small and $\mu_*$ is large. As $a_*$ increases (or $\mu_*$ decreases) $\Gamma(0)$ decreases to zero. If $\Gamma(0) < l^4/(4\pi^2\gamma^2)$ then the first mode becomes unstable. Higher modes become unstable as $\Gamma(0)$ decreases further. Finally for $B + C \geq 0$ all modes are unstable.

3. $\bar{u} = s_2, \bar{v} = 0$
   Here $C < 0$. For large values of $\mu_*$ in addition $B < 0$ and the situation is stable. As $\mu_*$ decreases $B$ increases above zero and low modes become unstable if $\Gamma(0)$ is small enough.

To summarize, the case $\bar{u} = 0$ is always stable. A group of very few individuals cannot survive even if they stay in one group. At the extinction threshold $\bar{u} = s_1$ a population can grow if the influence of alignment is strong enough. A population can even grow to exceed the capacity if the aligning forces are very strong and the influence of random turning is very small.

### Recovery

If a population starting below the extinction threshold rises above it, this process is called *recovery*. Recovery can be transient or permanent. If there is no alignment, i.e. $a_* = 0$ in (2.38), then the population cannot recover. But if $a_*$ is large enough, then recovery is possible.

We formulate (2.38) in terms of $u^{\pm}$ on some bounded interval with periodic boundary conditions. Since we are interested only in the behavior of $u$ around the threshold $s_1$ we may use the continuously differentiable linear continuation $\tilde{p}$ instead of $p$ at $s_2$, i.e. $\tilde{p}(u) = p(u)$ for $0 \leq u \leq s_2$ and $\tilde{p}(u) = p_* s_2(s_1 - s_2)u$ for $u > s_2$. Hence we study

$$\begin{aligned} u^+_t + \gamma u^+_x &= \mu(u^+, u^-)(u^+ - u^-) + \frac{1}{2}\tilde{p}(u), \\ u^-_t - \gamma u^-_x &= \mu(u^+, u^-)(u^- - u^+) + \frac{1}{2}\tilde{p}(u), \end{aligned} \tag{2.41}$$

with $\mu(u^+, u^-) = a_* u^+ u^-/(1 + u^3) - \mu_*$. We assume nonnegative smooth initial data which satisfy the boundary conditions such that we have smooth solutions. If $\mu_* > \max\{p_* s_1 s_2, p_* s_2(s_2 - s_1)\}$ then positivity is preserved [24]. By Lemma 2.2.6 there are two values $\Sigma_{1,2}$ such that alignment only occurs for densities $\Sigma_1 < u^{\pm} < \Sigma_2$. We show that recovery is possible iff the extinction threshold is in the interval $[\Sigma_1, \Sigma_2]$.

THEOREM 2.4.1
*Suppose for (2.41) parameters $\mu_*, p_*, s_1, s_2$ are given such that positivity is preserved. If we choose $a_*$ such that $\frac{s_1}{2} \notin [\Sigma_1, \Sigma_2]$ then $[0, s_1/2]^2$ is invariant. For sufficiently large $a_*$ we have $\frac{s_1}{2} \in [\Sigma_1, \Sigma_2]$ and there are trajectories starting in $[0, s_1/2]^2$ for which at least one of the components $u^\pm$ rises above $s_1/2$.*

PROOF.
We first assume $\frac{s_1}{2} \notin [\Sigma_1, \Sigma_2]$ and show that the vectorfield points inward on the part of the boundary where $u^- = s_1/2$. The condition reads

$$-\mu(u^+, s_1/2)(u^+ - s_1/2) + 1/2p(u^+ + s_1/2) \leq 0. \tag{2.42}$$

From the definition of $\Sigma_{1,2}$ and the assumption on $s_1$ it follows that $\mu(\cdot, s_1/2) < 0$. Hence the first term in (2.42) is non-positive for $0 \leq u^+ \leq s_1/2$. Since $p(u^+ + s_1/2) \leq 0$ for $0 \leq u^+ \leq s_1/2$ also the second term is non-positive. Hence (2.42) is satisfied. Together with preservation of positivity we find that $[0, s_1/2]^2$ is invariant by the invariance principle [24].

If we increase $a_*$ then $\mu$ increases and hence $\Sigma_2$ increases and $\Sigma_1$ decreases. Hence, for $a_*$ sufficiently large we find $\frac{s_1}{2} \in [\Sigma_1, \Sigma_2]$. Then we choose initial data as follows: $0 < u_0^+(x) \leq s_1/2$ with at least one point $x_0 \in (0, l)$ where $u_0^+(x_0) = s_1/2$. Since $s_1/2 \in [\Sigma_1, \Sigma_2]$ we can choose $0 < u^- < s_1/2$ such that $\mu > 0$ at $x_0$. We can follow the characteristics forward and backward in time such that at least for some time $\tau > 0$ there are solutions $u^\pm(t)$ to the system for $-\tau \leq t \leq \tau$ with $u^\pm(0) = u_0^\pm$. At $x_0$ we have $\dot{u}_0^+ > 0$ along the characteristic. By continuity this holds in a small neighborhood of $(0, x_0)$. But then for some $\tau_1 > 0$ we have $u^\pm(t) < s_1/2$ for $-\tau_1 < t < 0$ and $\max u^+(t) > s_1/2$ for $0 < t < \tau_1$. ∎

**Simulations**

For simulations we choose parameters $s_1 = 0.5, s_2 = 2, p_* = 0.3, \mu_* = 0.3$ and $\gamma = 1$. We have periodic boundary conditions and use a rotating coordinate system to plot the total density $u = u^+ + u^-$. Initial values are spatially constant and equal $u^+ = u^- = 0.2$ and a small peak of maximal height 0.1 is added in $u^+$.

The three plots show the behavior for varying strength of alignment. In the first case $a_* = 7$, and the population dies out. For $a_* = 9$ in the second case, the population recovers initially but it does not grow fast enough to survive. In the last picture $a_* = 11$ and we see that the population grows fast enough to reach the capacity.

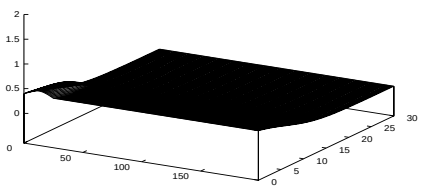


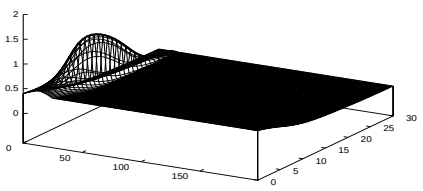

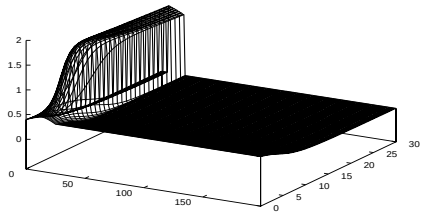


**Remarks**

1. Splitting the reaction term equally into the two directions as in (2.41) may lead to a modeling mistake if the reaction term is negative. Particles can only be deleted from $u^+$ if they are actually in $u^+$. A more accurate model treats the birth and death term of the population dynamics separately. Then no additional condition for preservation of positivity is necessary. For a thorough discussion of this question see [21].

2. Some error is made since for most species movement and reproduction happens on different time scales. There is a relatively recent discussion about the importance of different scales in general [12].

3. This approach to aggregation and predation closely follows Lizana and Padron [38]. Their spatially discrete model consists of a finite number of ordinary differential equations and uses (discrete) density dependent diffusion to model aggregation and a function similar to $p(u)$ for the population dynamics. The continuum analogue to the discrete model is a diffusion equation with density dependent diffusion coefficient, which changes sign, i.e. it is ill–posed.

# Chapter 3

# Alignment Models in 2-D

The present chapter consists of two parts. First we generalize the one-dimensional alignment model from Chapter 2 to two space dimensions still assuming constant speed. A partial integro-differential equation describes the orientation process at each point in space. Together with the transport equation (1.1) we obtain a model in form of a semilinear reaction transport equation. We prove existence and uniqueness of solutions, investigate the model for a discrete set of velocities and show simulations.

In the second part we present a master equation which comprises our model as well as models which already exist in the literature. This master equation allows us to compare these models and to get an interpretation of our model equation on the particle level. The application of the master equation to the one-dimensional case gives better insight to the model from Chapter 2.

## 3.1 The Semilinear Model Equation

The alignment process can be viewed as a competition of different velocity classes. To describe this competition we start from the equations for exponentially growing and competing species. Given $n$ types with densities $y_i$, $i = 1, \dots, n$, which increase exponentially at rates $m_i$, i.e. $\dot{y}_i = m_i y_i$, we form proportions $p_i = y_i / \sum y_j$. These satisfy

$$\dot{p}_i = m_i p_i - \frac{\sum_j m_j p_j}{\sum p_j} p_i. \tag{3.1}$$

The right hand side for type $i$ depends on its growth rate $m_i$ and on the average growth rate. This system preserves total mass (not only if this mass is unity). Eventually the whole mass will be concentrated in the types with the largest $m_i$.

Now we let $V = \gamma S^1$ be the set of velocities, interpret $i$ above as a continuous variable $s \in V$ and write $m(s)$ instead of $m_i$. The alignment process leads to a concentration in the direction of the average velocity. Hence we assume the coefficient $m(s) = s \cdot \bar{s}$ to be the inner product of the velocity of an individual with the average velocity $\bar{s}$, and also write $m(s) = s\bar{s}$ for short. Note that the coefficients $m_i$ in (3.1) are constants whereas the coefficients $m(s)$ are functions of $s$.

Denote by $u(t,s)$ the density at time $t$ with respect to the velocity $s \in V$. The total density is

$$\bar{u}(t) = \int_V u(t,\sigma)d\sigma, \tag{3.2}$$

where the integral is taken over all velocities, and the average velocity is

$$\bar{s}(t) = \frac{1}{\bar{u}(t)} \int_V \sigma u(t,\sigma)d\sigma \in \mathbb{R}^2. \tag{3.3}$$

With this notation the continuum analogue of (3.1) is

$$\frac{\partial}{\partial t}u(t,s) = a\left[(s\bar{s})u(t,s) - \frac{\int_V \sigma\bar{s}u(t,\sigma)d\sigma}{\int_V u(t,\sigma)d\sigma}u(t,s)\right],$$

where $a$ is some constant or a function of $\bar{u}$ and has a similar meaning as $a(u)$ in (2.3). This equation can be written in a simpler form as

$$u_t(t,s) = A(u)(t,s) \colon = a(\bar{u})[s\bar{s} - \bar{s}\bar{s}]u(t,s). \tag{3.4}$$

By construction, this equation preserves the total mass $\bar{u}$ (3.2). The function $A(u)$ gives the net rate of change in direction $s$. Given some average velocity $\bar{s} \neq 0$ the following picture shows which directions gain particles ($A > 0$) and which directions loose particles ($A < 0$).

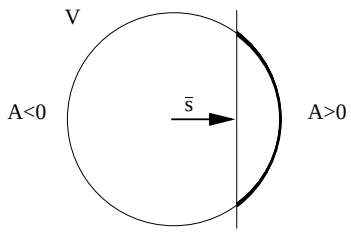


Finally we introduce the space variable $x \in \Omega \subset \mathbb{R}^2$. The full alignment transport equation for the function $u(t,x,s)$ reads

$$u_t + s \cdot \nabla_x u \quad = \quad A(u)(t,x,s) = a(\bar{u})[s\bar{s} - \bar{s}\bar{s}]u(t,x,s), \tag{3.5}$$

where $\bar{u}$ and $\bar{s} = \bar{s}(u)$ are given by (3.2) and (3.3). We are not interested in the behavior at the boundary and therefore we assume either $\Omega = \mathbb{R}^2$ or $\Omega = [0,1]^2$ with periodic boundary conditions.

The equations for $u$ along the characteristics are of the form $\dot{u} = \tilde{A}(u)u$ and hence the model preserves positivity. If all individuals are oriented in the same direction we speak of total alignment. This is a limiting case in which $u$ is a $\delta$-distribution with respect to $s$. In the sense of distributions such a situation is stationary for the reaction differential equation (3.4) and gives a traveling profile in (3.5).

### Reduction to one Dimension

In the special case $V = \{\pm\gamma\}$ and $x \in \mathbb{R}$ the system reduces to the one-dimensional model introduced in Chapter 2 when integrals are replaced by sums. This can be seen as follows. We have $s = \pm\gamma$, $\bar{u} = u^+ + u^-$ and

$$\bar{s} = \frac{(+\gamma)u^+ + (-\gamma)u^-}{\bar{u}} = \frac{\gamma v}{\bar{u}},$$

where as always $v = u^+ - u^-$. Thus (3.5) becomes for $s = +\gamma$

$$\begin{aligned} u_t^+ + \gamma u_x^+ &= a(\bar{u})\left[\gamma\frac{\gamma v}{\bar{u}} - \frac{\gamma^2 v^2}{\bar{u}^2}\right]u^+ \\ &= \frac{\gamma^2 a(\bar{u})}{\bar{u}^2}\left[v\bar{u} - v^2\right]u^+ \\ &= \frac{\gamma^2 a(\bar{u})}{\bar{u}^2}\left[(u^+ - u^-)(u^+ + u^-) - (u^+ - u^-)^2\right]u^+ \\ &= \frac{2\gamma^2 a(\bar{u})}{\bar{u}^2}[(u^+)^2 u^- - (u^-)^2 u^+] \\ &= \tilde{a}(\bar{u})u^+ u^-(u^+ - u^-). \end{aligned}$$

The computation for $s = -\gamma$ is analogous and we get system (2.3). Therefore (3.5) is a generalization of the one-dimensional model (2.3).

### Conservation of Mass

Integrating $\bar{u}$ over a spatial domain we get the overall number of particles in this domain. This number is invariant for the reorientation process. Suppose $u$ is a nonnegative smooth solution of (3.5) which has compact support in $\mathbb{R}^2$. Then for the overall number we have

$$\begin{aligned} \frac{d}{dt}\int_{\mathbb{R}^2}\int_V u(t,x,s)dsdx &= \int_{\mathbb{R}^2}\int_V -s\cdot\nabla u + A(u)dsdx \\ &= -\int_V\int_{\mathbb{R}^2} s\cdot\nabla u(t,x,s)dxds + \int_{\mathbb{R}^2}\int_V a(s\cdot\bar{s} - |\bar{s}|^2)udsdx. \end{aligned}$$

The first integral vanishes by Green's theorem. The second integral is zero by the definition of the average velocity. Hence the overall number is constant in time.

### Linearization

Any function which is constant in $\Omega \times V$ is a stationary solution to equation (3.5) since in this case the average velocity is zero at each point. We set $u = M + w$, where $w$ is a small perturbation of the constant $M > 0$, and let $\tilde{M} = 2\pi\gamma M$. For $w$ we find

$$\begin{aligned} A(u) &= a(\bar{u})(s\cdot\bar{s} - |\bar{s}|^2)u \\ &= \left(a(\tilde{M}) + a'(\tilde{M})\bar{w}\right)\left(s\cdot\frac{1}{\tilde{M}}\int\sigma w(x,\sigma)d\sigma\right)(M+w) + \text{h.o.t.}(w) \\ &= \frac{a(\tilde{M})}{2\pi\gamma}\left(s\cdot\int\sigma w(x,\sigma)d\sigma\right) + \text{h.o.t.}(w). \end{aligned}$$

Hence the linear equation for $w$ reads

$$w_t + s \cdot \nabla_x w = \bar{a}\, s \cdot \int \sigma w(x,\sigma) d\sigma, \tag{3.6}$$

where $\bar{a} = a(\tilde{M})/(2\pi\gamma)$. Equivalently we write $x = (x_1, x_2)$ and $s = \gamma\binom{\cos\varphi}{\sin\varphi}$ with $\varphi \in [-\pi, \pi]$ and obtain the equation

$$w_t + \gamma(\cos\varphi\, w_{x_1} + \sin\varphi\, w_{x_2}) = \gamma\bar{a}\int_{-\pi}^{\pi} \cos(\varphi - \psi) w(t,x,\psi) d\psi. \tag{3.7}$$

The subspace of spatially constant functions $u(t,x,s) = u(t,s)$ is invariant for equations (3.5) and (3.6). The convolution operator on the right hand side of (3.7) acts only on the orientation variable $\varphi$. With respect to this variable the operator has rank one and hence is compact on $L^2(S^1)$. Its only nonzero eigenvalue is $\lambda_1 = \pi$ with corresponding eigenfunction $w_e = e^{i\varphi}$.

Using $w_e$ we can construct spatially constant eigenfunctions for (3.7): The function

$$w(t,x,\varphi) = e^{\lambda t} w(x,\varphi) = e^{\lambda t} w_e(\varphi)$$

is an eigenfunction of (3.7) to the eigenvalue

$$\lambda = \frac{a(\tilde{M})}{2}.$$

Hence the constant solution is linearly unstable.

### Allowing Random Turning

Like in the one dimensional case (2.3) we add a random reorientation process to the alignment interaction. Equation (3.5) becomes

$$u_t + s\nabla_x u = -\mu_* u(t,x,s) + \mu_*(Ku)(t,x,s) + A(u), \tag{3.8}$$

where $\mu_* > 0$ is the rate at which particles choose a new direction and $Ku = \int_V K_{s,s'} u(s') ds'$ gives the distribution of new directions (see (1.1)). In the simplest case particles choose the new direction without any preference, i.e. $K_{s,s'} = 1/|V|$. Repeating the linearization procedure from above we get that

$$w(t,x,\varphi) = e^{\lambda t} w_e(\varphi)$$

solves the linearized equation with

$$\lambda = \frac{\bar{a}}{2\gamma} - \mu_*. \tag{3.9}$$

Hence we get the same threshold behavior as in the one dimensional case.

### Discrete Sets of Velocities

We consider the non-spatial reaction differential equation (3.4), where we may assume $a = 1$, and hence the equation reads

$$u_t(t,s) = (s \cdot \bar{s} - |\bar{s}|^2) u(t,s), \qquad s \in S^1. \tag{3.10}$$

We observe that $u(0,s) = 0$ for some $s \in S^1$ implies $u(t,s) = 0$ for all $t \geq 0$. Individuals turn only into directions in which there are already some individuals. If we assume that initially individuals are oriented in finitely many directions, then we can reduce (3.10) to a system of finitely many ordinary differential equations as follows: We denote by $s_1, ..., s_n \in S^1$ the set of directions and by $u_i(t) = u(t, s_i), i = 1, ..., n$ the number of individuals in each direction. In the definition of $\bar{u}, \bar{s}$ we have to replace the integrals by sums, i.e.

$$\bar{u} = \sum_{i=1}^{n} u_i, \qquad \bar{s} = \frac{1}{\bar{u}} \sum_{i=1}^{n} s_i u_i.$$

Then we obtain the system

$$\dot{u}_i = f_i(u_1, ..., u_n) = (s_i \cdot \bar{s} - |\bar{s}|^2) u_i, \quad i = 1, ..., n. \tag{3.11}$$

The same procedure was used in [42] to approximate the solution of the alignment model presented there by a set of infinitely sharp peaks. Therefore the method is called the peak ansatz.

We investigate stationary solutions of (3.11) and their stability. If all individuals are concentrated in one direction, then $u_1 > 0, u_i = 0$ for $i = 2, ..., n$. Hence we have $\bar{s} = s_1$ which implies that $f_i = 0$ for all $i = 1, ..., n$, i.e. we have a stationary solution.

Next, for two nonzero directions we have $u_{1,2} > 0, u_i = 0$ for $i = 3, ..., n$. This situation is stationary if

$$(s_1 - \bar{s}) \cdot \bar{s} = 0, \qquad i = 1, 2, \tag{3.12}$$

where $\bar{u}\bar{s} = u_1 s_1 + u_2 s_2$. Obviously the condition is satisfied if $\bar{s} = 0$, i.e. $s_1 = -s_2, u_1 = u_2$. Equally many individuals are oriented in two opposite directions. Now suppose $\bar{s} \neq 0$. If we subtract the two equations in (3.12) we get

$$(s_1 - s_2) \cdot (u_1 s_1 + u_2 s_2) = 0.$$

Using $|s_i| = 1$ we get

$$(u_1 - u_2)(1 - s_1 \cdot s_2) = 0.$$

By assumption, the two directions are different, i.e. $s_1 \cdot s_2 \neq 1$. Necessarily then $u_1 = u_2$ as above for $\bar{s} = 0$. Hence, the situation with $u_1 = u_2 > 0, u_i = 0$ for $i = 3, ..., n$ is stationary.

For more than two nonzero directions, i.e. $u_1, ..., u_k > 0, u_{k+1}, ..., u_n = 0, k \geq 3$, stationary solutions are given by the condition $\bar{s} = 0$. Individuals in the directions $s_1, ..., s_k$ must be distributed such that the average velocity is zero. Note that a stationary solution for a given set of directions is not unique, not even up to scalar multiple, if $k \geq 4$. To see that there are no stationary solutions with $\bar{s} \neq 0$ consider again (3.12) which now has to be satisfied for $i = 1, ..., k$. If $0 < |\bar{s}| < 1$ then the equation $(s_i - \bar{s}) \cdot \bar{s} = 0$ together with $|s_i| = 1$ determines exactly two different directions $s_{1,2}$. Hence (3.12) cannot be satisfied for more than two different directions $s_i$.

LEMMA 3.1.1
*For $1 \leq k \leq n$ assume that $u_1, ..., u_k > 0, u_{k+1}, ..., u_n = 0$. Then the stationary states of (3.11) are given by*

1. *$u_1 > 0$ for $k = 1$.*
2. *$u_1 = u_2 > 0$ for $k = 2$.*
3. *$\bar{s} = 0$ for $k \geq 3$.*

We now investigate the stability of the stationary solutions of (3.11). The Jacobian of (3.11) is $J = (\partial f_i / \partial u_j)_{i,j}$ where

$$\frac{\partial f_i}{\partial u_j} = \frac{u_i}{\bar{u}} s_i \cdot s_j + \left(1 - \frac{u_i}{\bar{u}}\right) s_i \cdot \bar{s} - \frac{2u_i}{\bar{u}} s_j \cdot \bar{s} + \left(\frac{2u_i}{\bar{u}} - 1\right) \bar{s} \cdot \bar{s}. \tag{3.13}$$

The corresponding linear system $\dot{\xi} = J\xi, \qquad \xi = (\xi_1, ..., \xi_n)$, reduces to

$$\dot{\xi}_i = \frac{1}{n} s_i \sum s_j \xi_j$$

in the case $u_i = \bar{u}/n$ and $\bar{s} = 0$, which is the discrete non-spatial analogue of (3.6).

We first consider the case $k = 1$, i.e. $u_1 > 0, u_i = 0$ for $i = 2, ..., n$. Then $\bar{u} = u_1, \bar{s} = s_1$ and hence

$$J = \begin{pmatrix} 0 & a_2 & a_3 & ... & a_n \\ -a_2 & -a_2 & -a_2 & ... & -a_2 \\ -a_3 & -a_3 & -a_3 & ... & -a_3 \\ \vdots & \vdots & \vdots & & \vdots \\ -a_n & -a_n & -a_n & ... & -a_n \end{pmatrix},$$

where $a_i = 1 - s_1 \cdot s_i > 0, i = 2, ..., n$. We determine the eigenvalues of $J$. To this end we write $(a_2, a_3, ..., a_n) = g^T$, where $g^T$ denotes the transpose of the vector $g$, and set $e_{n-1}^T = (1, ..., 1)$, a vector of length $n - 1$. Then $J$ can be written as

$$J = \begin{pmatrix} 0 & g^T \\ -g & -ge_{n-1}^T \end{pmatrix},$$

and the eigenvalue problem $J\binom{x}{y} = \lambda\binom{x}{y}$ becomes

$$\begin{aligned} g^T y &= \lambda x, \\ -gx - ge_{n-1}^T y &= \lambda y, \end{aligned} \tag{3.14}$$

where $x$ is a scalar and $y$ is a vector of length $n - 1$.
Multiplying the second equation of (3.14) by $e_{n-1}^T$ from the left gives

$$e_{n-1}^T y = -\frac{e_{n-1}^T g x}{\lambda + e_{n-1}^T g}. \tag{3.15}$$

Multiplication of the same equation by $g^T$ from the left gives

$$-g^T g x - g^T g e_{n-1}^T y = \lambda g^T y. \tag{3.16}$$

Now we insert (3.15) and (3.16) into the first equation of (3.14) and get

$$\lambda^2 x = -g^T g x + g^T g \frac{e_{n-1}^T g x}{\lambda + e_{n-1}^T g}.$$

Substituting $G_1 = e_{n-1}^T g = \sum_{k>1} a_k$ and $G_2 = g^T g = \sum_{k>1} a_k^2$ and multiplying by $\lambda + G_1$ leads to

$$\lambda(\lambda^2 + G_1\lambda + G_2) = 0,$$

where we assumed $x \neq 0$. We have seen above that $G_1$ is a sum of positive numbers and hence it is positive. Obviously $G_2$ is positive as well. The nonzero eigenvalues $\lambda_{1,2}$ are given by

$$\lambda_{1,2} = -\frac{G_1}{2} \pm \frac{1}{2}\sqrt{G_1^2 - 4G_2}.$$

We see that either $\lambda_{1,2}$ are real and negative or they are complex conjugate with negative real part. In any case, the situation is stable.

Next we consider the case $k = 2$ and follow the same steps as above for $k = 1$. The Jacobian is

$$J = \begin{pmatrix} \alpha & \alpha & a_3 & ... & a_n \\ \alpha & \alpha & b_3 & ... & b_n \\ c_3 & c_3 & c_3 & ... & c_3 \\ \vdots & \vdots & \vdots & & \vdots \\ c_n & c_n & c_n & ... & c_n \end{pmatrix},$$

where $\alpha = (1 - s_1 \cdot s_2)/4 > 0$. The other coefficients are $a_j = (|\bar{s}| - s_j \cdot s_2)/2$, $b_j = (|\bar{s}| - s_j \cdot s_1)/2$ and $c_j = s_j \cdot \bar{s} - |\bar{s}| = -(a_j + b_j)$. Similarly as above we write

$$g^T = \begin{pmatrix} a_2 & a_3 & ... & a_n \\ b_2 & b_3 & ... & b_n \end{pmatrix}$$

and $e_k$ for the vector of length $k$ with all entries equal to one. Then

$$J = \begin{pmatrix} \alpha e_2 e_2^T & g^T \\ -g e_2 e_2^T & -g e_2 e_{n-2}^T \end{pmatrix}.$$

The eigenvalue problem $J\binom{x}{y} = \lambda\binom{x}{y}$ can be treated as above, except that now $x$ is a vector of length 2 and $y$ is a vector of length $n - 2$. Setting

$$G_1 = e_{n-2}^T g e_2 = \sum_{k>2}(a_k + b_k) \quad \text{and} \quad G_2 = e_2^T g^T g e_2 = \sum_{k>2}(a_k + b_k)^2$$

we find the following characteristic equation for $\lambda$:

$$\lambda^2 + (G_1 - \alpha)\lambda + G_2 - \alpha G_1 = 0,$$

and hence

$$\lambda_{1,2} = \frac{\alpha - G_1}{2} \pm \frac{1}{2}\sqrt{(G_1 - \alpha)^2 - 4(G_2 - \alpha G_1)}.$$

We consider the special case of $n$ equally spaced directions, i.e. $s_j = \binom{\cos\varphi_j}{\sin\varphi_j}$ with $e^{in\varphi_j} = 1$. Then we can compute $a - G_1$ simply as

$$\alpha - G_1 = \frac{1}{2} - \left(\frac{1}{4} + \frac{n}{2}\right)(1 + s_1 \cdot s_2).$$

We observe the following: In the limiting case $s_1 = s_2$ the value $\alpha - G_1$ is negative and $\alpha = 0$. Therefore the real part of both eigenvalues is negative and the situation is stable. In the other limiting case $s_1 = -s_2$ we have $\alpha - G_1 > 0$ and hence there is at least one eigenvalue with positive real part. The situation is unstable. By continuity we find that the situation of two nonzero directions is unstable if the two directions are far apart and stable if they are close together.

Finally we consider the case of $k \geq 3$ nonzero directions. We know that at a stationary solution, we necessarily have $\bar{s} = 0$. Then the entries of the Jacobian simplify to

$$\frac{\partial f_i}{\partial u_j} = \frac{u_i}{\bar{u}} s_i \cdot s_j$$

and hence the rank of the Jacobian is at most $k$. The nonzero eigenvalues are the eigenvalues of the upper left $k \times k$ submatrix. We consider only the two special cases $k = 3$ and $k = 4$ with $k$ equally spaced nonzero directions. We can order the directions to get $s_j = e^{2\pi i/j}$ for $j = 1, ..., k$. Then the characteristic polynomial of the $k \times k$ submatrix is

$$\begin{aligned} \lambda^3 - 3\lambda^2 + \frac{9}{4}\lambda - \frac{3}{4} = 0 \quad \text{for} \quad k = 3, \\ (1 - \lambda)^4 + 1 = 0 \quad \text{for} \quad k = 4. \end{aligned}$$

In the first case we use Descartes' rule of signs to see that there is a root with positive real part and hence the situation is unstable. In the second case we see that $(1 - \lambda)$ is of the form $e^{2\pi il/8}$ for $l = 1, 3, 5, 7$. Hence the real part of $\lambda$ is positive and the situation is unstable.

**The NEWS-System**

We now fix the four velocities $V = \{e^{\frac{ik\pi}{2}} \ : \ k = 0, .., 3\} \subset S^1$ and consider the two-dimensional alignment model with spatial movement. The four directions are called North, East, West and South and the corresponding densities are denoted by $E(t, x_1, x_2) = u(t, x_1, x_2, e^0)$, $W(t, x_1, x_2) = u(t, x_1, x_2, e^{i\pi})$ and so on.

This choice of $V$ is very convenient for numerical simulations. It was first introduced by Broadwell [6] to approximate the plane non-linear Boltzmann equation.

Equation (3.8) with constant kernel $K = 1/|V| = 1/4$ is rewritten as a hyperbolic system of the four densities as

$$\begin{aligned} N_t + N_{x_1} &= -\mu_* N + \mu_* U/4 + a(U)[S_2 - S_1^2 - S_2^2]N, \\ E_t + E_{x_2} &= -\mu_* E + \mu_* U/4 + a(U)[S_1 - S_1^2 - S_2^2]E, \\ W_t - W_{x_2} &= -\mu_* W + \mu_* U/4 + a(U)[-S_1 - S_1^2 - S_2^2]W, \\ S_t - S_{x_1} &= -\mu_* S + \mu_* U/4 + a(U)[-S_2 - S_1^2 - S_2^2]S, \end{aligned}$$

where $U = N + E + S + W$ and $\bar{s} = (S_1, S_2) = \frac{1}{U}(E - W, N - S)$.

In the simulation below we take $a = \text{const.} = 1$ and $\mu_* = 0.005$ such that the homogeneous solution is unstable. Initial values are equal and spatially constant in all four directions and a small peak is added in the North-direction on a little square within the domain. We impose periodic boundary conditions, plot the solution every time the peak has completed one round and compare the snapshots.

The peak moves parallel to the East-West axis and grows in height as particles from the other directions align with the majority that moves North. Until round 13, the density where the peak has passed is lower than where it did not pass. Then from round 14 on, the density in the track of the peak is higher than outside of it.

The following happens: The aligning forces at the location of the peak are strongest for the South-direction. At the peak, most of the South going particles turn into the North-direction and align with the majority in the peak. Then also behind the peak the average velocity points North and hence the North-direction slowly gains particles although the peak has moved on. From round 14 on this gain is higher than the loss in the other directions and the total density in the trace rises above that outside the trace.

**Total Density $U$ of the NEWS System**

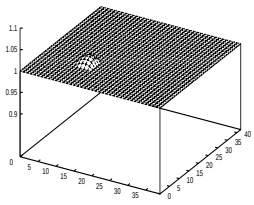

Initial values

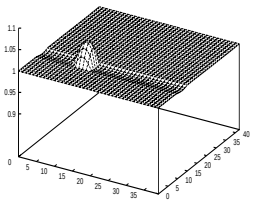

Round 9

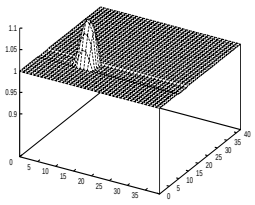

Round 13

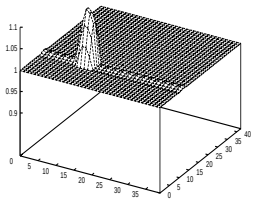

Round 14

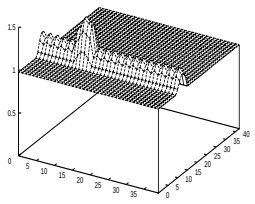

Round 20

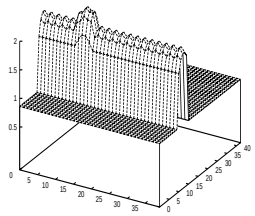

Round 30

## 3.2 Existence of Solutions

There are several possibilities to choose appropriate function spaces for the model equation (3.5) and to show existence of solutions. Below we show existence and uniqueness of global in time solutions which are integrable on $\mathbb{R}^2 \times V$. We use the method of characteristics and assume $a = 1$.

If one chooses $a = a_\delta(\bar{u}) = \bar{u}^2/(\delta + \bar{u}^2)$ for some $\delta > 0$ then the proof below can be adapted to show existence and uniqueness of global in time solutions in

the space of bounded functions, $L^\infty(\mathbb{R}^2 \times V)$.

Working on bounded space domains $\Omega \subset \mathbb{R}^2$, one could impose boundary conditions as described in [59]. If one chooses again $a = a_\delta$ as above, then the conditions of Theorem 4.5 in [59] are satisfied and local existence of solutions follows.

To show existence of solutions in $L^1(\mathbb{R}^2 \times V)$ we now assume $a = 1$ and set

$$Y\colon = L^\infty([0,T], L^1(\mathbb{R}^2 \times V))$$

with the usual norm. A function $u \in Y$ is called a *mild solution* of (3.5) if it satisfies the equation after integration along characteristics (compare (2.14)). For given $u_0 \in L^1(\mathbb{R}^2 \times V)$ and $w \in Y$ we define the operator

$$\mathcal{G}(w)(t,x,s)\colon = u_0(x - st, s) + \int_0^t A(w)(\tau, x - s(t-\tau), s)d\tau \tag{3.17}$$

by integration along the characteristics. We show that $\mathcal{G}$ is a contraction in the space $Y$ for sufficiently small $T$. The resulting fixed point is the unique mild solution of (3.5) in $Y$.

LEMMA 3.2.1
*The operator $A$ from (3.5) is homogeneous of degree 1. We set $A(0) = 0$. Then the reaction term $A\colon Y \to Y$ is well defined and Lipschitz.*

PROOF.
Suppose $\bar{u}(t,x) > 0$. Then the average velocity does not exceed the particle speed:

$$\begin{aligned} \|\bar{s}(u)(t,x,s)\|_{\mathbb{R}^2} &= \frac{1}{|\int_V u(t,x,s)ds|} \left\| \int_V \sigma u(t,x,\sigma)d\sigma \right\|_{\mathbb{R}^2} \\ &\leq \frac{\gamma}{\|u(t,x,\cdot)\|_{L^1}} \int_V |u(t,x,\sigma)|d\sigma \leq \gamma. \end{aligned}$$

The function $\bar{s}$ is homogeneous of degree 0. We may set $\bar{s}(0) = 0$ to get an everywhere defined bounded function. The function $A$ maps $Y$ into itself and is sublinear. Pick $w \in Y$ and compute

$$\begin{aligned} \|A(w)\|_Y &= \sup_{0\leq t\leq T} \int_V \int_{\mathbb{R}^2} \left| s \cdot \bar{s} - |\bar{s}|^2 \right| |w(t,x,s)|dxds \\ &\leq 2\gamma^2 \sup_{0\leq t\leq T} \|w(t)\|_{L^1(\mathbb{R}^1\times V)} = 2\gamma^2 \|w\|_Y. \end{aligned}$$

The function $A$ is globally Lipschitz on $Y$. Write

$$A(w) = A_1(w)w \qquad \text{with} \qquad A_1(w) = s \cdot \bar{s}(w) - |\bar{s}(w)|^2 \leq 2\gamma^2.$$

Then for $0 \neq w, \tilde{w} \in Y$ we compute

$$\|A(w) - A(\tilde{w})\|_Y \leq \sup_{0\leq t\leq T} \int_V \int_{\mathbb{R}^2} |(A_1(w) - A_1(\tilde{w}))w| + |A_1(\tilde{w})(w - \tilde{w})|dxds.$$

The second term can be estimated by $2\gamma^2\|w-\tilde{w}\|$ since $A_1$ is bounded. To estimate the first term we write $\bar{s}w = \bar{s}(w)$, keeping in mind that the function $\bar{s}$ is not linear in $w$. We also neglect the $t$-dependence for the moment.

$$\begin{aligned}
& \int_V \int_{\mathbb{R}^2} |(s\cdot \bar{s}w - |\bar{s}w|^2 - s\cdot\bar{s}\tilde{w} + |\bar{s}\tilde{w}|^2)||w| dx ds \\
= & \int_V \int_{\mathbb{R}^2} |[s - (\bar{s}w + \bar{s}\tilde{w})]\cdot(\bar{s}w - \bar{s}\tilde{w})|\,|w| dx ds \\
\leq & \int_V \int_{\mathbb{R}^2} 3\gamma |\bar{s}w - \bar{s}\tilde{w}||w| dx ds \\
= & 3\gamma \int_{\mathbb{R}^2} \left( \left| \frac{1}{\bar{w}} \int \sigma w d\sigma - \frac{1}{\bar{\tilde{w}}} \int \sigma \tilde{w} d\sigma \right| \int_V |w| ds \right) dx \\
\leq & 3\gamma \int_{\mathbb{R}^2} \left( \left| \frac{1}{\bar{w}} \int \sigma (w-\tilde{w}) d\sigma \right| + \left| (\frac{1}{\bar{w}} - \frac{1}{\bar{\tilde{w}}}) \int \sigma \tilde{w} d\sigma \right| \right) \|w(x,\cdot)\|_{L^1} dx \\
\leq & 3\gamma \int_{\mathbb{R}^2} \left| \int \sigma (w-\tilde{w}) d\sigma \right| dx + \int_{\mathbb{R}^2} \left| \frac{\bar{\tilde{w}} - \bar{w}}{\bar{w}\bar{\tilde{w}}} \int \sigma \tilde{w} d\sigma \right| \|w(x,\cdot)\|_{L^1} dx \\
\leq & 4\gamma^2 \|w - \tilde{w}\|_{L^1(\mathbb{R}^1 \times V)}
\end{aligned}$$

Taking into account the dependence on $t$ again and putting the two estimates together we get

$$\|A(w) - A(\tilde{w})\|_Y \leq 6\gamma^2 \|w - \tilde{w}\|_Y.$$

This estimates also holds in the case $\tilde{w} = 0$. By sublinearity we find

$$\|A(w) - A(\tilde{w})\|_Y = \|A(w)\|_Y \leq 2\gamma^2 \|w\|_Y \leq 6\gamma^2 \|w - \tilde{w}\|_Y.$$

■

THEOREM 3.2.2
*For all nonnegative initial data $u_0 \in L^1(\mathbb{R}^2 \times V)$ there exists a unique mild solution $u \in L^\infty([0,\infty), L^1(\mathbb{R}^2 \times V))$ to equation (3.5) with $u(0) = u_0$.*

PROOF.
To show local existence we adapt the proof of Theorem 2.2.1. Suppose $\|u_0\|_{L^1(V\times\mathbb{R}^2)} \leq k_0$ and choose $N = k_0 + \varepsilon$ for some $\varepsilon > 0$. The operator $\mathcal{G}$ from (3.17) leaves the ball $B(N) \subset Y$ of radius $N$ invariant. Take $w \in B(N)$ with $\|w\|_Y \leq N$. Then

$$\begin{aligned}
\|\mathcal{G}(w)\|_Y &\leq \|u_0\|_{L^1} + \left\| \int_0^t A(w)(\tau) d\tau \right\|_Y \\
&\leq \|u_0\|_{L^1} + \sup_{0\leq t\leq T} \int_0^t \|A(w)\|_Y d\tau \\
&\leq \|u_0\|_{L^1} + 2\gamma^2 T \|w\|_Y.
\end{aligned}$$

Hence for $T < \varepsilon/(2\gamma^2 N)$ the norm of $\mathcal{G}(w)$ is less than $N$. To show that $\mathcal{G}$ is a contraction we make use of the Lipschitz property of $A$.

$$\begin{aligned}\|\mathcal{G}(w) - \mathcal{G}(\tilde{w})\|_Y &= \left\| \int_0^t (A(w) - A(\tilde{w}))(\tau) d\tau \right\|_Y \\ &\leq \sup_{0\leq t\leq T} \int_0^t 4\gamma^2 \|w - \tilde{w}\|_Y d\tau \\ &\leq 4\gamma^2 T \|w - \tilde{w}\|_Y\end{aligned}$$

For $T < 1/(4\gamma^2)$ we get a contraction. By construction the unique fixed point $u \in Y$ is the solution of the equation. Using again equation (3.17) for $u$ we find that

$$\|u(t)\|_{L^1} \leq \|u_0\|_{L^1} + \int_0^t 2\gamma^2 \|u(\tau)\|_{L^1} d\tau.$$

An application of Gronwall's lemma finishes the proof. ∎

## 3.3 General Models for Orientation Processes

We compare the alignment model presented here with the two approaches described in the introduction. To that end we formulate a general (non-spatial) model equation for orientation processes. Then we show that for suitable choices of parameter functions we get as special cases the model equation (3.4) or the Model III of Edelstein-Keshet et al. for $\varepsilon = 0$, i.e.

$$u_t(t,\varphi) = u(t,\varphi) \int_{-\pi}^{\pi} Q_1(u(\varphi) - u(\varphi_1)) Q_2(\varphi - \varphi_1) u(\varphi_1) d\varphi_1, \tag{3.18}$$

or the model of Geigant et al., which reads

$$\begin{aligned}\frac{\partial}{\partial t} u(t,\varphi) &= -u(t,\varphi) \int_{-\pi}^{\pi} \zeta(\varphi - \varphi_1) u(t,\varphi_1) d\varphi_1 \\ &+ \int_{-\pi}^{\pi} \int_{-\pi}^{\pi} \omega(\varphi_0 - \varphi, \varphi_0 - \varphi_1) \zeta(\varphi_0 - \varphi_1) u(t,\varphi_1) u(t,\varphi_0) d\varphi_1 d\varphi_0.\end{aligned} \tag{3.19}$$

(For a detailed description of the models see the introduction.)

We observe that (3.19) contains only quadratic terms of the density. The interaction rate $\zeta$ and the turning probability $\omega$ are independent of the density. On the contrary, (3.4) and (3.18) contain terms of third order. Furthermore, suppose that there is a direction $\varphi_*$, say, in which there are no particles initially. Then in the models (3.4) and (3.18) no particles turn into this direction, i.e. $u(t,\varphi_*) = 0$ for all $t > 0$. To the contrary, in model (3.19) particles can turn into intermediate angles and hence in general $u(t,\varphi_*) \neq 0$, depending on $\omega$.

We generalize (3.19) for some given (compact) state space $V$. First, like in the population dominance model [30], we let $\zeta, \omega$ depend on the different angles instead of the differences only. Second, we let $\zeta, \omega$ depend on the particle density.

In the most general case, the turning probability and the interaction rate depend on the whole density distribution $u(\cdot)$, and hence we write

$$\omega = \omega^u(\varphi, \varphi_0, \varphi_1) = \omega(u(\cdot), \varphi, \varphi_0, \varphi_1) \tag{3.20}$$

for the probability that a particle in state $\varphi_0$ upon interaction with a particle in state $\varphi_1$ ends up in state $\varphi$. And the interaction rate of a particle in state $\varphi$ with another one in state $\varphi_1$ is

$$\zeta = \zeta^u(\varphi, \varphi_1) = \zeta(u(\cdot), \varphi, \varphi_1). \tag{3.21}$$

We require that $\zeta$ and $\omega$ are nonnegative and that $\omega$ satisfies

$$\int_{-\pi}^{\pi} \omega^u(\varphi, \varphi_0, \varphi_1) d\varphi = 1.$$

Then the following general model equation preserves the total mass $\int u d\varphi$ :

$$\begin{aligned} u_t(\varphi) &= -u(\varphi) \int_V \zeta^u(\varphi, \varphi_1) u(\varphi_1) d\varphi_1 \\ &+ \int_V \int_V \omega^u(\varphi, \varphi_0, \varphi_1) \zeta(\varphi_0, \varphi_1) u(\varphi_0) u(\varphi_1) d\varphi_0 d\varphi_1. \end{aligned} \tag{3.22}$$

This formulation for a gain-loss process is too general for most applications. Usually the process to be modeled imposes natural restrictions. For example, a model for a reorientation process on $V = S^1 \cong [-\pi, \pi]$, which is independent of external influences, should be rotationally invariant. If the interaction rate is independent of the density, then it should be symmetric with respect to interchanging its arguments, i.e.

$$\zeta(\varphi, \varphi_0) = \zeta(\varphi_0, \varphi).$$

One finds that $\zeta(\varphi, \varphi_0) = \zeta(\varphi - \varphi_0)$ must be an even function of the difference. Otherwise the first integral on the right hand side of (3.22) is not rotationally invariant. If the interaction rate does depend on the density, then the equation can be rotationally invariant even though the symmetry condition above is not satisfied.

It is obvious that (3.19) is a special case of (3.22). In the following we show how to derive (3.4) and (3.18) from (3.22).

THEOREM 3.3.1
*If one chooses*

$$\zeta^u(\varphi, \varphi_1) = \frac{1}{2\pi} (1 - \cos(\varphi - \varphi_1)) \quad \text{and} \quad \omega^u(\varphi, \varphi_0, \varphi_1) = \frac{u(\varphi)}{\int_V u(\psi) d\psi}$$

*then the general model (3.22) becomes (3.4).*

PROOF.
Obviously the requirements for the functions $\zeta$ and $\omega$ are fulfilled. Then equation (3.19) conserves total mass $\bar{u}$. We write $s = \binom{\cos\varphi}{\sin\varphi}$ and $\sigma = \binom{\cos\varphi_1}{\cos\varphi_1}$ and find

$s \cdot \sigma = \cos(\varphi - \varphi_1)$. We compute (neglecting the normalizing factor $1/2\pi$ and defining $\bar{s}$ analogously to (3.3))

$$\begin{aligned} & -u(\varphi) \int_{-\pi}^{\pi} \zeta^u(\varphi - \varphi_1) u(\varphi_1) d\varphi_1 \\ = \; & -u(\varphi) \int_{-\pi}^{\pi} u(\varphi_1) d\varphi_1 + u(\varphi) \int_{-\pi}^{\pi} \cos(\varphi - \varphi_1) u(\varphi_1) d\varphi_1 \\ = \; & -u(\varphi)\bar{u} + u(\varphi)\, s \cdot \int_{-\pi}^{\pi} \sigma u(\varphi_1) d\varphi_1 \\ = \; & -u(\varphi)\bar{u} + u(\varphi)\bar{u}\, s \cdot \bar{s}. \end{aligned}$$

And the second term gives (up to a factor $1/2\pi$)

$$\begin{aligned} & \int_{-\pi}^{\pi} \int_{-\pi}^{\pi} \omega^u(\varphi, \varphi_0, \varphi_1) \zeta(\varphi_0 - \varphi_1) u(\varphi_1) u(\varphi_0) d\varphi_1 d\varphi_0 \\ = \; & \frac{u(\varphi)}{\bar{u}} \int_{-\pi}^{\pi} \int_{-\pi}^{\pi} (1 - \cos(\varphi_0 - \varphi_1)) u(\varphi_1) u(\varphi_0) d\varphi_1 d\varphi_0 \\ = \; & \frac{u(\varphi)}{\bar{u}} \bar{u}^2 \left[1 - \bar{s} \cdot \bar{s}\right]. \end{aligned}$$

Inserting these two results in equation (3.22) we get

$$\begin{aligned} u_t &= -u(\varphi)\bar{u} + u(\varphi)\bar{u}s\bar{s} + u(\varphi)\bar{u} - u(\varphi)\bar{u}|\bar{s}|^2 \\ &= u(\varphi)\bar{u}(s\bar{s} - |\bar{s}|^2), \end{aligned}$$

which is (3.4). ∎

THEOREM 3.3.2
*If one chooses*

$$\zeta^u(\varphi, \varphi_0) = Q_1^-(u(\varphi) - u(\varphi_0))Q_2(\varphi - \varphi_0) \quad \text{and} \quad \omega^u(\varphi, \varphi_0, \varphi_1) = \delta(\varphi - \varphi_1),$$

*where $Q_1^-$ is the negative part of $Q_1$, then the general model (3.22) becomes (3.18).*

PROOF.
We write $Q_1 = Q_1^+ - Q_1^-$ for the positive and negative part. Since $Q_1$ is odd, we have $Q_1^+(x) = Q_1^-(-x)$. Then we compute, starting from equation (3.18),

$$\begin{aligned} u_t &= u(\varphi) \int_{-\pi}^{\pi} Q_1(u(\varphi) - u(\varphi_1)) Q_2(\varphi - \varphi_1) u(\varphi_1) d\varphi_1 \\ &= -u(\varphi) \int_{-\pi}^{\pi} Q_1^-(u(\varphi) - u(\varphi_1)) Q_2(\varphi - \varphi_1) u(\varphi_1) d\varphi_1 \\ &\quad + u(\varphi) \int_{-\pi}^{\pi} Q_1^+(u(\varphi) - u(\varphi_1)) Q_2(\varphi - \varphi_1) u(\varphi_1) d\varphi_1 \\ &= -u(\varphi) \int_{-\pi}^{\pi} Q_1^-(u(\varphi) - u(\varphi_1)) Q_2(\varphi - \varphi_1) u(\varphi_1) d\varphi_1 \\ &\quad + \int_{-\pi}^{\pi} \int_{-\pi}^{\pi} \delta(\varphi - \varphi_0) Q_1^-(u(\varphi_0) - u(\varphi_1)) Q_2(\varphi_0 - \varphi_1) u(\varphi_1) u(\varphi_0) d\varphi_1 d\varphi_0. \end{aligned}$$

The last equation has the form of the general model (3.22). Note that here we have $\zeta^u(\varphi, \varphi_0) = -\zeta^u(\varphi_0, \varphi)$, i.e. the turning function is not symmetric with respect

to interchanging its arguments. But the equation is rotationally invariant. To see this, assume that $u$ is a solution and set $v(\varphi) = u(\Phi + \varphi)$. Then

$$\begin{aligned} v_t &= u(\Phi+\varphi)\int_{-\pi}^{\pi} Q_1(u(\Phi+\varphi)-u(\varphi_1))Q_2(\Phi+\varphi-\varphi_1)u(\varphi_1)d\varphi_1 \\ &= u(\Phi+\varphi)\int_{-\pi}^{\pi} Q_1(u(\Phi+\varphi)-u(\Phi+\varphi_0))Q_2(\varphi-\varphi_0)u(\Phi+\varphi_0)d\varphi_0 \\ &= v(\phi)\int_{-\pi}^{\pi} Q_1(v(\varphi)-v(\varphi_0))Q_2(\varphi-\varphi_0)v(\varphi_0)d\varphi_0. \end{aligned}$$

■

Interpreting the parameter functions we see that for the model equation (3.4) the turning probability is independent of the interaction angles. The probability that an individual turns into some direction depends simply on the relative density of individuals in that direction. The interaction rate increases as the angular difference between interaction partners increases. Individuals in opposite directions interact strongly, which can be interpreted as a mechanism to avoid collisions, whereas almost aligned individuals interact only weakly, which may account for the fact that fish in a school are never perfectly aligned.

In deriving (3.18) it was assumed that particles can turn only into the direction of their interaction partner. This restriction is reflected in the fact that the turning probability for (3.18) is a delta-distribution.

### The General Model Applied to 1D

The general equation (3.22) can also be applied to model alignment together with speed adaptation in one space dimension. If we denote by $V \subset \mathbb{R}$ the set of speeds, then the time evolution of the density $u = u(t, x, s)$ is given by the following equation:

$$\begin{aligned} u_t + su_x &= -u(t,x,s)\int_V \zeta^u(s,s')u(s')ds' \\ &+ \int_V\int_V \omega^u(s,s',s'')\zeta(s',s'')u(s')u(s'')ds'ds''. \end{aligned} \tag{3.23}$$

We do not discuss possible choices of parameters. Instead we show that if the parameter functions do not depend on the density and if we only have two speeds $V = \{\pm\gamma\}$ as in Chapter 2, then one cannot model alignment with this approach. This is why our one dimensional model (2.3) had to contain terms of order at least three in the density.

Lemma 3.3.3
*In any interaction based orientation model on the line with speeds $s \in \{\pm\gamma\}$, density independent parameters and without external bias, the stationary solution $u^+ = u^- = \text{const.}$ is linearly stable.*

Proof.
We abbreviate $\pm$ for $\pm\gamma_*$. The non bias condition that the model itself does not prefer any direction gives some symmetry conditions for $\zeta$ and $\omega$, namely

$$\begin{aligned} &\zeta(+,-) = \zeta(-,+), \qquad \zeta(+,+) = \zeta(-,-), \\ &\omega(s_1,s_2,s_3) = \omega(-s_1,-s_2,-s_3). \end{aligned}$$

We abbreviate $\zeta^{s_1}_{s_2} = \zeta(s_1, s_2)$ and $\omega^{s_1}_{s_2}(s_3) = \omega(s_1, s_2, s_3)$. The model equation for $u^+$ reads

$$\begin{aligned} & u^+_t + \gamma_* u^+_x = \\ = \; & -u^+[\zeta^+_+ u^+ + \zeta^+_- u^-] \\ & +\omega^+_+(+)\zeta^+_+(u^+)^2 + \omega^+_-(+)\zeta^+_- u^+u^- + \omega^-_+(+)\zeta^-_+ u^+u^- + \omega^-_-(+)\zeta^-_-(u^-)^2 \\ \\ = \; & \zeta^+_+ \left(\omega^+_+(+) - 1\right)(u^+)^2 + \omega^-_-(+)\zeta^-_-(u^-)^2\zeta^+_- \left(\omega^+_-(+) + \omega^-_+(+) - 1\right) u^+u^-. \end{aligned}$$

Now we use the symmetry conditions and the fact that $\omega$ is a probability distribution, i.e.

$$\begin{aligned} \omega(+,-,+) &= 1 - \omega(+,-,-) = 1 - \omega(-,+,+), \\ \omega(-,-,+) &= \omega(+,+,-) = 1 - \omega(+,+,+). \end{aligned}$$

The factor for the mixed term $u^+u^-$ is zero and setting $\bar{\omega} := \omega^+_+(+)\zeta^+_+$ we arrive at

$$u^+_t \gamma_* u^+_x = -\bar{\omega} {u^+}^2 + \bar{\omega} {u^-}^2 = \bar{\omega} u(u^- - u^+).$$

A similar calculation for $u^-_t$ gives the system

$$\begin{aligned} u^+_t + \gamma u^+_x &= \bar{\omega} u(u^- - u^+), \\ u^-_t - \gamma u^-_x &= \bar{\omega} u(u^+ - u^-), \end{aligned}$$

where $\bar{\omega} > 0$ and $u = u^+ + u^- > 0$. Since the factor $\bar{\omega} u$ is positive, the solution $u^+ = u^- = \text{const.}$ is linearly stable. ■

# Chapter 4

# Speed Adaptation

So far we assumed that individuals move with constant speed and change only their direction of motion in order to form moving polarized groups.

It has long been observed and documented that fish (and other individuals forming moving polarized groups) also adjust their speed, i.e. slow down or speed up, in order to join a school or stay with it (cf. [55]). Some models even suggest that constant speed in groups would lead to break up of these groups [12].

Here we derive a model for the speed adaptation process in one space dimension. Individuals move on the line to the right and to the left with speeds $\gamma^{\pm}$, respectively. They change direction according to the turning function $\mu$ in (2.8). The speeds $\gamma^{\pm}$ depend on the density and the density gradient.

First we derive the model equation for a somewhat simpler situation where all particles move in one direction. We investigate some properties of this model. We prove existence results for a parabolically regularized version of the model and use the vanishing viscosity approach to show existence of solutions for the hyperbolic model as well. Finally we formulate the full system with two directions of movement and check which of the results for the simpler equations carry over to the full system.

## 4.1 The Model Equations

At the end of the previous chapter we briefly indicated one possibility how movement on the line with non constant speed can be modeled. One chooses some set of velocities $V \subset \mathbb{R}^2$. At each point in space there may be individuals with different velocities. These individuals interact.

Here we want to follow another approach which can also be found in reaction random walk models for chemotaxis, for example in [27, 28]. We assume that the conditions at each space point $x$ determine exactly two different speeds $\gamma^{\pm}(x)$. All individuals at $x$ which move to the right have the speed $\gamma^{+}(x)$ and all individuals at $x$ which move to the left have the speed $\gamma^{-}(x)$.

In the first part of this chapter we consider the following simpler situation: Suppose that, as a result of the alignment process, all individuals move in the same direction, to the right, say. Then we may drop the superscript "+". The

school as a one-dimensional moving object is described by a conservation law

$$\frac{\partial}{\partial t}u(t,x) + \frac{\partial}{\partial x}(\gamma(t,x)u(t,x)) = 0, \tag{4.1}$$

where the speed $\gamma$ is positive. The process by which individuals adapt their speed to that of their neighbors is modeled by a partial differential equation for $\gamma$ and hence, we obtain a system of two equations for the density $u$ and the speed $\gamma$.

To model the speed adaptation, we assume that there is an *optimal* or *target density* $u_*$ and a *preferred velocity* $\gamma_*$ (see [39] and references therein, [18, 55]). Individuals try to approach areas with optimal density. In order to do so, they deviate by some amount $\eta$ from their preferred speed so that the actual speed can be written as

$$\gamma(t,x) = \gamma_* + \eta(t,x). \tag{4.2}$$

The deviation $\eta$ depends on whether individuals want to reach areas of higher or lower densities. It also depends on whether these areas of higher or lower density can be found in front of the individuals or behind them. Mathematically this means that $\eta(t,x)$ cannot depend on the value $u(t,x)$ alone but must incorporate some non-local information. This information is given by the gradient of $u$.

In the literature about conservation laws, the speed depends on the density but not on the gradient. As we just saw, dependence on the density alone is not sufficient to model speed adaptation. Some directional information is needed. These considerations are supported by a result of Flierl et al. [12]. Starting from a stochastic model, they derive a partial differential equation for the density of a socially aggregating population. Higher order moments are needed to describe the density flux.

At any given time $t$ an individual at position $x$ perceives the given density $u(t,x)$ and compares it with the optimal density $u_*$. Suppose $u(t,x) < u_*$. Remember, all individuals are moving in the same direction. If the gradient $u_x(t,x)$ is positive, then by speeding up the individual can reach areas in which the density is closer to $u_*$ than $u(t,x)$ is. Hence we want $\eta(t,x) > 0$. If $u(t,x) < u_*$ and $u_x(t,x) < 0$ then similarly we want $\eta(t,x) < 0$. The considerations for $u(t,x) > u_*$ are similar. To capture this qualitative behavior we define an auxiliary function $\tilde{F} = \tilde{F}(u, u_x)$ which has the following properties

$$\tilde{F} \quad \text{is bounded,} \qquad \tilde{F} > 0 \quad \text{in I and III,} \qquad \tilde{F} < 0 \quad \text{in II and IV.}$$

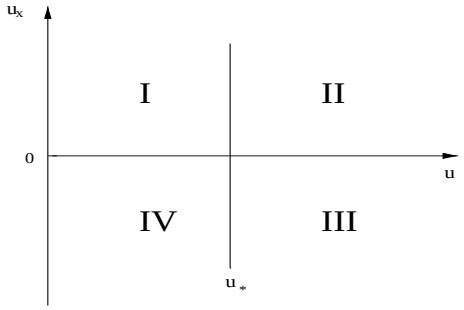


A function with these properties is for example

$$\tilde{F}(u, u_x) = \tanh[(u_* - u)u_x]. \tag{4.3}$$

We introduce a sensitivity parameter $\chi > 0$ and set $F = \chi\tilde{F}$. In the simplest case one might try to set $\eta = F$. If we substitute this into equation (4.1) and perform the differentiation with respect to $x$, then we obtain the equation

$$u_t + [F_2(u, u_x)u]u_{xx} + [F_1(u, u_x)u + F(u, u_x)]u_x = 0,$$

where $F_j$ denotes the derivative of $F$ with respect to the $j$-th variable. From the properties of the function $F$ it is clear that the coefficient in front of $u_{xx}$ changes sign. Hence the problem is ill-posed. This seems to be a typical situation for velocity dependent aggregation phenomena (compare [3, 16, 39] and also [53, 54] in a different context).

To circumvent this difficulty we assume that individuals adjust their velocity with a small time lag and a small error. Then $\eta$ satisfies the following equation.

$$\tau\eta_t = \beta\eta_{xx} - \eta + F(u, u_x), \tag{4.4}$$

where $\tau$ measures the time lag and $\beta$ determines the variance of the error. Now we assume in addition some random movement of individuals which we model by adding $\varepsilon u_{xx}$ on the right hand side of (4.1). Then equations (4.1), (4.2) and (4.4) form the following system which is our model problem for the first part of this chapter:

$$\begin{aligned} u_t + (\gamma u)_x &= \varepsilon u_{xx}, && (4.5)\\ \tau\eta_t &= \beta\eta_{xx} + F(u, u_x) - \eta, && (4.6)\\ \gamma &= \gamma_* + \eta, \end{aligned}$$

where $\varepsilon, \beta > 0, \tau \geq 0$ are (small) constants. Alternatively we write

$$E = F + \gamma_* = \chi\tilde{F} + \gamma_*$$

and call it the *expected velocity* since it is the velocity that occurs if the adjustment process is precise, i.e. $\tau = \beta = 0$. Since we model a school moving in one direction only, we choose $\chi$ such that

$$E \geq 0.$$

We assumed that $F$ is bounded, and hence $E$ is also bounded by some value $E_{\max}$. We get the following equivalent formulation of our model system.

$$\begin{aligned} u_t + (\gamma u)_x &= \varepsilon u_{xx}, && (4.7)\\ \tau\gamma_t &= \beta\gamma_{xx} + E(u, u_x) - \gamma. && (4.8) \end{aligned}$$

We use both notations (4.5), (4.6) and (4.7), (4.8) whichever is the more convenient. For $\tau > 0$ the system is parabolic. If we prescribe initial data $u_0, \gamma_0$ in appropriate spaces then the initial value problem is well-posed. For $\tau = 0$ the second equation is an elliptic equation which has to be satisfied for all $t$. We can prescribe initial data only for the density, i.e. $u_0$. The values of $\gamma$ at $t = 0$ are determined by the elliptic equation. We show later that the system is well-posed for $\tau = 0$ in some appropriate function space.

LEMMA 4.1.1
*The system (4.7), (4.8) preserves positivity of $u$.*

PROOF.
Suppose a solution $(u, \gamma)$ exists up to some time $T > 0$ and is smooth. Suppose also that $u_0 > 0$. We write (4.7) as

$$-u_t + \varepsilon u_{xx} - \gamma u_x - \gamma_x u = 0$$

and apply the maximum principle to get $u \geq 0$ [57]. ∎

Positivity of $\gamma$ is not more difficult to show. We give a proof together with other estimates on $\gamma$ for the different cases $\tau > 0, \tau = 0$ later.

### 4.1.1 Linearization

The pair of constant functions $(\bar{u}, \gamma_*)$ is a stationary solution to the system (4.7), (4.8) for all values $\bar{u} \geq 0$. We investigate the stability of this solution in both cases $\tau > 0$ and $\tau = 0$. Whether this solution is stable or not depends on the difference $\bar{u} - u_*$. The biological reason for this dependence is clear: Suppose the actual density $\bar{u}$ is lower than the preferred density $u_*$. Then a small perturbation of $\bar{u}$ triggers the formation of denser patches and the formation of empty places since individuals try to approach areas of higher densities. In contrast, if $\bar{u} > u_*$ then small perturbations of $\bar{u}$ are flattened out. Individuals seek areas of lower densities.

**Case 1:** $\tau = 0$
Here and in the following we frequently use the Green's function for $1 - \beta\Delta$ on $\mathbb{R}$ and its Fourier transform and denote it by $G$ and $\hat{G}$. The explicit formulas are

$$G(x) = \sqrt{\frac{\pi}{2\beta}}\, e^{-\frac{|x|}{\sqrt{\beta}}} \qquad \text{and} \qquad \hat{G}(\kappa) = \frac{1}{\beta\kappa^2 + 1}.$$

We write the solution of (4.8) as

$$\gamma(t, \cdot) = E(u, u_x)(t) * G. \tag{4.9}$$

We now let $u = \bar{u} + v$ and expand

$$E(u, u_x) = E(\bar{u}, 0) + E_1(\bar{u}, 0)v + E_2(\bar{u}, 0)v_x + \text{h.o.t.}(v), \tag{4.10}$$

where subscripts of $E$ denote partial derivatives with respect to the first and second variable. The special choice of $\tilde{F}$ in (4.3) gives $E(\bar{u}, 0) = \gamma_*$, $E_1(\bar{u}, 0) = 0$ and $E_2(\bar{u}, 0) = \gamma_* \chi(u_* - \bar{u})$. The sign change for $E_2$ at $\bar{u} = u_*$ is a natural consequence of the modeling assumptions. It determines the stability behavior. Plugging the expansion of $E$ into the representation of $\gamma$ we obtain

$$\gamma = E(\bar{u}, 0) * G + E_1(\bar{u}, 0)v * G + E_2(\bar{u}, 0)v_x * G + \text{h.o.t.}(v) \tag{4.11}$$

and

$$\gamma_x = E_1(\bar{u}, 0)v_x * G + E_2(\bar{u}, 0)v_{xx} * G + \text{h.o.t.}(v). \tag{4.12}$$

Putting this into equation (4.7) for $u$ and retaining only linear terms in $v$ we get the following equation

$$v_t = \varepsilon v_{xx} - A v_x - B(v_x * G) - C(\bar{u})(v_{xx} * G), \tag{4.13}$$

where $A = E(\bar{u}, 0) \int G(y)dy$, $B = \bar{u}E_1(\bar{u}, 0)$ and $C = \bar{u}E_2(\bar{u}, 0)$ are constants. The Fourier transform of (4.13) is

$$\hat{v}_t = \kappa^2(C\hat{G} - \varepsilon)\hat{v} + i\kappa(A + B\hat{G})\hat{v}, \tag{4.14}$$

where $\hat{G}$ is real and positive. The growth of $\hat{v}$ is determined by the factor of $\kappa^2$. If $\bar{u} > u_*$ then we know from the considerations about $E_2$ that $C$ is negative and hence all modes decay and the solution is stable. On the other hand, if $\bar{u} < u_*$ then $C > 0$. Then $C\hat{G}(\kappa)$ is a positive decreasing function of $\kappa$. For small enough $\varepsilon > 0$ the factor $C\hat{G} - \varepsilon$ is positive for small values of $\kappa$. Low modes grow and the situation is unstable.

**Case 2:** $\tau > 0$
Choosing again $u = \bar{u} + v$ and $\gamma = \gamma_* + \eta$ and expanding gives the following system of two equations

$$\begin{aligned} v_t &= \varepsilon v_{xx} - \gamma_* v_x - \bar{u}\eta_x + \text{h.o.t.}(v), \\ \tau\eta_t &= \beta\eta_{xx} - \eta + E_1 v + E_2 v_x + \text{h.o.t.}(\eta), \end{aligned} \tag{4.15}$$

where we put $E_j = E_j(\bar{u}, 0)$. The Fourier transform of the linear part is

$$\begin{pmatrix} \hat{v}_t \\ \tau\hat{\eta}_t \end{pmatrix} = \begin{pmatrix} -\varepsilon\kappa^2 + i\kappa\gamma_* & i\kappa\bar{u} \\ E_1 - i\kappa E_2 & -\beta\kappa^2 - 1 \end{pmatrix} \begin{pmatrix} \hat{v} \\ \hat{\eta} \end{pmatrix}. \tag{4.16}$$

We investigate the real part of the eigenvalues $\lambda$ of the system. In order to avoid too complicated expressions, we assume at first $\tau = 1$ and $E_1 = 0$. Then the trace of the matrix in (4.16) is

$$-(\varepsilon + \beta)\kappa^2 - 1 + i\kappa\gamma_* =: S_1 + iS_2$$

and its determinant is

$$\kappa^2(\varepsilon\beta\kappa^2 + \varepsilon - E_2\bar{u}) - i\kappa(\beta\gamma_*\kappa^2 + \gamma_*^2) =: D_1 + iD_2.$$

The characteristic polynomial $\lambda^2 - (S_1 + iS_2)\lambda + D_1 + iD_2$ has two roots $\lambda_{1,2} = a_{1,2} + ib_{1,2}$. The real and imaginary parts satisfy

$$\begin{aligned} a_1 + a_2 &= S_1, \qquad & b_1 + b_2 &= S_2, \\ a_1a_2 - b_1b_2 &= D_1, \qquad & a_1b_2 + a - 2b_1 &= D_2. \end{aligned} \tag{4.17}$$

If we substitute $\kappa \mapsto -\kappa$, then $S_2, D_2$ change sign whereas $S_1, D_1$ do not. Therefore, from (4.17) we see that substituting $\kappa \mapsto -\kappa$ amounts to conjugating the roots. The real parts of $\lambda_{1,2}$ are not changed. Hence we may assume $\kappa > 0$. Then we have the following sign pattern:

$$S_1 < 0, \qquad S_2 > 0, \qquad D_2 < 0. \tag{4.18}$$

For $D_1$ we observe that

$$\begin{aligned} E_2 < 0 \quad &\Longrightarrow D_1 > 0, \\ E_2 > 0 \quad &\Longrightarrow D_1 < 0 \quad \text{for} \quad \varepsilon, \kappa \quad \text{small}. \end{aligned} \tag{4.19}$$

Eliminating $a_1, b_1, b_2$ from (4.17) we obtain a fourth order polynomial in $a = a_2$, namely

$$\begin{aligned} &4a^4 - 8S_1a^3 + (5S_1^2 + S_2^2 + 4D_1)a^2 - S_1(S_1^2 + S_2^2 + 4D_1)a \\ &\quad + S_1S_2D_2 - D_2^2 + D_1S_2^2 \\ =:&\alpha_4 a^4 + \alpha_3 a^3 + \alpha_2 a^2 \alpha_1 a + \alpha_0 \end{aligned} \tag{4.20}$$

We apply Descartes' rule of signs to find positive real solutions for $a$ [43]: Let $N$ be the number of sign changes in the sequence of coefficients

$$(\alpha_4, \alpha_3, \alpha_2, \alpha_1, \alpha_0).$$

Then there are at most $N$ positive real roots $a$ of (4.20) and the number of positive real roots is either $N$ or $N-2$ or $N-4$.

LEMMA 4.1.2
*If $E_2 < 0$ then there are no sign changes in the sequence of coefficients and hence there are no real positive roots. If $E_2 > 0$ then for all sufficiently small $\varepsilon, \kappa$ there is exactly one sign change in the sequence and hence there is exactly one positive real root.*

PROOF.
Suppose at first $E_2 < 0$. Then the coefficients satisfy $\alpha_4, \alpha_3, \alpha_2, \alpha_1 > 0$. It remains to show that $\alpha_0 > 0$. The expression for $\alpha_0$ can be computed explicitly as

$$\alpha_0 = S_1S_2D_2 - D_2^2 + D_1S_2^2 = 6\varepsilon\beta\gamma_*^2\kappa + (2\varepsilon - E_2\bar{u})\gamma^2\kappa^4. \tag{4.21}$$

For $E_2 < 0$ this expression is positive for all $\kappa \neq 0$. Now suppose $E_2 > 0$. Then we see from (4.21) that $\alpha_0 < 0$ for sufficiently small $\varepsilon, \kappa$. Similarly one can compute $\alpha_{2,3}$ and find a sign change for $E_2 > 0$ and suitably small $\varepsilon, \kappa$. Hence all but the first two coefficients in (4.20) are negative and there is exactly one sign change. ■

If we now let $\tau$ vary, we find that the sign pattern of the coefficients $\alpha_i$ is not changed. The values of $\varepsilon, \kappa$ for which the sign changes occur are different in general. Next we observe that the eigenvalues $\lambda_{1,2}$ depend continuously on $E_1$. Then for small values of $|E_1|$ we find the same behavior. We summarize the stability behavior in the following lemma.

LEMMA 4.1.3
*Let $\varepsilon, \beta > 0$ and $\tau \geq 0$. In case $\tau > 0$ assume in addition that $\|E_1(\cdot, 0)\|_\infty$ is small. Then the stationary solution $(\bar{u}, \gamma_*)$ to (4.7), (4.8) is linearly stable if $\bar{u} > u_*$. If on the other hand $\bar{u} < u_*$, then for all sufficiently small $\varepsilon$ the solution is unstable and the modes for a finite range of wave numbers grow.*

**Perfect Schools**

A perfect school has a uniform density in the interior and sharp edges (compare 2.1.1). It is described mathematically by a characteristic function of some interval. This is not a classical solution. We only expect it to arise in the absence of random motion.

A weak solution to (4.7) with $\varepsilon = 0$ is a function $u \in L^1_{\text{loc}}([0,T] \times \mathbb{R})$ such that

$$\int_0^T \int_{\mathbb{R}} u\psi_t + (\gamma u)\psi_x dx dt = -\int_{\mathbb{R}} u_0 \psi dx \tag{4.22}$$

for all $\psi \in C^1(\mathbb{R}^+ \times \mathbb{R})$ with compact support in $[0,T) \times \mathbb{R}$ (cf. [37]). Under the assumption that $\gamma \equiv \gamma_*$ is constant it is obvious that for $u_0 = \chi_{[a,b]}$ a weak solution is $u(t,x) = u_0(x - \gamma_* t)$. We show that the converse is also true: if the density is a traveling rectangle, then $\gamma = \gamma_*$.

LEMMA 4.1.4
*Suppose $u_0 = \alpha\chi_{[a,b]}$ for some $\alpha > 0$ and set $u(t,x) = u_0(x - ct)$ for some $c > 0$. For $\tau > 0$ assume in addition $\gamma_0 = \gamma_*$. Then the solution to (4.8) is $\gamma \equiv \gamma_*$.*

PROOF.
Take the case $\tau = 0$ first. We have $E = \gamma_*$ a.e. on $[0,T] \times \mathbb{R}$ and hence $E \in L^2_{\text{loc}}(\mathbb{R})$ for almost all $t \in [0,T]$. Then by Theorem 8.9 in [15] there is a unique $\gamma(t) \in W^{2,2}_{\text{loc}}(\mathbb{R})$ which satisfies the elliptic equation in (4.8) for $\varepsilon = 0$ a.e. Since $\mathbb{R}$ is one-dimensional $\gamma(t)$ is continuous in $x$. But $\gamma \equiv \gamma_*$ solves (4.8) a.e. and by uniqueness and continuity this is the solution.

Similarly for $\tau > 0$. With $E \in L^2_{\text{loc}}(\mathbb{R})$ the parabolic equation for $\gamma$ has a unique solution which satisfies $\gamma(t) \in W^{2,2}_{\text{loc}}$ (cf. [36]). It satisfies the equation a.e. on $\mathbb{R}$. Again $\gamma(t)$ is continuous in $x$ hence $\gamma = \gamma_*$ is the solution. ∎

We have not yet specified the speed of the school. From the interpretation of the model only $c = \gamma_*$ should be admissible. The Rankine-Hugoniot jump conditions [37] generally determine the shock speed $c$ in a conservation law of the form $u_t + f(u)_x = 0$ by the formula

$$\frac{f(u_l) - f(u_r)}{u_l - u_r} = c,$$

where $u_r, u_l$ is the density right and left from the shock. In the case at hand this condition is satisfied for $c = \gamma_*$ only. We collect these results in the following lemma.

LEMMA 4.1.5
*The system of equations (4.7), (4.8) for $\varepsilon = 0$ has weak solutions in the form of traveling characteristic functions of intervals with speed $\gamma_*$.*

### 4.1.2 Numerical Simulations

To simulate solutions of system (4.7), (4.8) we impose Neumann boundary conditions on the interval $[0,1]$, choose $\tilde{F}$ as in (4.3) and parameters

$$\gamma_* = 1, \quad u_* = 0.5, \quad \varepsilon = \beta = 10^{-4}, \quad \tau = 10^{-3}, \quad \chi = 0.3.$$

The initial density is a pulse with compact support, the initial velocity is identically equal to the preferred velocity. We distinguish the two cases

$$(1) \quad \max u_0 < u_* \quad \text{and} \quad (2) \quad \max u_0 > u_*.$$

**Case (1): Initial data below $u_*$.**

**t = 0** **t = T**

**Density:**

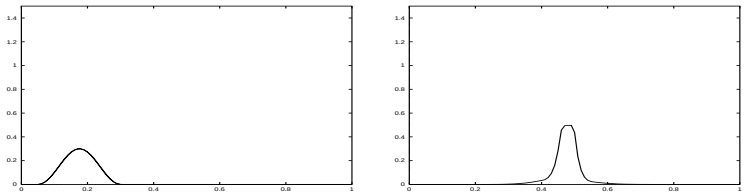

**Expected Velocity:**

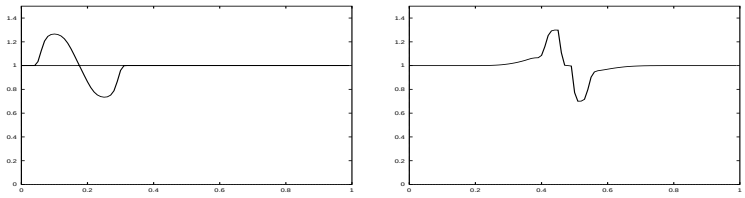

**Velocity:**

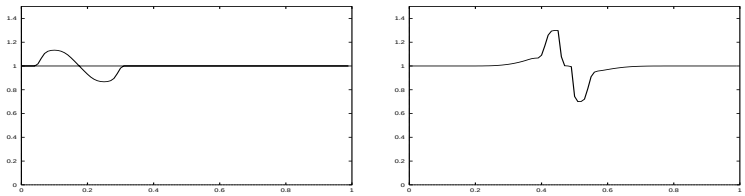

**Density development in time**

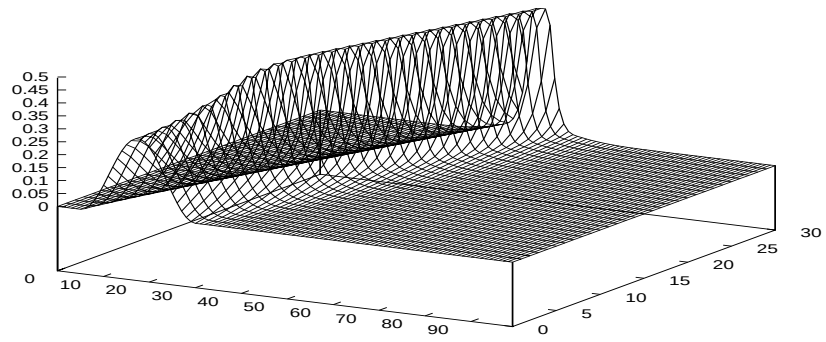

**Case (2): Initial data above $u_*$.**

**t = 0** **t = T**

**Density:**

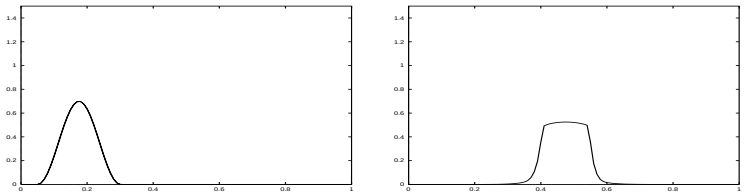

**Expected Velocity:**

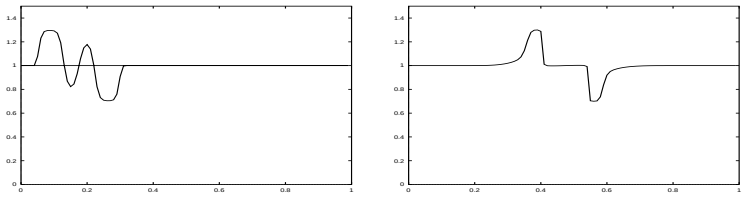

**Velocity:**

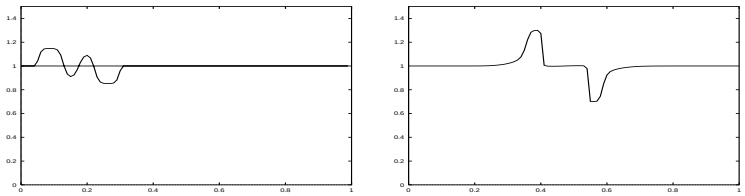

**Density development in time**

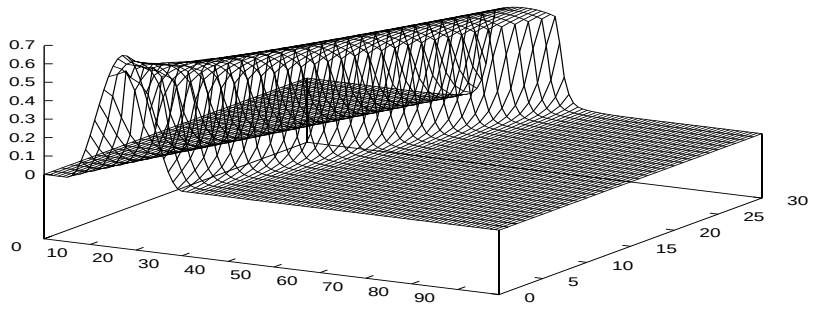

In both cases we plot the shapes of the density $u$, the expected velocity $E$ and the actual velocity $\gamma$ at the beginning $t = 0$ and at the end $t = T$ of the simulation. Then the density development is plotted for $0 \le t \le T$.

We observe the following: In case (1) the pulse becomes higher and more narrow. Individuals crowd more closely together to attain the optimal density. In case (2) the peak spreads out and its height decreases. In both cases the velocity at the end of the school is greater than $\gamma_*$ and in front of the school it is lower than $\gamma_*$. Gradients of $u$ are flattened out where the density is too high and become more steep where the density is below the optimal density. The steep gradients naturally poses problems for numerical schemes but we show below that smooth solutions exist for all times.

## 4.2 Existence of Solutions

We show local and also global existence of solutions of the system of equations (4.7), (4.8) in spaces of differentiable functions for $\varepsilon, \beta > 0$. The equation for $\gamma$ is parabolic for $\tau > 0$ and elliptic for $\tau = 0$. These two cases are discussed separately. We always assume that $0 \le E \le E_{\max}$ is Lipschitz, which is true for the special case given above. It is clear that the total mass of $u$ is conserved by the system.

**Existence for $\tau > 0$**

THEOREM 4.2.1
*Let $\varepsilon, \tau, \beta > 0$ and $E \in \mathcal{C}_b^{0,1}$. For all nonnegative initial data $(u_0, \gamma_0) \in \mathcal{C}_b^1(\mathbb{R})^2$ there exists a unique solution $(u, \gamma) \in \mathcal{C}([0,T], \mathcal{C}_b^1(\mathbb{R})^2)$ of system (4.7), (4.8) for some $T > 0$.*

PROOF.
We write the equations as

$$\nu_t = \mathcal{A}\nu + \mathcal{F}(\nu)$$

with $\nu = (u, \gamma)^T$ and $\mathcal{A} = \operatorname{diag}(\varepsilon\Delta, (\beta/\tau)\Delta)$, which generates an analytic semigroup on $X = \mathcal{C}_b^1(\mathbb{R})^2$. The nonlinearity is

$$\mathcal{F} = (-(\gamma u)_x, (E(u, u_x) - \gamma)/\tau)^T.$$

The norm on $X$ is $\|(u,\gamma)\|_X = \|u\|_{C^1} + \|\gamma\|_{C^1}$. Furthermore let $Y = \mathcal{C}(\mathbb{R})^2$ with norm $\|u\|_{C^0} + \|\gamma\|_{C^0}$. Then $\|(u_x, \gamma_x)\|_Y \le \|(u,\gamma)\|_X$. We show that $\mathcal{F}\colon X \to Y$ is locally Lipschitz. Choose $k_0 > 0$ and $(u,\gamma), (v,\xi) \in X$ with $\|(u,\gamma)\|_X, \|(v,\xi)\|_X \le k_0$. The second component of $\mathcal{F}((u,\gamma)) - \mathcal{F}((v,\xi))$ is estimated by

$$\begin{aligned} \tau\|(E(u,u_x) - \gamma) - (E(v,v_x) - \xi)\|_{C^0} &\le Lip(E)\|u - v\|_{C^1} + \|\gamma - \xi\|_{C^0} \\ &\le \tilde{L}\|(u - v, \gamma - \xi)\|_X, \end{aligned}$$

where $Lip(E)$ is the Lipschitz constant of $E$ and $\tilde{L} = \max\{Lip(E), 1\}$. For the first component we have

$$\begin{aligned} \|(\gamma u)_x - (\xi v)_x\|_{C^0} &\le \|u\|_{C^0}\|\gamma_x - \xi_x\|_{C^0} + \|u_x\|_{C^0}\|\gamma - \xi\|_{C^0} \\ &\quad + \|\xi_x\|_{C^0}\|u - v\|_{C^0} + \|\xi\|_{C^0}\|u_x - v_x\|_{C^0} \\ &\le 2\|u\|_{C^1}\|\gamma - \xi\|_{C^1} + 2\|\xi\|_{C^1}\|u - v\|_{C^1} \\ &\le L(k_0)\|(u - v, \gamma - \xi)\|_X, \end{aligned}$$

for some constant $L$ which depends only on $k_0$. The claim now follows from Proposition 1.1 in [62] §15. ∎

THEOREM 4.2.2
*In addition to the assumptions of Theorem 4.2.1 assume*

$$0 \leq \gamma_0(x) \leq E_{\max}. \tag{4.23}$$

*Then solutions to system (4.7), (4.8) exist globally, i.e.* $(u, \gamma) \in \mathcal{C}([0, \infty), \mathcal{C}_b^1(\mathbb{R})^2)$.

The proof of the theorem relies on several lemmas.

LEMMA 4.2.3
*With the assumptions of Theorem 4.2.2 let $\gamma$ be a solution of (4.8). Then*

$$0 \leq \gamma(t, x) \leq E_{\max},$$

*and the gradient of $\gamma$ can be estimated by*

$$\|\gamma(t)\|_{C^1} \leq \|\gamma_0\|_{C^1} + K_\beta \sqrt{t},$$

*where $K_\beta = K_\beta(\beta, \tau, E_{\max})$ is independent of $\varepsilon > 0$.*

PROOF.
By assumption we have $E \geq 0$, and hence the maximum principle gives $\gamma \geq 0$. Similarly we show that $\xi = E_{\max} - \gamma \geq 0$, which gives the upper bound for $\gamma$. To estimate the gradient of $\gamma$ we apply the variation of constants formula and denote by $T_\beta(t)$ the semigroup generated by $(\beta/\tau)\Delta$. Using the estimate (see [62])

$$\|T_\beta(t)\|_{L(\mathcal{C}, \mathcal{C}^1)} \leq C_\beta t^{-1/2}$$

we find

$$\begin{aligned}
\|\gamma(t)\|_{C^1} &\leq \|\gamma_0\|_{C^1} + \frac{1}{\tau} \int_0^t \|T_\beta(t-s)(E-\gamma)(s)\|_{C^1} ds \\
&\leq \|\gamma_0\|_{C^1} + \frac{1}{\tau} \int_0^t \frac{C_\beta}{\sqrt{t-s}} \|(E-\gamma)(s)\|_{C^0} ds \\
&\leq \|\gamma_0\|_{C^1} + \frac{2E_{\max} C_\beta}{\tau} \int_0^t \frac{1}{\sqrt{t-s}} ds \\
&\leq \|\gamma_0\|_{C^1} + \frac{4E_{\max} C_\beta}{\tau} \sqrt{t}.
\end{aligned}$$

∎

LEMMA 4.2.4
*With the assumptions of Theorem 4.2.2 the maximum of $u$ satisfies*

$$\|u(t)\|_{C^0} \leq \|u_0\|_{C^0} e^{\lambda t}$$

*for $\lambda = \|\gamma_0\|_{C^1} + K_\beta \sqrt{t}$.*

PROOF.
Fix $t > 0$ and set $\lambda = \|\gamma_0\|_{C^1} + K_\beta\sqrt{t}$. Then apply the maximum principle to $v(\tau, x) := e^{-\lambda\tau}u(\tau, x)$ and get that $\|v(\tau)\|_{C^0} \leq \|v(0)\|_{C^0}$ on $0 \leq \tau \leq t$. This implies in particular that $\|u(t)\|_{C^0} \leq \|u_0\|_{C^0}e^{\lambda t}$. ∎

LEMMA 4.2.5
*Let the assumptions of Theorem 4.2.2 be satisfied. Then for sufficiently small $T > 0$ the $C^1$-norm of $u$ on $[0, T]$ can be bounded by*

$$\sup_{0\leq t\leq T} \|u(t)\|_{C^1} \leq \frac{1 + C_\varepsilon\lambda e^{\lambda T}\sqrt{T}}{1 - K_\varepsilon\sqrt{T}}\|u_0\|_{C^1},$$

*where $\lambda = \|\gamma_0\|_{C^1} + K_\beta\sqrt{T}$ and $K_\varepsilon$ depends on $\varepsilon$ but not on the initial data.*

PROOF.
As above we denote by $T_\varepsilon(t)$ the semigroup generated by $\varepsilon\Delta$ and use the estimate

$$\|T_\varepsilon(t)\|_{L(\mathcal{C},\mathcal{C}^1)} \leq C_\varepsilon t^{-1/2}.$$

Then from the variation of constants formula and Lemmas 4.2.3 and 4.2.4 we get

$$\begin{aligned}
\|u(t)\|_{C^1} &\leq \|u_0\|_{C^1} + \int_0^t \|T_\varepsilon(t-s)(\gamma u_x + \gamma_x u)(s)\|_{C^1} ds \\
&\leq \|u_0\|_{C^1} + \int_0^t \frac{C_\varepsilon}{\sqrt{t-s}} \|(\gamma u_x + \gamma_x u)(s)\|_{C^0} ds \\
&\leq \|u_0\|_{C^1} + \int_0^t \frac{C_\varepsilon}{\sqrt{t-s}} \left(\|\gamma\|_{C^0}\|u\|_{C^1} + \|\gamma\|_{C^1}\|u\|_{C^0}\right)(s) ds \\
&\leq \|u_0\|_{C^1} + \int_0^t \frac{C_\varepsilon}{\sqrt{t-s}} E_{\max}\|u(s)\|_{C^1} ds \\
&\qquad + \int_0^t \frac{C_\varepsilon}{\sqrt{t-s}} \left(\|\gamma_0\|_{C^1} + K_\beta\sqrt{T}\right)\|u_0\|_{C^0}e^{\lambda T} ds \\
&\leq \|u_0\|_{C^1} + C_\varepsilon\lambda\|u_0\|_{C^0}e^{\lambda T}\sqrt{t} + C_\varepsilon E_{\max}\int_0^t \frac{\|u(s)\|_{C^1}}{\sqrt{t-s}} ds.
\end{aligned}$$

Now we introduce the norm

$$\|u\|^T := \sup_{0\leq t\leq T} \|u(t)\|_{C^1}.$$

Taking sup on both sides in the inequality above gives

$$\|u\|^T \leq \|u_0\|_{C^1} + C_\varepsilon\lambda\|u_0\|_{C^0}e^{\lambda T}\sqrt{T} + E_{\max}C_\varepsilon\|u\|^T\sqrt{T}.$$

Putting together the terms $\|u\|^T$ on both sides and dividing by $1 - K_\varepsilon\sqrt{T}$ with $K_\varepsilon = E_{\max}C_\varepsilon$ we get

$$\|u\|^T \leq \frac{\|u_0\|_{C^1} + C_\varepsilon\lambda\|u_0\|_{C^0}e^{\lambda T}\sqrt{T}}{1 - K_\varepsilon\sqrt{T}}.$$

Finally, since $\|u_0\|_{C^0} \leq \|u_0\|_{C^1}$, the claim follows. ∎

Proof of Theorem 4.2.2.
Choose

$$\sqrt{T} = \frac{1}{2E_{\max}C_\varepsilon},$$

then with Lemma 4.2.5 we get

$$\|u(T)\|_{C^1} \leq \|u_0\|_{C^1} G(\lambda) := \|u_0\|_{C^1} \frac{1 + C_\varepsilon \lambda e^{\lambda T}\sqrt{T}}{1 - K_\varepsilon \sqrt{T}}.$$

We choose the values of $u$ and $\gamma$ at $T$ as new initial values, i.e. $u^{(1)}(0) = u(T)$, $\gamma^{(1)}(0) = \gamma(T)$ and solve the equations again. As above we get

$$\begin{aligned} \|\gamma^{(1)}(t)\|_{C^1} &\leq \|\gamma(T)\|_{C^1} + K_\beta\sqrt{t} \\ &\leq \|\gamma_0\|_{C^1} + K_\beta(\sqrt{T} + \sqrt{t}), \end{aligned}$$

and set $\lambda^{(1)} = \|\gamma_0\|_{C^1} + 2K_\beta\sqrt{T}$. Since $K_\varepsilon$ is independent of the initial data, we apply Lemma 4.2.5 for the same value of $T$ as above to get

$$\|u(2T)\|_{C^1} = \|u^{(1)}(T)\|_{C^1} \leq \|u^{(1)}(0)\|_{C^1} G(\lambda^{(1)}) \leq \|u_0\|_{C^1} G(\lambda) G(\lambda^{(1)}).$$

We can iterate this argument and find

$$\|u((n+1)T)\|_{C^1} \leq \|u_0\|_{C^1} G(\lambda) G(\lambda^{(1)}) \cdot \ldots \cdot G(\lambda^{(n)}) < \infty,$$

where $\lambda^{(k)} = \|\gamma_0\|_{C^1} + (k+1)K_\beta\sqrt{T}$. This finishes the proof. ∎

**Existence for $\tau = 0$**

Suppose the adjustment to the expected velocity is instantaneous, i.e. $\tau = 0$, but with an error, i.e. $\beta > 0$. Then equation (4.8) is an elliptic equation which has to be satisfied at every time $t$. The system reads

$$\begin{aligned} u_t &= \varepsilon u_{xx} - (\gamma u)_x \\ 0 &= \beta\gamma_{xx} - \gamma + E(u, u_x). \end{aligned} \tag{4.24}$$

Suppose two functions $f$ and $\gamma$ satisfy the simple elliptic equation

$$\gamma = f + \beta\gamma_{xx}. \tag{4.25}$$

Then $\gamma$ is in some sense "close" to $f$ but it is "smoother". Taking Fourier transforms gives

$$\hat{\gamma}(\kappa) = \frac{1}{1 + \beta\kappa^2}\hat{f}(\kappa), \tag{4.26}$$

so that high wave numbers of $f$ are damped out in $\gamma$. Applied to the second equation in (4.24) we find that the velocity is not as sensitive to local variations in the density as the expected velocity is.

LEMMA 4.2.6
*For all $f \in \mathcal{C}_b^1(\mathbb{R})$ there is a unique function $\gamma \in \mathcal{C}_b^2(\mathbb{R})$ which solves (4.25). The following estimates hold*

$$\|\gamma\|_{C^1} \leq C(\beta)\|f\|_{C^0} \text{ and } \|\gamma\|_{C^2} \leq C(\beta)\|f\|_{C^1}$$

*for some constant $C$ which depends on $\beta$.*

PROOF.
We use $f$ and the Green's function of $\beta\Delta - 1$ to represent $\gamma = f * G$. Then the estimates are straightforward. ∎

THEOREM 4.2.7
*Suppose $E \in \mathcal{C}_b^{1,1}$ and let $\varepsilon > 0$. For all nonnegative initial data $u_0 \in \mathcal{C}_b^2(\mathbb{R})$ there exists a unique solution $(u, \gamma) \in \mathcal{C}([0,T], \mathcal{C}_b^2(\mathbb{R})^2)$ of system (4.24) for some time $T > 0$.*

PROOF.
For any function $u \in \mathcal{C}_b^2(\mathbb{R})$ we have $u_x \in \mathcal{C}_b^1(\mathbb{R})$. By Lemma 4.2.6 we can define a continuous map $u \mapsto \gamma^u$ from $\mathcal{C}_b^2(\mathbb{R})$ to $\mathcal{C}_b^2(\mathbb{R})$, where $\gamma^u$ is the unique solution of the second equation in (4.24). With this notation we can write the system in the single equation:

$$u_t = \varepsilon u_{xx} - (\gamma^u u)_x. \tag{4.27}$$

We apply the semigroup approach to this equation. We have to estimate the nonlinearity $u \mapsto (\gamma^u u)_x$. Obviously $u \in \mathcal{C}_b^2(\mathbb{R})$ implies $(\gamma^u u)_x \in \mathcal{C}_b^1(\mathbb{R})$. We need to show that the map is locally Lipschitz.
Choose $k_0 > 0$ and $u, v \in \mathcal{C}_b^2(\mathbb{R})$ such that $\|u\|_{C^2}, \|v\|_{C^2} < k_0$. Then $\gamma^u, \gamma^v$ are well defined. The difference $\xi = \gamma^u - \gamma^v$ satisfies an equation of the form (4.25) since the equation for $\gamma$ is linear. We have the following inequalities

$$\begin{aligned}
\|\xi\|_{C^1} &\leq C(\beta)\|E(u,u_x) - E(v,v_x)\|_{C^0} \\
&\leq C(\beta)L_E\|u - v\|_{C^1}, \\
\|\xi_x\|_{C^1} &\leq C(\beta)\left\|\frac{d}{dx}E(u,u_x) - \frac{d}{dx}E(v,v_x)\right\|_{C^0} \\
&\leq C(\beta)\|E_1^u u_x + E_2^u u_{xx} - E_1^v v_x - E_2^v v_{xx}\|_{C^0} \\
&\leq C(\beta)\|(E_1^u + E_1^v)(u_x - v_x) + (E_1^u - E_1^v)(u_x + v_x)\|_{C^0} \\
&\quad + C(\beta)\|(E_2^u + E_2^v)(u_{xx} - v_{xx}) + (E_2^u - E_2^v)(u_{xx} + v_{xx})\|_{C^0} \\
&\leq C(\beta, k_0, \|E\|_{C^{1,1}})\|u - v\|_{C^2},
\end{aligned}$$

where $E^u_j$ stands for the derivative of $E(u, u_x)$ with respect to the $j-$th component. With this we get the Lipschitz estimate:

$$\begin{aligned}\|(\gamma^u u)_x - (\gamma^v v)_x\|_{C^1} &\leq \|\gamma^u_x - \gamma^v_x\|_{C^1}\|u+v\|_{C^1} \\ &\quad +\|\gamma^u_x + \gamma^v_x\|_{C^1}\|u-v\|_{C^1} \\ &\quad +\|\gamma^u - \gamma^v\|_{C^1}\|u_x+v_x\|_{C^1} \\ &\quad +\|\gamma^u + \gamma^v\|_{C^1}\|u_x-v_x\|_{C^1} \\ &\leq C(\beta, k_0, \|E\|_{C^{1,1}})\|u-v\|_{C^2}.\end{aligned}$$

Now, Proposition 1.1 §15 in [62] gives the local existence result. The fact that $\gamma^u$ is continuous in $t$ follows by applying Lemma 4.2.6 to $\xi = \gamma^u(t) - \gamma^u(s)$. ∎

The elliptic equation for $\gamma$ yields stronger estimates than the parabolic equation with $\tau > 0$. These estimates give global in time existence for the case $\tau = 0$.

LEMMA 4.2.8
*Let the assumptions of Theorem 4.2.7 be satisfied and denote by $(u, \gamma)$ a solution of (4.24). Then*

$$0 \leq \gamma(t,x) \leq E_{\max}.$$

*Furthermore, $\gamma$ together with its first and second derivatives is bounded independently of $u$, i.e. there is a constant $K > 0$ such that*

$$\|\gamma\|_{C^2} \leq K. \tag{4.28}$$

PROOF.
By Lemma 4.2.6 $\gamma$ is bounded and smooth. From the elliptic equation for $\gamma$ we see that if $\gamma$ is concave, i.e. $\gamma_{xx}(x_0) < 0$, then necessarily $\gamma(x_0) \leq E_{\max}$. Now suppose there is some $x_0 \in \mathbb{R}$ with $\gamma(x_0) > E_{\max}$. Suppose further that $\gamma_x(x_0) > 0$. Since $\gamma$ cannot become concave as long as it exceeds $E_{\max}$, it has to grow at least linearly for $x \geq x_0$. But then it cannot be bounded as $x \to +\infty$. If $\gamma_x(x_0) < 0$ then similarly it cannot be bounded as $x \to -\infty$. Hence, $\gamma \leq E_{\max}$ on $\mathbb{R}$. Analogous considerations with "convex" instead of "concave" give $\gamma \geq 0$.
Going back to the equation for $\gamma$ we see that

$$\|\gamma_{xx}\|_{C^0} \leq \frac{1}{\beta}\|E - \gamma\|_{C^0} \leq \frac{2E_{\max}}{\beta}.$$

Given these two bounds and the positivity of $\gamma$ we apply the interpolation estimate 3.2.9. in [34] and get

$$|\gamma_x(t,x)|^2 \leq N\gamma(t,x)\|\gamma_{xx}(t,\cdot)\|_{C^0} \leq \frac{2NE_{\max}}{\beta},$$

for some constant $N$. This proves the claim. ∎

THEOREM 4.2.9
*With the assumptions of Theorem 4.2.7 solutions to (4.24) exist globally, i.e. $(u, \gamma) \in \mathcal{C}([0,\infty), \mathcal{C}^2_b(\mathbb{R})^2)$.*

PROOF.
As in the case $\tau > 0$ one could get an exponential bound for the maximum of $u$ via the maximum principle (see Lemma 4.2.4) and proceed like in the proof of Theorem 4.2.2. Due to the estimate (4.28) we do not need this exponential bound here and proceed differently. Later, when we work with the system of $u^{\pm}$ and $\gamma^{\pm}$ an exponential bound for $u^{\pm}$ is not available. But the proof presented here can be adapted there.
As before we denote by $T_\varepsilon(t)$ the semigroup generated by $\varepsilon\Delta$ and use the estimate

$$\|T_\varepsilon(t)\|_{L(C^1,C^2)} \leq C_\varepsilon t^{-1/2}.$$

By the same arguments as in the proof of Theorem 4.2.2 we find, using (4.28)

$$\begin{aligned}
\|u(t)\|_{C^2} &\leq \|u(0)\|_{C^2} + \int_0^t \|T_\varepsilon(t-s)(\gamma^u u)_x(s)\|_{C^2} ds \\
&\leq \|u(0)\|_{C^2} + \int_0^t \frac{C_\varepsilon}{\sqrt{t-s}} \|(\gamma^u u)_x(s)\|_{C^1} ds \\
&\leq \|u(0)\|_{C^2} + C_\varepsilon K \int_0^t \frac{\|u(s)\|_{C^2}}{\sqrt{t-s}} ds.
\end{aligned}$$

Introducing the norm $\|u\|^T = \sup_{0\leq t\leq T} \|u(t)\|_{C^2}$ as before, we estimate

$$\|u\|^T \leq \frac{\|u_0\|_{C^2}}{1 - C_\varepsilon K\sqrt{T}},$$

for sufficiently small $T > 0$. Note that in contrast to the proof of Theorem 4.2.2 there is no dependence on $\gamma$ in this inequality. A continuation argument like in the proof of 4.2.2 gives

$$\|u(nT)\|_{C^2} \leq \|u_0\|_{C^2} \left(\frac{1}{1 - C_\varepsilon K\sqrt{T}}\right)^n$$

which finishes the proof. ∎

## 4.3 Solutions for $\varepsilon = 0$

We now show existence of (weak) solutions for the hyperbolic/elliptic system

$$\begin{aligned}
u_t + (\gamma u)_x &= 0, \\
\eta &= \beta\eta_{xx} + F(u, u_x), \\
\gamma &= \eta + \gamma^*, \\
u(0,\cdot) &= u_0,
\end{aligned} \tag{4.29}$$

which was introduced above.

In conservation laws like Burgers' equation even arbitrarily smooth initial functions with small absolute values can lead to discontinuous solutions in finite time. Interpretation and simulation suggest that also for system (4.29) gradients of $u$ could become arbitrarily steep. The natural function space for conservation laws is the space of functions of bounded variation [8]. But in the equation for $\eta$ the

expression $F(u, u_x)$ must make sense. For $u \in BV$, by definition, $u_x$ is a finite measure and $F(u, u_x)$ is not necessarily well defined. Which then is the appropriate function space to work with?

Instead of aiming for the greatest generality, we show that for sufficiently smooth initial data there exist solutions which are continuous in $x$ for arbitrarily long times. After what had been said before, this claim seems surprising. There the strong influence of the elliptic equation for $\eta$ shows up.

We multiply by suitable test functions and integrate by parts to get

$$\int_0^T \int_{\mathbb{R}} u\phi_t + \gamma u\phi_x dx dt = -\int_{\mathbb{R}} u_0 \phi dx \tag{4.30}$$

and

$$\int_{\mathbb{R}} -\beta\eta_x\psi_x - \eta\psi dx = \int_{\mathbb{R}} F(u, u_x)\psi dx. \tag{4.31}$$

As long as $\gamma$ is bounded, the first equation makes sense for $u \in L^1_{\text{loc}}([0,T] \times \mathbb{R})$. In the second equation we impose some integrability conditions on $F(u, u_x)$. Always assuming that $F$ is Lipschitz we get further conditions on $u_x$. One could work with $u_x \in L^1$ which implies $u \in W^{1,1} \subset \mathcal{C}$. Here we choose to work with $u \in W^{1,2} = H^1 \subset \mathcal{C}$.

The main theorem of this section is the following.

THEOREM 4.3.1
*Let $F$ be in $\mathcal{C}^{2,1}_b$, $T > 0$ and $\Omega_T = [0,T] \times \mathbb{R}$. Then for any nonnegative initial datum $u_0 \in H^3(\mathbb{R}) \cap L^1(\mathbb{R})$ there exists a solution $(u, \eta)$ of system (4.29) with $u \geq 0$ in the following sense*

- *$u \in L^1(\Omega_T) \cap L^\infty([0,T], H^1(\mathbb{R}))$ and $u$ satisfies (4.30) for all $\phi \in \mathcal{C}^1(\Omega_T)$ with compact support in $[0,T) \times \mathbb{R}$.*
- *$\eta \in L^\infty([0,T], H^2(\mathbb{R}))$ and for almost all $t \in [0,T]$ the function $\eta$ satisfies (4.31) for all $\psi \in \mathcal{C}^1(\mathbb{R})$ with compact support.*
- *initial values are assumed in the weak sense, i.e. there exists a set $\mathcal{L} \subset [0,T]$ of Lebesgue measure 0, such that $u(t,\cdot), \eta(t,\cdot)$ are defined a.e. on $\mathbb{R}$ for $t \in [0,T]\backslash\mathcal{L}$ and satisfy*

$$\limsup_{t \to 0, t \in [0,T]\backslash\mathcal{L}} \|u(t,\cdot) - u_0(\cdot)\|_{H^1(I)} = 0$$

*and*

$$\limsup_{t \to 0, t \in [0,T]\backslash\mathcal{L}} \|\eta(t,\cdot) - \eta(0,\cdot)\|_{H^2(I)} = 0$$

*for all bounded intervals $I = [-\rho, \rho]$.*

COROLLARY 4.3.2
*Let $F$ be in $\mathcal{C}^{2,1}_b$, and $T > 0$. Then for all nonnegative initial data $u_0 \in \mathcal{C}^3(\mathbb{R})$ with compact support there exists a solution of (4.29) such that $u(t)$ remains continuous in $x$ for $t \in [0,T]$.*

The proof of this theorem, given in 4.3.2, is an adaptation of the vanishing viscosity method. The equation for $u$ is regularized by $\varepsilon\Delta$ and estimates on several norms of $u$ and $\eta$ are shown to hold independently of $\varepsilon$ provided the initial function is sufficiently smooth. A compact imbedding argument then provides the desired solutions. The $\varepsilon$-independent estimates which are needed are given in several lemmas preceeding the proof.

The letter $C$ always denotes a generic constant and may change its value even within one proof. The notation $C(a,b)$ means that $C$ depends on $a,b$ but not on other quantities. As always the norm of a space $X$ is denoted by $\|\cdot\|_X$ the only exception being $\|\cdot\|_{L^2} = \|\cdot\|_2$.

### 4.3.1 Estimates independent of $\varepsilon$

The function $\eta$ differs from $\gamma$ only by a constant $\eta = \gamma - \gamma_*$ and hence by Lemma 4.2.8 we can assume that if $\eta$ is a $C^2$-solution of the elliptic equation in (4.29) then also

$$\|\eta(t)\|_{\mathcal{C}^2} \leq K. \tag{4.32}$$

LEMMA 4.3.3
*Let $F \in \mathcal{C}_b^{p-1,1}$ and $u \in H^p(\mathbb{R})$ for some integer $p \geq 1$. Then there exists a unique solution $\eta \in H^{p+1}(\mathbb{R})$ of*

$$\beta\eta_{xx} - \eta = F(u, u_x),$$

*which satisfies*

$$\|\eta\|_{H^{p+1}} \leq C(\beta, \|F\|_{C^{p-1,1}})\|u\|_{H^p}.$$

*In particular there is a continuous injective map $H^p \to H^{p+1} : u \mapsto \eta^u$, where $\eta^u$ denotes the unique solution of the second equation in (4.29).*

PROOF.
Take Fourier transforms like in Lemma 4.26. ∎

Now we set up the framework for the vanishing viscosity method. The equation for $u$ in (4.29) is regularized by $\varepsilon\Delta$. Then the equation looks like the first equation in (4.24), where we proved existence of solutions for fixed $\varepsilon > 0$. Now we fix initial values $u_0$ and look at solutions depending on the parameter $\varepsilon$. We write $u^\varepsilon(t,x) = u(t,x,\varepsilon)$ and $\eta^\varepsilon$ instead of $\eta^{u^\varepsilon}$. As always we have $\gamma^\varepsilon = \eta^\varepsilon + \gamma_*$. Then the equation becomes

$$\begin{aligned} u_t^\varepsilon - \varepsilon u_{xx}^\varepsilon + (\gamma^\varepsilon u^\varepsilon)_x &= 0, \\ u(0,\cdot) &= u_0. \end{aligned} \tag{4.33}$$

First we show local existence of solutions in $H^p$ for $p \geq 1$. Then we prove estimates of $\|D_k u^\varepsilon(t,\cdot)\|_2$ successively for $0 \leq k \leq 3$ which are independent of $\varepsilon > 0$. Finally we bound $\|D_k u_t^\varepsilon(t,\cdot)\|_2$ for $k \in \{0,1\}$, where $D_k = \partial^k/\partial x^k$. To ease notation we drop the superscript $\varepsilon$ for the moment since no confusion can arise.

LEMMA 4.3.4
*Let $F \in \mathcal{C}_b^{p-1,1}$ and $u_0 \in H^p(\mathbb{R})$ for some $p \geq 1$, $u_0 \geq 0$. Then there exists a time $T > 0$ such that there is a unique solution $u \in \mathcal{C}([0,T], H^p(\mathbb{R}))$ of equation (4.33) with $\eta(t) \in H^{p+1}(\mathbb{R})$ for all $0 \leq t \leq T$.*

PROOF.
Semigroup approach. To show that the map $u \mapsto (\gamma u)_x$ is locally Lipschitz we use Lemma 4.3.3 and the fact that the equation for $\eta$ is linear. ∎

LEMMA 4.3.5
*Let $F$ and $u_0$ as in Lemma 4.3.4 with $p \geq 3$. For all $t \geq 0$ we have*

$$\|u(t)\|_2 \leq e^{Kt}\|u_0\|_2, \tag{4.34}$$

*with $K$ being the constant from (4.32).*

PROOF.
Since $u \in H^3(\mathbb{R})$ we have $\eta(t) \in H^4(\mathbb{R}) \subset \mathcal{C}^3(\mathbb{R})$ and so estimate (4.32) holds true. Then

$$\begin{aligned}\frac{d}{dt}\int u^2(t,x)dx &= 2\int u(t,x)(\varepsilon u_{xx}(t,x) - (\gamma(t,x)u(t,x))_x dx \\ &= -2\varepsilon\int u_x^2(t,x)dx - 2\int \left(\gamma u u_x + \gamma_x u^2\right)(t,x)dx.\end{aligned}$$

Now we use the equality $(\gamma u^2)_x = \gamma_x u^2 + 2\gamma u u_x$. The integral of $(\gamma u^2)_x$ vanishes since $\gamma$ is bounded and $u \in L^2$. The integral of $u_x^2$ is positive and $\gamma_x$ is bounded by $K$. Hence we estimate

$$\frac{d}{dt}\|u(t)\|_2^2 \leq \int |\gamma_x(t,x)|u^2(t,x)dx \leq K\|u(t)\|_2^2.$$

The claim then follows. ∎

LEMMA 4.3.6
*Let $F$ and $u_0$ as in Lemma 4.3.4 with $p \geq 3$. For all $T > 0$ there exists a constant $C = C(T, K, \|u_0\|_2)$ independent of $\varepsilon > 0$ such that*

$$\|u_x(t)\|_2 \leq C\left(\|u_{0x}\|_2 + 1\right) \tag{4.35}$$

*for $0 \leq t \leq T$. The constant grows in $T$ at most like $e^{e^T T}$.*

PROOF.
Differentiating equation (4.33) with respect to $x$ and setting $v = u_x$ gives

$$v_t = \varepsilon v_{xx} - \gamma v_x - 2\gamma_x v - \gamma_{xx} u. \tag{4.36}$$

We use the same idea as above to estimate $\|v\|_2$. There is an additional term in the equation which we estimate by the Cauchy-Schwarz inequality.

$$\begin{aligned}\frac{d}{dt}\int v^2(t,x)dx &= 2\int v(t,x)\left(\varepsilon v_{xx} - \gamma v_x - 2\gamma_x v - \gamma_{xx} u\right)(t,x)dx \\ &= -2\varepsilon\int v_x^2(t,x)dx - \int(\gamma v^2)_x(t,x)dx \\ &\quad +3\int(\gamma_x v^2)(t,x)dx - 2\int(\gamma_{xx} uv)(t,x)dx\end{aligned}$$

This gives the inequality

$$\frac{d}{dt}\|v(t)\|_2^2 \leq 3K\|v(t)\|_2^2 + 2K\|u(t)\|_2\|v(t)\|_2.$$

On comparing for $z, \zeta > 0$ the differential equations $\dot{z} \leq az + b\sqrt{z}$, $a, b > 0$, and $\dot{\zeta} = g(\zeta)$ with

$$g(\zeta) = \begin{cases} a+b, & 0 < \zeta \leq 1 \\ (a+b)\zeta, & \zeta \geq 1 \end{cases}$$

such that $az + b\sqrt{z} \leq g(z)$ for $z > 0$ one finds $z(t) \leq e^{(a+b)t}(1 + z(0))$. Here we have $a = 3K$ and $b = 2Ke^{KT}$. This proves the claim. ∎

LEMMA 4.3.7
*Let $F$ and $u_0$ as in Lemma 4.3.4 with $p \geq 3$. For all $T > 0$ there exists a constant $C = C(T, K, \|u_0\|_{H^1}, \beta, \|F\|_{C^1})$ independent of $\varepsilon > 0$ such that*

$$\|u_{xx}(t)\|_2 \leq C\left(\|u_{0xx}\|_2 + 1\right) \tag{4.37}$$

*for $0 \leq t \leq T$.*

PROOF.
Differentiating equation (4.33) twice and setting $v = u_{xx}$ we get

$$v_t = \varepsilon v_{xx} - \gamma v_x - 3\gamma_x v - 3\gamma_{xx}u_x - \gamma_{xxx}u.$$

We can treat this equation as above except for the last term. Differentiating the equation for $\eta$ we can replace

$$\eta_{xxx} = \frac{1}{\beta}\left(\eta_x - F_1(u, u_x)u_x - F_2(u, u_x)u_{xx}\right).$$

As usual, subscripts of $F$ denote partial derivatives. We get an additional term containing $v$. We arrive at the equation

$$\begin{aligned} \frac{d}{dt}\|v(t)\|_2^2 &= -2\varepsilon\int v_x^2(t,x)dx - \int(\gamma v^2)_x^2(t,x)dx \\ &\quad -5\int(\gamma_x v^2)(t,x)dx - \int\left(3\gamma_{xx}u_x - \frac{1}{\beta}\gamma_x + \frac{F_1}{\beta}u_x\right)uv(t,x)dx \\ &\quad -\int\frac{F_2}{\beta}uv^2(t,x)dx. \end{aligned}$$

Hence we estimate

$$\begin{aligned} \frac{d}{dt}\|v(t)\|_2^2 &\leq \left(5K + \frac{\|F_2\|_\infty}{\beta}e^{KT}\|u_0\|_2\right)\|v(t)\|_2^2 \\ &\quad + C(K, \beta, \|F_1\|_\infty)\|u(t)\|_{H^1}\|v(t)\|_2. \end{aligned}$$

This inequality hat the same structure as in the preceeding lemma. Here we have $a = (5K + \frac{\|F_2\|_\infty}{\beta}e^{KT}\|u_0\|_2)$ and $b = C(T, K, \beta, \|F_1\|_\infty, \|u_0\|_{H^1})$. A similar argument as above finishes the proof. ∎

LEMMA 4.3.8
*Let $F$ and $u_0$ as in Lemma 4.3.4 with $p \geq 3$. For all $T > 0$ there exists a constant $C = C(T, K, \|u_0\|_{H^2}, \beta, \|F\|_{C^2})$ such that*

$$\|u_{xxx}(t)\|_2 \leq e^{Ct} \left( \|u_{0xxx}\|_2 + 1 \right) \tag{4.38}$$

*for $0 \leq t \leq T$.*

PROOF.
Similarly to the above lemma. ∎

COROLLARY 4.3.9
*Let $F$ and $u_0$ as in Lemma 4.3.4 with $p \geq 3$. Then there exists a unique solution $u \in \mathcal{C}([0, \infty), H^3(\mathbb{R}))$ to system (4.29) with $\eta \in \mathcal{C}([0, \infty), H^4(\mathbb{R}))$.*

LEMMA 4.3.10
*Let $F$ and $u_0$ as in Lemma 4.3.4 with $p \geq 3$. Then for all $t \geq 0$ there is a constant $C = C(t)$ independent of $0 < \varepsilon \leq 1$ such that*

$$\|u_t(t)\|_2 \leq C \|u(t)\|_{H^2}. \tag{4.39}$$

PROOF.
A simple computation and the Cauchy-Schwarz inequality give

$$\begin{aligned} \int u_t^2(t,x)dx &= \int \left( \varepsilon u_{xx} - (\gamma u)_x \right)^2 (t,x)dx \\ &= \varepsilon^2 \int u_{xx}^2(t,x)dx - 2\varepsilon \int u_{xx}(\gamma u)_x(t,x)dx + \int (\gamma u)_x^2(t,x)dx \\ &\leq \varepsilon^2 \|u_{xx}(t)\|_2^2 + 2\varepsilon \|u_{xx}(t)\|_2 \|(\gamma u)_x(t)\|_2 + \|(\gamma u)_x(t)\|_2^2. \end{aligned}$$

By Lemma 4.3.7 the norm of $u_{xx}$ can be bounded independently of $\varepsilon > 0$. For the last term we find the estimate

$$\begin{aligned} \int (\gamma u)_x^2 dx &= \int \gamma_x^2 u^2 + \gamma \gamma_x u u_x + \gamma^2 u_x^2 dx \\ &\leq 2K^2 \left( \|u\|_2 + \|u_x\|_2 \right), \end{aligned}$$

where we use boundedness of $\gamma$. The last two terms are bounded independently of $\varepsilon > 0$ by Lemmas 4.3.5 and 4.3.6. ∎

LEMMA 4.3.11
*Let $F$ and $u_0$ as in Lemma 4.3.4 with $p \geq 3$. Then for all $t \geq 0$ there is a constant $C = C(t)$ independent of $0 < \varepsilon \leq 1$ such that*

$$\|u_{xt}(t)\|_2 \leq C \|u(t)\|_{H^3}. \tag{4.40}$$

PROOF.
Similarly as above. ∎

### 4.3.2 Proof of Theorem 4.3.1

From now on we write the superscript $\varepsilon$ again. Suppose that the initial data satisfy $u_0 \in H^3 \cap L^1(\mathbb{R})$, $u_0 \geq 0$.

**(i) Boundedness independent of** $0 < \varepsilon \leq 1$
By the preceeding Lemmas 4.3.5 through 4.3.11 we know that there is a constant $C$ independent of $0 < \varepsilon \leq 1$ such that on $\Omega_T$ we have

$$\|u^\varepsilon\|_{H^1(\Omega_T)}, \|u^\varepsilon_x\|_{H^1(\Omega_T)} \leq C.$$

Lemma 4.3.3 applied to $\eta$ and $\eta_x$ gives an $\varepsilon$-independent bound

$$\|\eta^\varepsilon\|_{H^1(\Omega_T)}, \|\eta^\varepsilon_x\|_{H^1(\Omega_T)} \leq C,$$

where $\eta^\varepsilon$ denotes the solution of the elliptic equation for $\eta$ with $u^\varepsilon, u^\varepsilon_x$ on the right hand side. Positivity of $u^\varepsilon$ and the conservation law structure of the equation for $u^\varepsilon$ give $\|u^\varepsilon(t)\|_{L^1(\mathbb{R})} = \text{const.}$ and hence we may assume also that

$$\|u^\varepsilon\|_{L^1(\Omega_T)} \leq C.$$

**(ii) Convergence**
Given some domain $\Omega \subset \mathbb{R}^n$ the imbedding $W^{k,p}(\Omega) \hookrightarrow L^q_{\text{loc}}(\Omega)$ is compact for $kp \leq \dim(\Omega)$ and $1 \leq q < \infty$ (see Theorem 6.2 in [1]). Here we have $k = 1, p = 2, \dim(\Omega_T) = 2$. Hence there is a sequence $\varepsilon_n \to 0$ and there are functions $u \in L^1 \cap L^2(\Omega_T)$ and $v, \eta, \zeta \in L^2(\Omega_T)$ such that

$$\left.\begin{array}{ll} u^{\varepsilon_n} \longrightarrow u, & u^{\varepsilon_n}_x \longrightarrow v \\ \eta^{\varepsilon_n} \longrightarrow \eta, & \eta^{\varepsilon_n}_x \longrightarrow \zeta \end{array}\right\} \text{ in } L^2_{\text{loc}}(\Omega_T) \text{ as } n \to \infty.$$

For all $\varepsilon > 0$ and all test functions $\psi \in \mathcal{C}^1(\mathbb{R})$ with compact support we have

$$\int \eta^\varepsilon_x \psi dx = -\int \eta^\varepsilon \psi_x dx,$$

and hence $\zeta = \eta_x$ in the weak sense and similarly $v = u_x$. Even though the convergence need not be in $L^2(\Omega_T)$ the $L^2$-norm of the limit is nonetheless bounded by the $L^2$-norm of the sequences. In particular $u$ is measurable with respect to $t$ and $u(t) \in H^1(\mathbb{R})$ for almost all $t$. This then gives

$$u \in L^1(\Omega_T) \cap L^\infty([0,T], H^1(\mathbb{R})) \text{ and } \eta \in L^\infty([0,T], H^1(\mathbb{R})).$$

**(iii) The limit satisfies the equation**
Multiplying equation (4.33) for $u^\varepsilon$ with a test function $\phi \in \mathcal{C}^1(\mathbb{R}^2)$ with compact support in $[0,T) \times \mathbb{R}$ and integrating over $\Omega_T$ we get after partial integration

$$\int_0^T \int u^\varepsilon \phi_t + \gamma^\varepsilon u^\varepsilon \phi_x dx dt = -\varepsilon \int_0^T \int u^\varepsilon_x \phi_x dx dt - \int u_0 \phi dx. \tag{4.41}$$

The weak convergence $u^{\varepsilon_n} \to u$ as $\varepsilon_n \to 0$ implies

$$\int_0^T \int u^{\varepsilon_n} \phi_t dx dt \longrightarrow \int_0^T \int u \phi_t dx dt.$$

Convergence of the second term is obvious since the scalar product in $L^2$ is continuous in both variables, hence

$$\int_0^T \int \gamma^{\varepsilon_n} u^{\varepsilon_n} \phi_x dx dt \longrightarrow \int_0^T \int \gamma u \phi_x dx dt.$$

The convergence of $u_x^{\varepsilon_n}$ implies the boundedness of the first integral on the right hand side of equation (4.41). Then, as $\varepsilon_n \to 0$, this term vanishes. Altogether we have shown that in the limit

$$\int_0^T \int u\phi_t + \gamma u \phi_x dx dt = -\int u_0 \phi dx,$$

which means that the limit satisfies equation (4.29) in the weak sense.

The fact that $\eta$ satisfies the elliptic equation for almost all $t \in [0,T]$ follows similarly when we take into account that there are subsequences which converge a.e. Regularity theory for the elliptic equation gives $\eta(t) \in H^2$ for almost all $t \in [0,T]$ and

$$\|\eta(t)\|_{H^2} \leq C \|u(t)\|_{H^1}.$$

**(iv) Initial Conditions**
We define the set $\mathcal{L} \subset [0,T]$ such that for all $t \in [0,T]\backslash\mathcal{L}$ and for almost all $x \in \mathbb{R}$ the point $(t,x)$ is a Lebesgue point of $u$ and $\eta$. The measure of $\mathcal{L}$ is zero by the regularity properties of $u$ and $\eta$. Fix $\rho > 0$ and set $I = [-\rho, \rho]$. We show that

$$\limsup_{t \to 0, t \in [0,T]\backslash\mathcal{L}} \|u(t,\cdot) - u_0(\cdot)\|_{H^1(I)} = 0.$$

For all $\varepsilon > 0$ and $t \in [0,T]\backslash\mathcal{L}$ we have

$$\|u(t,\cdot) - u_0(\cdot)\|_{H^1(I)} \leq \|u(t,\cdot) - u^\varepsilon(t,\cdot)\|_{H^1(I)} + \|u^\varepsilon(t,\cdot) - u_0(\cdot)\|_{H^1(I)}.$$

For the first term on the right hand side we note that by passing to a subsequence, also denoted by $\varepsilon_n$ we can assume that $u^{\varepsilon_n} \to u$, $u_x^{\varepsilon_n} \to u_x$ a.e. Hence the first term is arbitrarily small for almost all $t$.

The second term can be split as

$$\|u^\varepsilon(t,\cdot) - u_0(\cdot)\|_{H^1} \leq \|(T_\varepsilon(t) - Id)u_0\|_{H^1} + \int_0^t \|T_\varepsilon(t-s)(\gamma^\varepsilon u^\varepsilon)_x(s)\|_{H^1} ds.$$

Since $T_\varepsilon$ is a strongly continuous semigroup, the first term vanishes as $t \to 0$. The integral can be estimated by

$$C_\varepsilon K e^{CT} \|u_0\|_{H^1(\mathbb{R})} \sqrt{t},$$

which vanishes as $t \to 0$.

To show the initial condition for $\eta$ we use that $F$ is Lipschitz and that the equation for $\eta$ is linear. With Lemma 4.3.3 and the convergence $u^{\varepsilon_n} \to u$ the assertion follows.

**(v) Uniqueness and Regularity**
Solutions of conservation laws are not unique in general. Additional conditions like entropy conditions have to be imposed [33]. One might be able to adapt the entropy method to the equations here.

For initial data in $H^3$ we get solutions in $H^1$. This loss of differentiability is partly due to the formulation of the problem (the explicit appearance of $u_x$ in the equations) and partly due to the method of proof (using the compact imbedding results). In order to achieve better regularity properties one might be able to use different compactness results like the Fréchet-Kolmogoroff Theorem.

■

Remark
Probably one can show that Theorem 4.3.1 remains true if $H^q(\mathbb{R}) = W^{q,2}(\mathbb{R})$ is replaced by $W^{q,1}(\mathbb{R})$ wherever it occurs in the theorem. To show statements like Lemmas 4.3.5 through 4.3.11 one could use an estimate by Vol'pert (Theorem 17.2 in [64]). Lemma 4.3.3 has to be replaced by the following lemma, which ensures solvability of elliptic equations in $L^1$.

Lemma 4.3.12
*Let $f \in L^1(\mathbb{R})$. Then there exists a unique solution $\eta \in W^{2,1}(\mathbb{R})$ of the elliptic equation $(\beta\Delta - 1)\eta = f$ and $\|\eta\|_{W^{2,1}} \leq C(\beta)\|f\|_{L^1}$. Furthermore $\eta \in \mathcal{C}^1(\mathbb{R})$ and $\|\eta\|_{\mathcal{C}^1} \leq C(\beta)\|f\|_{L^1}$.*

Proof.
Suppose $f \in L^1(\mathbb{R})$. It suffices to treat the case $\beta = 1$. Taking Fourier transforms we get

$$\hat{\eta}(\kappa) = \frac{-1}{\kappa^2 + 1}\hat{f}(\kappa),$$

where by the Riemann-Lebesgue Lemma $\hat{f} \in \mathcal{C}_{uc}(\mathbb{R})$ and $\hat{f}(\kappa) \to 0$ as $|\kappa| \to \infty$ as well as $\|\hat{f}\|_{C^0} \leq \|f\|_{L^1}$. Obviously $\hat{\eta}$ is integrable and we apply the inverse Fourier transform to get a function $\check{\hat{\eta}} = \zeta \in \mathcal{C}_{uc}(\mathbb{R})$ which is the candidate for the solution. As above we know $\zeta(x) \to 0$ as $|x| \to \infty$ and $\|\zeta\|_{C^0} \leq \|\hat{\eta}\|_{L^1} \leq C\|f\|_{L^1}$.

**Claim:** $\zeta \in L^1(\mathbb{R})$

$$\begin{aligned}\int |\zeta(x)|dx &= \frac{1}{2\pi}\int \left|\int \frac{-\hat{f}(\kappa)}{\kappa^2+1}e^{i\kappa x}d\kappa\right| dx \\ &\leq \frac{\|\hat{f}\|_\infty}{2\pi}\int \frac{\pi}{2}e^{-|x|}dx \leq \|f\|_{L^1}\end{aligned}$$

From this we conclude that $\eta = \zeta = \check{\hat{\eta}}$. From the equation we furthermore get that $\eta_{xx} \in L^1(\mathbb{R})$ with $\|\eta_{xx}\|_{L^1} \leq 2\|f\|_{L^1}$.

Suppose for the moment that $|\hat{f}(\kappa)| \leq \frac{C}{\kappa}$ for large enough $|\kappa|$. Then

$$\kappa\hat{\eta}(\kappa) = \frac{-\kappa}{\kappa^2+1}\hat{f}(\kappa) \in L^1(\mathbb{R}).$$

We can repeat the process above to get $\eta_x \in \mathcal{C}_{uc}(\mathbb{R})$ and $\eta_x(x) \to 0$ as $|x| \to \infty$ as well as $\|\eta_x\|_{L^1} \leq C\|f\|_{L^1}$. Furthermore we can integrate

$$\eta_x(y) = \int_{-\infty}^{y} \eta_{xx}(s)ds \leq \|\eta_{xx}\|_{L^1} \leq 2\|f\|_{L^1}$$

which gives the desired $\mathcal{C}^1$-estimate for $\eta$.
It remains to show that actually $|\hat{f}(\kappa)| \leq \frac{C}{\kappa}$ for large enough $|\kappa|$. To this end consider a step function

$$g(x) = A\chi_{[a,b]}(x)$$

which has the Fourier transform

$$\hat{g}(\kappa) = \frac{iA}{2\kappa}\left(e^{ia\kappa} - e^{ib\kappa}\right).$$

We can find a sequence of finite linear combinations of such step functions (on disjoint intervals)

$$g_m = \sum_{n=1}^{l_m} A_n^m \chi_{[a_n^m, b_n^m]}$$

such that $g_m \to f$ in $L^1$ as $m \to \infty$. This implies that $\hat{g}_m \to \hat{f}$ uniformly. We get a bound

$$\left| \lim_{m\to\infty} \sum_{n=1}^{l_m} A_n^m (e^{ia_n^m\kappa} - e^{ib_n^m\kappa}) \right| \leq 2C|\kappa| \leq 2\pi C$$

for $\kappa \in [-\pi, \pi]$. The term in absolute values is a periodic function in $\kappa$ and hence the claim follows. ∎

## 4.4 The Full System for $u^{\pm}$

Finally, we combine the speed adaptation process with the alignment process. There are individuals moving to the right and to the left. The respective densities are denoted by $u^{\pm}$. Individuals change direction according to the turning function from Chapter 2. They also adapt their speed $\gamma^{\pm}$ according to the equations derived at the beginning of the present chapter. We assume that each individual adapts its speed only to the speed of others which move in the same direction as the individual itself. The system then reads

$$\begin{aligned} u_t^{\pm} \pm (\gamma^{\pm} u^{\pm})_x &= \varepsilon u_{xx}^{\pm} \pm \mu(u^+, u^-)(u^{\pm} - u^{\mp}), \\ \tau\eta^{\pm} &= \beta\eta_{xx}^{\pm} + F(u^{\pm}, \pm u_x^{\pm}), \\ \gamma^{\pm} &= \eta^{\pm} + \gamma_*, \end{aligned} \tag{4.42}$$

where $\mu(u^+, u^-) = a(u)u^+u^- - \mu_*/2$ and $a(u) = a_*/(1 + u^k)$ for $k = 2, 3$, $a_* > 0$.

We may fix small values of $\varepsilon, \beta, \tau$ and consider the behavior of the system depending on the "biological parameters" preferred density $u_*$, preferred speed $\gamma_*$, strength of alignment $a_*$, rate of turning $\mu_*$ and strength of speed adaptation $\chi$. For $a_* = \chi = 0$, $\mu_* > 0$ the system reduces to (1.5) and the stationary state $u^+ = u^- = \text{const.}$ is stable. Increasing $a_*$ destabilizes this stationary state. If

$a_* = \mu_* = 0$ then the equations for $u^\pm$ decouple and increasing $\chi$ destabilizes the constant solution $u^+ = u^- < u_*$, $\gamma^\pm = \gamma_*$. We expect that also for small $\mu_*$ increasing $\chi$ can destabilize this stationary state.

We can conjecture what happens for $\mu_* = 0$. By alignment all individuals tend to move in the same direction, by speed adaptation individuals tend to move in patches of density $u_*$ in either direction. The bifurcation behavior from $u^+ = u^- =$ const. should depend on the relative strength $a_*/\chi$.

Due to the number of parameters, analytical stability results are difficult to obtain. Numerical simulations could give some information about possible phenomena. From our point of view, model (4.42) is a good starting point for further studies to understand the behavior of moving polarized groups. Here we show existence of solutions for $\tau = 0, \varepsilon > 0$ and then prove that the vanishing viscosity approach can be adapted to the system of four equations.

Under the assumption $\tau = 0$ the second and the third equation of (4.42) can be replaced by

$$\gamma^\pm = \beta\gamma^\pm_{xx} + E(u^\pm, \pm u^\pm_x). \tag{4.43}$$

THEOREM 4.4.1
*Let $E \in \mathcal{C}^{1,1}_b$, $\varepsilon > 0$ and $\tau = 0$. Choose initial data $u^\pm_0 \in \mathcal{C}^2_b(\mathbb{R})$ with $u^\pm_0 \geq 0$. Then there exists a unique global nonnegative solution $(u^\pm, \gamma^\pm) \in \mathcal{C}([0,\infty), \mathcal{C}^2_b(\mathbb{R})^4)$ of (4.42). The speed functions satisfy*

$$0 \leq \gamma^\pm \leq E_{\max}, \qquad \|\gamma^\pm\|_{C^2} \leq C(\beta)\|u^\pm\|_{C^2} \qquad \text{and} \qquad \|\gamma^\pm\|_{C^2} \leq K.$$

PROOF.
By (4.43) the equations for $\gamma^\pm$ decouple and Lemmas 4.2.6 and 4.2.8 apply to both $\gamma^+$ and $\gamma^-$. We abuse notation and write $\gamma^\pm$ instead of $\gamma^{u^\pm}$ for the solution of (4.43). Then system (4.42) can be written as a system of two equations for the densities $u^\pm$. Let $X = \mathcal{C}^2(\mathbb{R})^2$ with norm $\|(u,v)\|_X = \|u\|_{C^2} + \|v\|_{C^2}$ and $Y = \mathcal{C}^1(\mathbb{R})^2$ accordingly. We set $\nu = (u^+, u^-)^T$. Then (4.42) becomes

$$\nu_t = \mathcal{A}\nu + \mathcal{F}(\nu) = \mathcal{A}\nu + \mathcal{F}_1(\nu) + \mathcal{F}_2(\nu), \tag{4.44}$$

where $\mathcal{A}$ =diag$(\varepsilon\Delta, \varepsilon\Delta)$ is the generator of an analytic semigroup on $X$. The nonlinearities are

$$\begin{aligned} \mathcal{F}_1(\nu) &= -((\gamma^+u^+)_x, (\gamma^-u^-)_x)^T, \\ \mathcal{F}_2(\nu) &= \mu(u^+, u^-)(u^+ - u^-, u^- - u^+)^T. \end{aligned}$$

From Theorem 4.2.7 we know that each component of $\mathcal{F}_1$ is locally Lipschitz from $\mathcal{C}^2(\mathbb{R})$ into $\mathcal{C}^1(\mathbb{R})$. Hence so is $\mathcal{F}_1$ from $X$ to $Y$. Now consider one component of $\mathcal{F}_2$. Note that $\mu$ and all its derivatives are bounded. The Lipschitz constant of $\mu$ and its first derivative can be bounded by $\|\mu\|_{C^2}$. Choose $u^\pm, \tilde{u}^\pm \in \mathcal{C}^1(\mathbb{R})$ with

$\|u^{\pm}\|_{C^1}, \|\tilde{u}^{\pm}\|_{C^1} \leq k_0$ for some $k_0 > 0$. Then

$$\begin{aligned}
& \|\mu(u^+,u^-)(u^+-u^-)-\mu(\tilde{u}^+,\tilde{u}^-)(\tilde{u}^+-\tilde{u}^-)\|_{C^1} \\
\leq\ & \frac{1}{2}\|(\mu(u^+,u^-)+\mu(\tilde{u}^+,\tilde{u}^-))(u^+-u^--\tilde{u}^++\tilde{u}^-)\|_{C^1} \\
& +\frac{1}{2}\|(\mu(u^+,u^-)-\mu(\tilde{u}^+,\tilde{u}^-))(u^+-u^-+\tilde{u}^+-\tilde{u}^-)\|_{C^1} \\
\leq\ & \|\mu\|_{C^1}\left(\|u^+-\tilde{u}^+\|_{C^1}+\|u^--\tilde{u}^-\|_{C^1}\right) \\
& +Ck_0\|\mu\|_{C^2}(\|u^+-\tilde{u}^+\|_2+\|u^--\tilde{u}^-\|_{C^1}).
\end{aligned}$$

Hence $\mathcal{F}_2$ is even locally Lipschitz from $\mathcal{C}^1(\mathbb{R})$ into $\mathcal{C}^1(\mathbb{R})$. Then of course $\mathcal{F}$ is locally Lipschitz and Proposition 1.1 §15 in [62] gives local existence of solutions and uniqueness.

Suppose $u^{\pm}(t,\cdot) > 0$ for $0 \leq t < t_0$ and $u^+(t_0,x_0) = 0$, say. Then by the differential equation

$$u_t^+(t_0,x_0) = \varepsilon u_{xx}^+ + \mu u^- > 0,$$

hence positivity is preserved.

To show global existence of solutions we adapt the proof of Theorem 4.2.9. We estimate the norm of $\nu$ in $X$ as follows.

$$\begin{aligned}
\|\nu(t)\|_X &= \|u^+(t)\|_{C^2}+\|u^-(t)\|_{C^2} \\
&\leq \|u_0^+\|_{C^2}+\|u_0^-\|_{C^2}+\int_0^t \|T_\varepsilon(t-s)(\gamma^+u^++\gamma^-u^-)_x(s)\|_{C^2}ds \\
&\quad +2\int_0^t \|T_\varepsilon(t-s)(\mu(u^+,u^-)(u^+-u^-))(s)\|_{C^2}ds \\
&\leq \|\nu_0\|_X+\int_0^t \frac{C_\varepsilon}{\sqrt{t-s}}2K\|\nu(s)\|_X ds \\
&\quad +2\int_0^t \frac{C_\varepsilon\mu_\infty}{\sqrt{t-s}}\|\nu(s)\|_X ds,
\end{aligned}$$

where $\mu_\infty = \sup_x|\mu(u^+,u^-)|+\sup_x|\mu_j(u^+,u^-)u^{\pm}|$. Subscripts of $\mu$ denote derivatives with respect to the $j$-th component. With the norm $\|\nu\|^T = \sup_{0\leq t\leq T}\|\nu(t)\|_X$ we have

$$\|\nu\|^T \leq \|\nu_0\|_X + 2KC_\varepsilon\|\nu\|^T\sqrt{T}+2C_\varepsilon r_\infty\|\nu\|^T\sqrt{T},$$

and hence

$$\|\nu\|^T \leq \frac{\|\nu_0\|_X}{1-C\sqrt{T}},$$

where $C = 2C_\varepsilon(K+\mu_\infty)$ does not depend on initial data. Hence we can apply a continuation argument to complete the proof. ∎

Finally we show that the vanishing viscosity approach from the previous section can be applied here also. There is a weak solution of (4.42) for $\varepsilon = 0$. If the initial data are sufficiently smooth then the solution $u^{\pm}(t,\cdot)$ remains continuous in $x$ for arbitrary long times $T$. The analogue of Theorem 4.3.1 is the following.

THEOREM 4.4.2
*Let $F$ be in $\mathcal{C}_b^{2,1}$, $T > 0$ and $\Omega_T = [0,T] \times \mathbb{R}$. Then for all nonnegative initial data $u_0^\pm \in H^3(\mathbb{R}) \cap L^1(\mathbb{R})$ there exists a solution $(u^\pm, \eta^\pm)$ which satisfies $u^\pm \geq 0$, to system (4.42) with $\varepsilon = 0$ following sense*

- *$u^\pm \in L^1(\Omega_T) \cap L^\infty([0,T], H^1(\mathbb{R}))$ and $u^\pm$ satisfy the weak formulation of (4.42) for all $\phi \in \mathcal{C}^1(\Omega_T)$ with compact support in $[0,T) \times \mathbb{R}$.*

- *$\eta^\pm \in L^\infty([0,T], H^2(\mathbb{R}))$ and for almost all $t \in [0,T]$ the functions $\eta^\pm$ satisfy the weak formulation of (4.42) for all $\psi \in \mathcal{C}^1(\mathbb{R})$ with compact support.*

- *initial values are assumed in the weak sense, i.e. there exists a set $\mathcal{L} \subset [0,T]$ of Lebesgue measure 0, such that $u^p m(t,\cdot), \eta^\pm(t,\cdot)$ are defined a.e. on $\mathbb{R}$ for $t \in [0,T]\backslash\mathcal{L}$ and satisfy*

$$\limsup_{t \to 0, t \in [0,T]\backslash\mathcal{L}} \|u^\pm(t,\cdot) - u_0^\pm(\cdot)\|_{H^1(I)} = 0$$

*and*

$$\limsup_{t \to 0, t \in [0,T]\backslash\mathcal{L}} \|\eta^\pm(t,\cdot) - \eta^\pm(0,\cdot)\|_{H^2(I)} = 0$$

*for all bounded intervals $I = [-\rho, \rho]$.*

COROLLARY 4.4.3
*Let $F$ be in $\mathcal{C}_b^{2,1}$ and $T > 0$. Then for all nonnegative initial data $u_0^\pm \in \mathcal{C}^3(\mathbb{R})$ with compact support there exists a solution to (4.42) with $\varepsilon = 0$ such that $u^\pm(t)$ remains continuous for $t \in [0,T]$.*

PROOF.
Since the proof closely follows the one in the previous section we only give the details where it deviate from what was done before.

**(i) The equations for $\eta^\pm$.**
The equation for $\eta^+$ is independent of $u^-$ and vice versa. Therefore Lemma 4.3.3 holds for $\eta^+$ as well as for $\eta^-$ : Given $u^\pm \in H^p(\mathbb{R})$ for some $p \geq 1$ there exist unique solutions $\eta^\pm \in H^{p+1}(\mathbb{R})$ of the equation for $\eta$ in (4.42) and

$$\|\eta^\pm\|_{H^{p+1}} \leq C(\beta, \|F\|_Z)\|u^\pm\|_{H^p}.$$

Also as before if $p \geq 3$ then $\eta^\pm \in \mathcal{C}^2$ and $\|\eta^\pm\|_{C^2} \leq K$.
Again, abusing notation, we denote by $\eta^\pm$ the unique solutions corresponding to $u^\pm$. With this notation system (4.42) reduces to two equations for the densities.

**(ii) Local Existence in $H^p(\mathbb{R})^2$**
It remains to show that $\mathcal{F}_2 : (H^p)^2 \to (H^{p-1})^2$ is locally Lipschitz. Let $u^\pm, v^\pm \in H^p$ with $\|u^\pm\|_{H^p}, \|v^\pm\|_{H^p} < k_0$. We use that $\mu$ and all its derivatives are Lipschitz. Furthermore $H^p(\mathbb{R})$ is a Banach algebra for $p \geq 1$ with continuous multiplication.

Then

$$\begin{aligned} & \|\mathcal{F}_2(u^+,u^-)-\mathcal{F}_2(v^+,v^-)\|_{(H^{p-1})^2} \\ \leq\ & \|(\mu(u^+,u^-)-\mu(v^+,v^-))(u^+-u^--v^++v^-)\|_{H^{p-1}} \\ & +\|(\mu(u^+,u^-)-\mu(v^+,v^-))(u^+-u^--v^++v^-)\|_{H^{p-1}} \\ \leq\ & L_p(\mu)C_1(k_0)\|u^{\pm}-v^{\pm}\|_{H^{p-1}} \\ & +C_2(\|\mu\|_{C^{p-1}})\|u^{\pm}-v^{\pm}\|_{H^{p-1}} \\ \leq\ & L(\mu,k_0)\|u^{\pm}-v^{\pm}\|_{H^{p-1}}. \end{aligned}$$

The different constants have the following meaning: $L_p(\mu)$ is the supremum of the Lipschitz constants of derivatives of $\mu$ up to order $p-1$, the factors $C_j$ are just suitable multiples of their arguments and $L$ is the sum of $L_pC_1$ and $C_2$.

**(iii) The Estimate of $\nu=(u^+,u^-)$ in $L^2(\mathbb{R})^2$**

$$\begin{aligned} \frac{d}{dt}\|u^{\pm}(t)\|_2^2 &= \int u^{\pm}\left(\varepsilon u^{\pm}_{xx}-(\gamma^{\pm}u^{\pm})_x+\mu(u^+,u^-)(u^+-u^-)\right)(t,x)dx \\ &\leq K\|u^{\pm}(t)\|_2^2+\|\mu\|_{C^0}\|u^{\pm}(t)\|_2^2+\|\mu\|_{C^0}\|u^+(t)\|_2\|u^-(t)\|_2, \end{aligned}$$

where the first term comes from Lemma 4.3.5. Due to the coupling, we cannot derive a bound for $u^+$ or $u^-$ alone from this inequality, but we can derive one for $\nu=(u^+,u^-)$ with respect to the norm $\|\nu\|_2=\|u^+\|_2+\|u^-\|_2$, namely

$$\|\nu(t)\|_2^2\leq e^{(K+2\|\mu\|)t}\|\nu_0\|_2^2.$$

From now on we assume $u_0^{\pm}\in H^3(\mathbb{R})$, $u_0^{\pm}\geq 0$ and denote by $\nu=(u^+,u^-)$ the unique solution of (4.42) with $t\in[0,T]$ for fixed $T>0$. We show estimates of different norms of $\nu$ which are independent of $\varepsilon$.

**(iv) The Estimate of $\nu_x=(u_x^+,u_x^-)$ in $L^2(\mathbb{R})^2$**
Like in Lemma 4.3.6 we compute

$$\begin{aligned} \frac{d}{dt}\|u_x^{\pm}(t)\|_2^2 &\leq 3K\|u_x^{\pm}(t)\|_2^2+2K\|u^{\pm}(t)\|_2\|u_x^{\pm}(t)\|_2 \\ &\quad+\int|u_x^{\pm}\frac{\partial}{\partial x}[\mu(u^{\pm}-u^{\mp})](t,x)|^2dx. \end{aligned}$$

We have to estimate the last term. First note that the derivatives of $\mu$ times the density, i.e. $\mu_{1,2}(u^+,u^-)u^{\pm}$, are bounded globally in $x$. Then

$$\begin{aligned} & \int u_x^+[(\mu_1u_x^++\mu_2u_x^-)(u^+-u^-)+\mu(u_x^+-u_x^-)]dx \\ \leq\ & \int[\mu_1u^+(u_x^+)^2+\mu_1u^-(u_x^+)^2+\mu_2u^+u_x^+u_x^-+\mu_2u^-u_x^+u_x^-]dx \\ & +A(\|u_x^+\|_2^2+\|u_x^+\|_2\|u_x^-\|_2) \\ \leq\ & 3A(\|u_x^+\|_2^2+\|u_x^+\|_2\|u_x^-\|_2), \end{aligned}$$

where $A=\max(\|\mu\|_0,\|\mu_ju^{\pm}\|_0)$. A similar estimate holds for $u_x^-$ and hence for the sum of both. This gives the estimate

$$\|\nu_x(t)\|_2^2\leq e^{Ct}(\|\nu_0\|_2^2+1),$$

where $C = 4K + 2Ke^{(K+2\|\mu\|)T}\|\nu_0\|_2^2 + 5A$.

**(v) Higher Order Estimates of $\nu$**
Successive differentiation and estimation give the analogue of Corollary 4.3.9. For nonnegative initial data $u_0^{\pm} \in H^3(\mathbb{R})$ there exists a unique solution $u^{\pm} \in \mathcal{C}([0,\infty), H^3(\mathbb{R}))$ to system (4.42) with $\eta^{\pm} \in \mathcal{C}([0,\infty), H^4(\mathbb{R}))$. Furthermore there is a constant $C$ independent of $\varepsilon > 0$ such that for $t \in [0,T]$ we have

$$\|\nu(t,\cdot)\|_{H^3} \leq C.$$

The estimates for $\nu_t$ and $\nu_{xt}$ are similar to Lemmata 4.3.10 and 4.3.11.

**(vi) Boundedness of Solutions**
Now we explicitly take into account the dependence on $\varepsilon$. We assume nonnegative initial data $u_0^{\pm} \in H^3(\mathbb{R})$ and denote the solution to (4.42) by $\nu^{\varepsilon} = (u^{+\varepsilon}, u^{-\varepsilon})$. Then the following expressions are bounded independently of $0 < \varepsilon \leq 1$.

$$\|\nu^{\varepsilon}\|_2, \quad \|\nu_x^{\varepsilon}\|_2, \quad \|\nu_t^{\varepsilon}\|_2, \quad \|\nu_{xx}^{\varepsilon}\|_2, \quad \|\nu_{xt}^{\varepsilon}\|_2,$$

and also with $z = (\eta^+, \eta^-)$ the following

$$\|z^{\varepsilon}\|_2, \quad \|z_x^{\varepsilon}\|_2, \quad \|z_t^{\varepsilon}\|_2, \quad \|z_{xx}^{\varepsilon}\|_2, \quad \|z_{xt}^{\varepsilon}\|_2.$$

**(vii) Convergence**
By a compact imbedding argument as before we find functions $u^{\pm} \in L^1 \cap L^2(\Omega_T)$ and $\eta^{\pm} \in L^2(\Omega_T)$ and a sequence $\varepsilon_n \to 0$ such that for $n \to \infty$

$$\begin{array}{l} u^{\pm\varepsilon_n} \longrightarrow u^{\pm} \qquad \text{in } L^1_{\text{loc}} \cap L^2_{\text{loc}}(\Omega_T) \\ \left.\begin{array}{l} u_x^{\pm\varepsilon_n} \longrightarrow u_x^{\pm} \\ \eta^{\pm\varepsilon_n} \longrightarrow \eta^{\pm} \\ \eta_x^{\pm\varepsilon_n} \longrightarrow \eta_x^{\pm} \end{array}\right\} \quad \text{in } L^2_{\text{loc}}(\Omega_T). \end{array}$$

The convergence is also pointwise convergence a.e. The rest of the proof is as in the proof of Theorem 4.3.1. ■

## 4.5 Remarks

1. Grindrod [16] derives the following system for density dependent aggregation due to the expected net reproduction rate $E$.

$$\begin{aligned} u_t &= \delta u_{xx} - (wu)_x + ruE(u), \\ 0 &= \varepsilon w_{xx} - w + \nabla E. \end{aligned}$$

The term $ruE(u)$ is a production term and the velocity $w$ is chosen as to maximize $E$. The elliptic damping for $w$ is introduced since $w = \nabla E$ would lead to an ill-posed problem. Simulations show aggregation phenomena and a linear analysis is performed. No analytical results on existence of solutions are given, the limit $\delta \to 0$ is not considered.
If the time scale for reproduction is much longer than for motion then, in the limit $r = 0$, and the system is similar to (4.29) with $\gamma_* = 0$. Due to the different nonlinearities in the elliptic equations the results obtained here do not easily carry over to the system there.

2. In a series of papers the question of swarm formation is discussed, which is closely related to the schooling model here. In particular the question is which type of models supports traveling pulse solutions. It is shown that purely local models are not applicable [11].
   Mogilner and Edelstein-Keshet [39] derive a non-local model for swarm-formation, assuming attractive and repulsive forces between individuals. It has the form

$$\begin{aligned} u_t &= Du_{xx} - (Vu)_x \\ V &= a_e u + (A_a - A_r u)(K * u), \end{aligned}$$

   where the convolution kernel $K$ is an odd kernel with compact support. The diameter of the support can be viewed as the radius of vision of individuals. The convolution $K * u$ acts as a generalized gradient which prevents the equation from being ill-posed. (The approximation by Taylor series expansion is ill-posed.)
   Attracting forces $A_a$ are stronger than repulsive forces $A_r u$ at low densities but weaker at high densities. A detailed linear analysis is carried out, it is shown that a rectangular traveling pulse is a solution to the system with $D = 0$. A stability analysis for a smooth perturbation of such a pulse in case of low diffusion $D << 1$ shows that traveling band solutions are only locally stable in time.

3. Chemotaxis in another example for density dependent aggregation. The particle velocity depends on some external signal which in turn depends on the density. Models consist of equations for the density and for the signal (see for example [32], [27], [28]). The coupling between speed and density is somewhat indirect whereas in the model here it is direct.

4. The vanishing viscosity approach has been used to prove existence of solutions to (systems of) conservation laws in one and several space dimensions in spaces of functions of bounded variation and of bounded measurable functions (cf. [64], [33]). The speed function depends pointwise on the density. There is no dependence on the gradient of the density. In [27] a chemotaxis model is studied with the vanishing viscosity approach. The gradient of the density does not appear there either.

5. Formally we can interpret the ill-posed form of equation (4.1) with $\gamma^u = F$ as follows: As long as the density is small, i.e. $u < u_*$, high values become higher and low values become lower. In other words: Contrasts are enhanced. Contrast enhancing is an important part of image processing and one of the methods used for it is the application of anisotropic nonlinear diffusion [53], [54]. The basic equation reads

$$u_t - (A(u_x^\varepsilon)u_x)_x = f(u),$$

   where $A \geq 0$ is a monotone decreasing function. If $u^\varepsilon = u$ then the problem is ill-posed since the diffusion coefficient may change sign. Hence the difficulty is the same as in the model presented here. The function $u^\varepsilon$ is an appropriate mollification introduced in order to make the equation well-posed.

# Bibliography


[1] **Adams, R.A.** *Sobolev Spaces.* Academic Press, New York, 1975.

[2] **Alt, W.** Models for mutual attraction and aggregation of motile individuals. In: Levin (ed.) *Mathematics in Biology and Medicine.* Lecture Notes in Biomathematics 57, Springer-Verlag, Berlin (1983), 33–38

[3] **Alt, W.** Degenerate diffusion equations with drift functionals modeling aggregation. *Nonlinear Analysis* **9** (1985), 811–836

[4] **Alt, W.** (ed.) *Dynamics of Cell and Tissue Motion,* Workshop Bonn–Röttgen 1995, Birkhäuser, Basel, 1997

[5] **Aronson, D.G.** The role of diffusion in mathematical population biology: Skellam revisited. In: Levin (ed.) *Mathematics in Biology and Medicine.* Lecture Notes in Biomathematics 57, Springer-Verlag, Berlin (1983), 2–6

[6] **Broadwell, J.E.** Shock structure in a simple velocity gas. *Phys. Fluids* **7** (1964), 1243–1247

[7] **Cahn, J.W., Hilliard, J.E.** Free energy of a non-uniform system, interfacial free energy. *J. Chem. Phys.* **28** (1958), 258–267

[8] **Dafermos, C.M.** *Hyperbolic Conservation Laws in Continuum Physics.* Grundlehren der mathematischen Wissenschaften 325, Springer Verlag, Berlin, 2000

[9] **Deutsch, A.** Orientation–induced pattern formation: swarm dynamics in a lattice-gas automaton model. *Int. J. of Bifurcation and Chaos* **6** (1995), 1735–1752

[10] **Edelstein-Keshet, L., Ermentrout, G.B.** Models for contact mediated pattern formation. *J. Math. Biol.* **29** (1990), 32–58

[11] **Edelstein-Keshet, L., Watmough, J., Grünbaum, D.** Do traveling band solutions describe cohesive swarms? *J. Math. Biol.* **36** (1998), 515–549

[12] **Flierl, G., Grünbaum, D., Levin, S., Olsen, D.** From individuals to aggregations: The interplay between behavior and physics. *J. Theor. Biol.* **196** (1999), 397–454

[13] **Geigant, E.** *Nichtlineare Integro-Differential-Gleichungen zur Modellierung von Musterbildungsprozessen auf $S^1$.* Dissertation Universität Bonn, 1999

[14] **Geigant, E., Ladizhansky, K., Mogilner, A.** An integro-differential model for orientational distributions of F-actin in cells. *SIAM J. Appl. Math.* **59** (1999), 787–809

[15] **Gilbarg, D., Trudinger, N.S.** *Elliptic Partial Differential Equations of Second Order.* Grundlehren der mathematischen Wissenschaften 224, Springer Verlag, 1977

[16] **Grindrod, P.** Models of individual aggregation or clustering in single and multi-species communities. *J. Math. Biol.* **26** (1988), 651–660

[17] **Grünbaum, D.** Translating stochastic density–dependent individual behavior with sensory constraints to an Eulerian model of animal swarming. *J. Math. Biol.* **33** (1994), 139–161

[18] **Grünbaum, D., Okubo, A.** Modelling social animal aggregations. In: Levin (ed.) *Frontiers in Mathematical Biology,* Lecture Notes in Biomathematics 100, Springer-Verlag, Berlin 1994, 296–325

[19] **Hadeler, K.P.** Travelling fronts for correlated random walks. *Canadian Applied Math. Quart.* **2** (1994), 27–43

[20] **Hadeler, K.P.** Spatial epidemic spread by correlated random walk with slow infectives. In: P.D. Smith (ed.) *Ordinary and Partial Differential Equations Vol. V* Proc. Conf. Dundee 1996, Pitman Research Notes Math. Ser. 378 (1997), 18–27

[21] **Hadeler, K.P.** Reaction Transport Systems. In: Capasso, Diekmann (eds.) *Mathematics inspired by Biology.* CIME Lectures 1997, Lecture Notes in Math. 1714, Springer, 1999

[22] **Hillen, T.** *Nichtlineare hyperbolische Systeme zur Modellierung von Ausbreitungsvorgängen und Anwendung auf das Turing Modell.* Dissertation, Universität Tübingen, 1995

[23] **Hillen, T.** A Turing model with correlated random walk. *J. Math. Biol.* **35** (1996), 49–72

[24] **Hillen, T.** Invariance principles for hyperbolic random walk systems. *J. of Math. Anal. and Appl.* **210** (1997), 360–374

[25] **Hillen, T., Othmer, H.** The diffusion limit of transport equations derived from velocity jump processes. *SIAM J. Appl. Math.* **61** (2000), 751–775

[26] **Hillen, T., Müller, J.** Modulation equations and parabolic limits of reaction random walk systems. *Math. Meth. Appl. Sci.* **21** (1998), 1207–1226

[27] **Hillen, T., Rohde, C., Lutscher, F.** Existence of weak solutions for a hyperbolic model for chemosensitive movement. *J. of Math. Anal. and Appl.* accepted

[28] **Hillen, T., Stevens, A.** Hyperbolic models for chemotaxis in 1-D. *Nonlinear Analysis: Real World Applications* **1** (2000), 409–433

[29] **Holmes, E.E.** Are diffusion models too simple? *Amer. Naturalist* **142** (1993), 779–795

[30] **Jäger, E., Segel, L.A.** On the distribution of dominance in populations of social organisms. *SIAM J. Appl. Math.* **52** (1992), 1444–1468

[31] **Kac, M.** A stochastic model related to the telegrapher's equation (1956), reprinted in *Rocky Mtn. Math. J.* **4** (1974) 497–509

[32] **Keller, E.F., Segel, L.A.** Initiation of slime mold aggregation viewed as an instability. *J. Theor. Biology* **26** (1970), 399–415

[33] **Kruẑkov, S.** First oder quasilinear equations in several independent variables. *Math. USSR Sbornik* **10** (1970), 217–243

[34] **Krylov, N.V.** *Lectures on Elliptic and Parabolic Equations in Hölder Spaces.* AMS, Providence, 1996

[35] **Kuttler, C.** *Freie Randwertprobleme für eindimensionale Transportgleichungen.* Dissertation, Universität Tübingen, 2000

[36] **Ladyzhenskaya, O.A., Solonnikov, V.A., Ural'tseva, N.N.** *Linear and quasi-linear Equations of Parabolic Type.* AMS, Providence, 1968

[37] **LeVeque, R.** *Numerical Methods for Conservation Laws.* Birkhäuser, Basel, 1992

[38] **Lizana, M., Padron,V.** A spatially discrete model for aggregating populations. *J. Math. Biol.* **38** (1999), 79–102

[39] **Mogilner, A. Edelstein-Keshet, L.** A non-local model for a swarm. *J. Math. Biol.* **38** (1999), 534–570

[40] **Mogilner, A., Edelstein-Keshet, L.** Spatio–angular order in populations of self aligning objects. *Physica D* **89** (1996), 346–367

[41] **Mogilner, A., Edelstein-Keshet, L.** Selecting a common direction I. *J. Math. Biol.* **33** (1995), 619–660

[42] **Mogilner, A., Edelstein-Keshet, L., Ermentrout, G.B.** Selecting a common direction II. *J. Math. Biol.* **34** (1996), 811–842

[43] **Murray, J.D.** *Mathematical Biology.* Springer Verlag, Berlin, 1993

[44] **Niwa, H.** Newtonian dynamical approach to fish schooling. *J. Theor. Biol.* **181** (1996), 47–63

[45] **Okubo, A.** Dynamical aspects of animal grouping: swarms, schools, flocks and herds. *Adv. in Biophysics* **22** (1986), 1–94

[46] **Othmer, H., Dunbar, S., Alt, W.** Models of dispersal in biological systems. *J. Math. Biol.* **26** (1988), 263–298

[47] **Padron, V.** Aggregation on a nonlinear parabolic functional differential equation. *Divulgaciones Matemáticas* **6** (1998), 149–164

[48] **Parrish, J.K., Edelstein-Keshet, L.** Complexity, pattern and evolutionary Trade-Offs in animal aggregation. *Science* **284** (1999), 99–101

[49] **Parrish, J.K., Hamner, W.M.** *Animal Groups in three Dimensions.* Cambridge University Press, 1997

[50] **Pfistner, B.** *A one dimensional model for the swarming behavior of Myxobacteria.* In: Alt, Hoffmann (eds.) *Biological Motion,* Lecture Notes in Biomathematics 89, Springer-Verlag, Berlin (1990), 556–563

[51] **Pfistner, B., Alt, W.** *A two dimensional random walk model for swarming behavior.* In: Alt, Hoffmann (eds.) *Biological Motion,* Lecture Notes in Biomathematics 89, Springer-Verlag, Berlin (1990), 568–569

[52] **Pitcher, T. J.** Shoaling and schooling in fishes. In: Greenberg, Haraway (eds.) *Comparative Psychology: a Handbook.* Garland, New York, 1998

[53] **Preußer, T., Rumpf, M.** An adaptive finite element method for large scale image processing. *Journal of Visual Comm. and Image Repres.*, to appear

[54] **Preußer, T., Rumpf, M.** Anisotropic nonlinear diffusion in flow visualization. *Report No.25, Sonderforschungsbereich 256*, Bonn, 1999

[55] **Radakov, D.V.** *Schooling in the Ecology of Fish.* Halsted Press, John Wiley & Sons, New York, 1973

[56] **Reed, M.C.** Propagation of singularities for non-linear wave equations in one dimension. *Comm. Diff. Eq.* **3** (1978), 135–199

[57] **Renardy, M., Rogers, R.C.** *An Introduction to Partial Differential Equations.* Springer, New York, 1993.

[58] **Reynolds, C.W.** Flocks, herds and schools: A distributed behavior model. *Computer Graphics* **21** (1987), 25–34,
`http://www.red3d.com/cwr/boids/`

[59] **Schwetlick, H.** *Reaktions-Transportgleichungen* Dissertation, Universität Tübingen, 1998

[60] **Schwetlick, H.** Travelling fronts for multidimensional nonlinear transport equations. *Ann. Inst. Henri Poincaré, Analyse non linéaire* **17** (2000), 523–550

[61] **Stöcker, S.** Models for tuna school formation. *Math. Biosci.* **156** (1999), 167–190

[62] **Taylor, M.** *Partial Differential Equations III,* Springer-Verlag, New York, 1996

[63] **Vabø, R., Nøttestad, L.** An individual model of fish school reactions: predicting antipredator behavior as observed in nature *Fish. Oceanogr.* **6** (1997), 155–171

[64] **Vol'pert, A.** The spaces BV and quasilinear equations. *Math USSR, Sb.* **2** (1967), 225–267